Sapienza Università di Roma
Facoltà di Farmacia, Dip. di Chimica e Tecnologie del Farmaco

Istituto Pasteur - Fondazione Cenci Bolognetti

Dottorato in Scienze Pasteuriane XXI Ciclo

Design, Synthesis and Anti-HIV Activity of New Indolyl Aryl Sulfones (IASs): Structure-Activity Relationship of Substituents on the 2-Carboxyamide Function

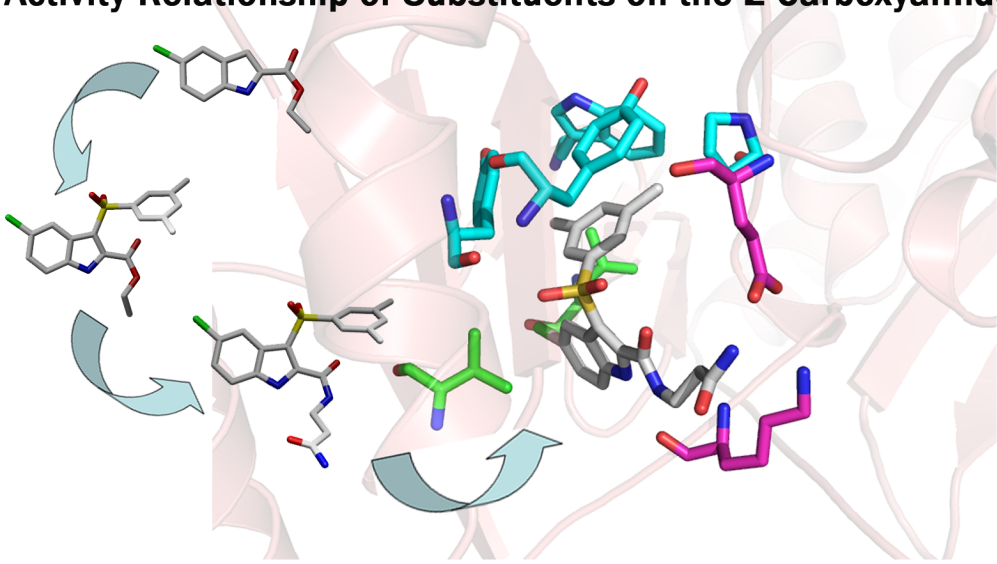

Tutor: Prof. Romano Silvestri
PhD Student: Francesco Piscitelli

Contents:

Introduction

In 1981, the acquired immunodeficiency syndrome (AIDS) appeared insidiously and mystified doctors and scientists alike. No one could have predicted then that it would become, arguably, the worst plague in human history.

Human immunodeficiency virus (HIV) is the etiological agent of AIDS; was estimated that 40 million of people living with HIV infection at the end of 2007.[1] The antiretroviral drugs or an eventual preventive HIV vaccine are the two strategies of combating AIDS/HIV infection.[2] More than twenty antiretroviral drugs approved by Food and Drugs Administration (FDA) are available falling in six classes: nucleoside and nucleotide reverse transcriptase inhibitors (NRTIs and NtRTIs), non-nucleoside reverse transcriptase inhibitors (NNRTIs), protease inhibitors (PIs), fusion inhibitors (FIs), integrase inhibitors (IIs) and CCR5 antagonists.[3] Three (recommended) or four antiretroviral drugs[4] are combined in the highly active antiretroviral therapy (HAART) that, since its introduction in 1996, proved to be effective in reducing morbidity and mortality of HIV-infected people.[5] However, HAART is unable to eradicate the viral infection; the needed long-term or permanent treatments favour the emergence of drug resistance, toxicity, and unwanted side effects.[6] The development of drugs for HIV infection began soon after the virus was discovered 25 years ago. Since then, progress has been substantial, but numerous uncertainties persist about the best way to manage this disease.

Figure 1. History of AIDS/HIV.

HIV Structure and Life Cycle

Structure. There are two types of HIV: HIV-1 and HIV-2. Worldwide, the predominant virus is HIV-1, and the relatively uncommon HIV-2 type is concentrated in West Africa and is rarely found elsewhere.

HIV is a lentivirus, from the family of retroviruses, which characteristically have an RNA genome contained within a capsid and a lipid envelope. The viral envelope contains 2 major viral glycoprotein, gp41 and gp120 that mediate viral entry and syncytium formation. The HIV core is composed of 3 structural proteins, p24, p16, and p9. The p24 protein forms the capsid that encloses 2 genomic RNA strands and the viral enzymes reverse transcriptase (RT), protease, ribonuclease, and integrase (IN). The matrix protein (MA), gp16, is anchored to the internal face of the envelope. P9 is a nucleocapsid protein not covalently attached to the viral RNA.[7]

The genome of HIV, similarly to retroviruses in general, contains three major genes: *gag*, *pol*, and *env*. These genes code for the major structural and functional components of HIV, including envelope proteins and reverse transcriptase. Accessory genes carried by HIV include *tat*, *rev*, *nef*, *vif*, *vpr*, and *vpu* (for HIV-1) or *vpx* (for HIV-2). The functions of some of these genes are known. Figure 3 shows an overview of the organization of the (approximately) 9-kilobase genome of the HIV provirus and a summary of the functions of its nine genes encoding 15 proteins.[8]

Life cycle. Like other viruses, HIV needs to proliferate inside its target cells; the HIV life cycle can be separated in different phases. A general overview is showed in Figure 4.

Entry. Infection begins when a virus encounters a cell with a high-affinity receptor for the virus. A specific high-affinity binding reaction occurs between the virus surface envelope glycoprotein (gp120) and the CD4 molecule[9] found on a variety of cells of haematopoietic origin. These cells include T lymphocytes, monocyte/macrophages, Langerhans cells, follicular dendritic

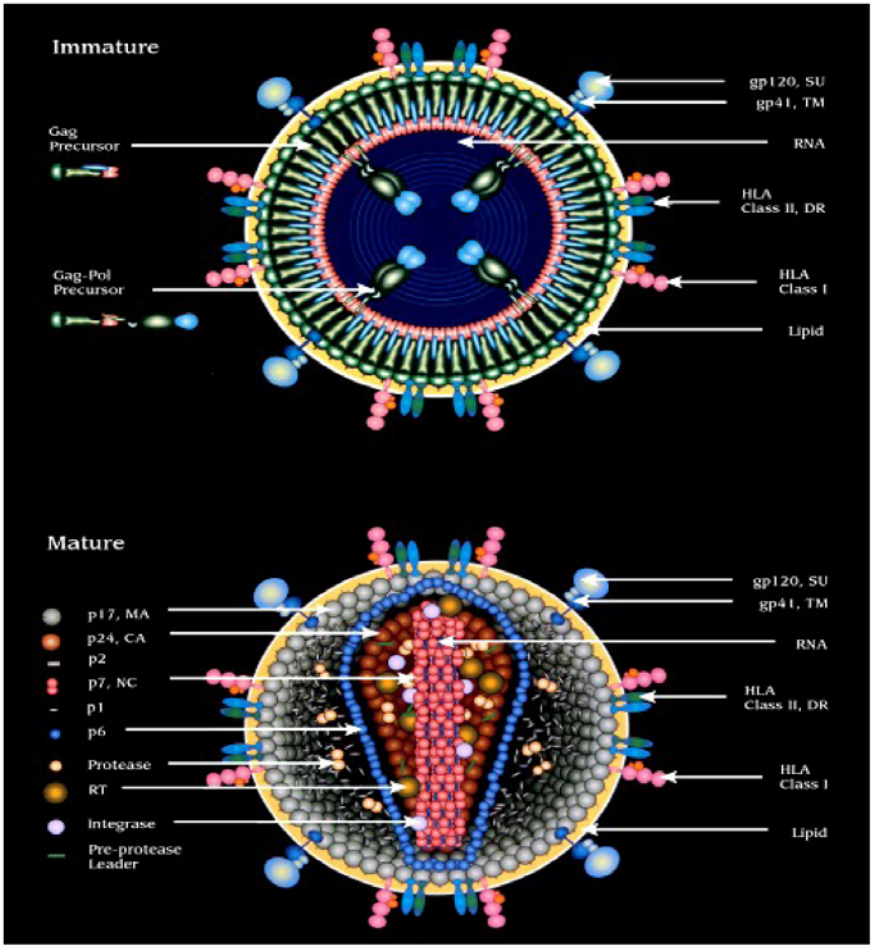

Figure 2. HIV Structure.

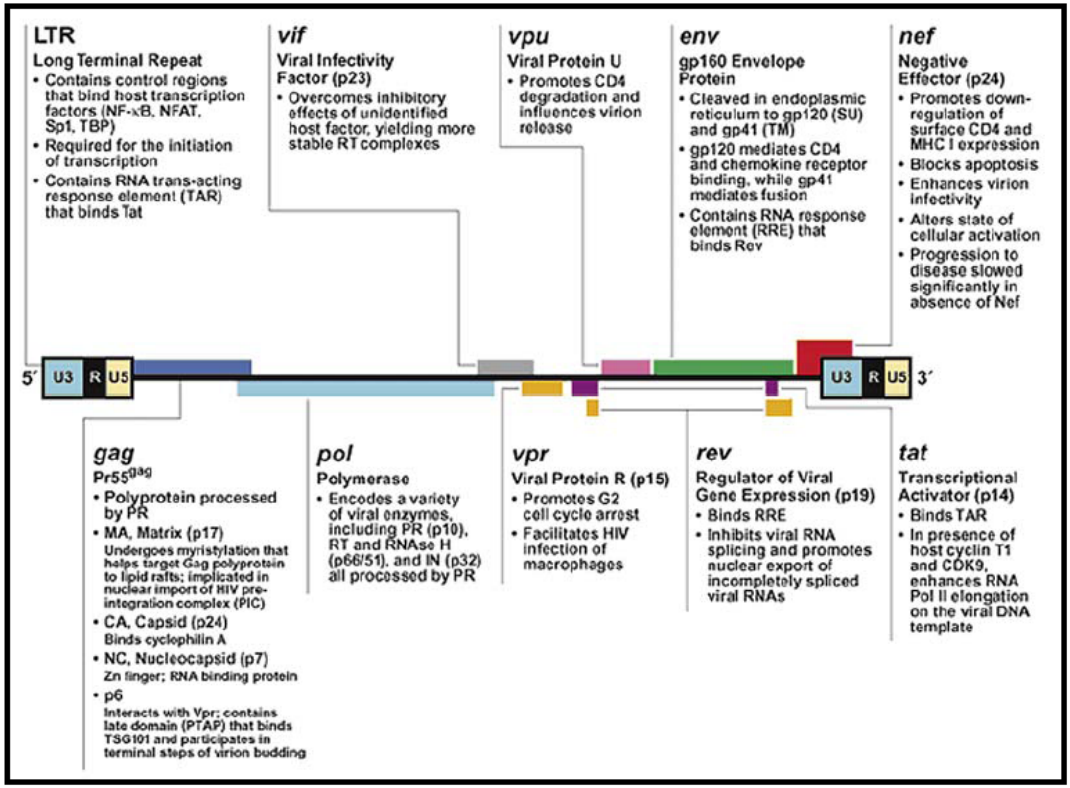

Figure 3. Organization of the HIV proviral genome and summary of gene product function.

cells, thymocyte precursors, and B cells.[10] CD4 binds to gp120 with extremely high affinity and serves as the major receptor for HIV-1 infection. Entry occurs by fusion of virus and cell membranes mediated by gp41 in a pH independent manner.[11] Expression of CD4 wasn't the only requisite for HIV infection of a cell. Recently was observed that HIV also needs a chemokine receptor adjacent to the CD4 receptor before it can enter the target cells and two types of chemokine receptors are used by HIV: CCR5 and, at later stages of infection, the CXCR4 receptors.

Reverse transcription and integration. This phase consist in the biosynthesis of the double-stranded DNA molecules from the single-stranded RNA, and takes place inside the cell cytoplasm with the aid of the enzyme viral RT (see Figure 5 for mechanism). The proviral DNA associated with MA, RT, and IN is translocated from the cytoplasm to the nucleus.[12] Although proviral DNA exists in both circular and linear forms, the linear DNA is the precursor for integration.[13] Cleavage of target DNA sequence within the host chromosome is then followed by legation of the 3' end of the proviral DNA to the 5' end of the chromosomal DNA by the viral IN.[14] Cellular repair enzymes finally complete the integration reaction. The activation of T cells, at least one round of cellular DNA synthesis, has been shown to be required for proviral DNA integration into the host chromosome.[12c]

Transcription. Transcription from the integrated proviral DNA requires cellular RNA polymerase II and transcription initiation factors, many of which are absent in non-activated, resting T cells. As a consequence, little or no virus production is detected in infected but non-cycling T cells obtained from patients. In addition to a defect in the cellular environment, the site of proviral DNA integration may also contribute to latency.[15]

HIV-1 mRNAs produced in infected cells are capped with $m^7G_{ppp}G$ at the 5' end and polyadenylated at the 3' end. Three types of HIV-1 mRNAs are produced as a result of differential splicing events.[16] Early viral mRNAs present in the cytoplasm of infected cells are completely spliced 1.7-2 kilobase (kb) mRNA species encoding regulatory proteins. These include three coding for *tat,*

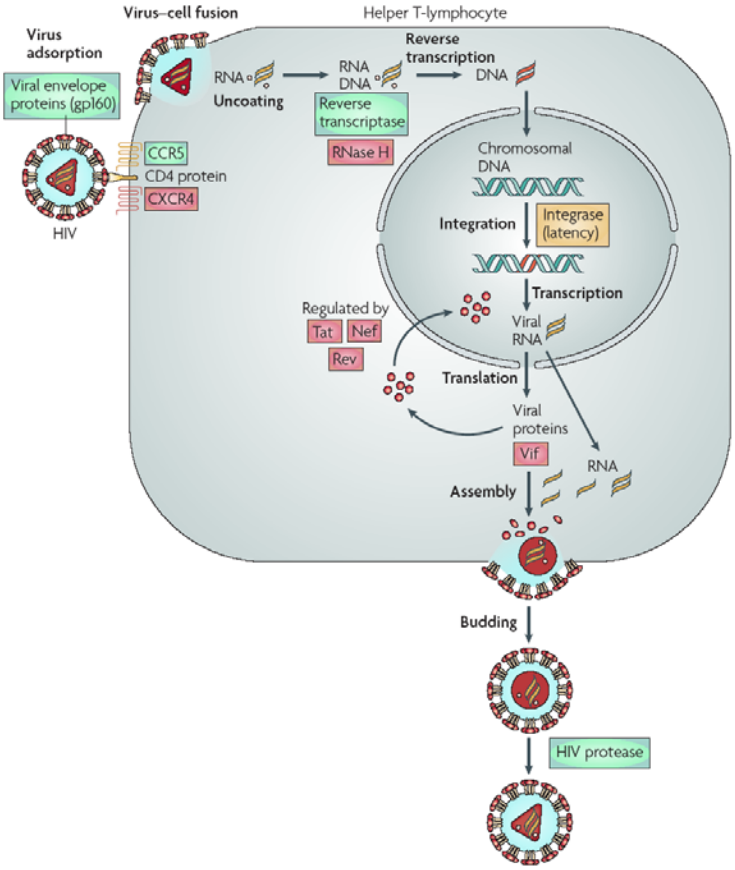

Figure 4. Replication cycle of HIV with current and possible targets for antiviral intervention. Proteins that are targets for approved drugs are coloured green: gp160, reverse transcriptase, HIV protease and chemokine (c-c motif) receptor 5 (CCR5). Integrase (yellow) is a target in advanced clinical development. Proteins that are more speculative drug targets are coloured red: chemokine (C-X-C motif) receptor 4 (CXCR4), RNase H, *tat*, *rev*, *nef* and *vif*.

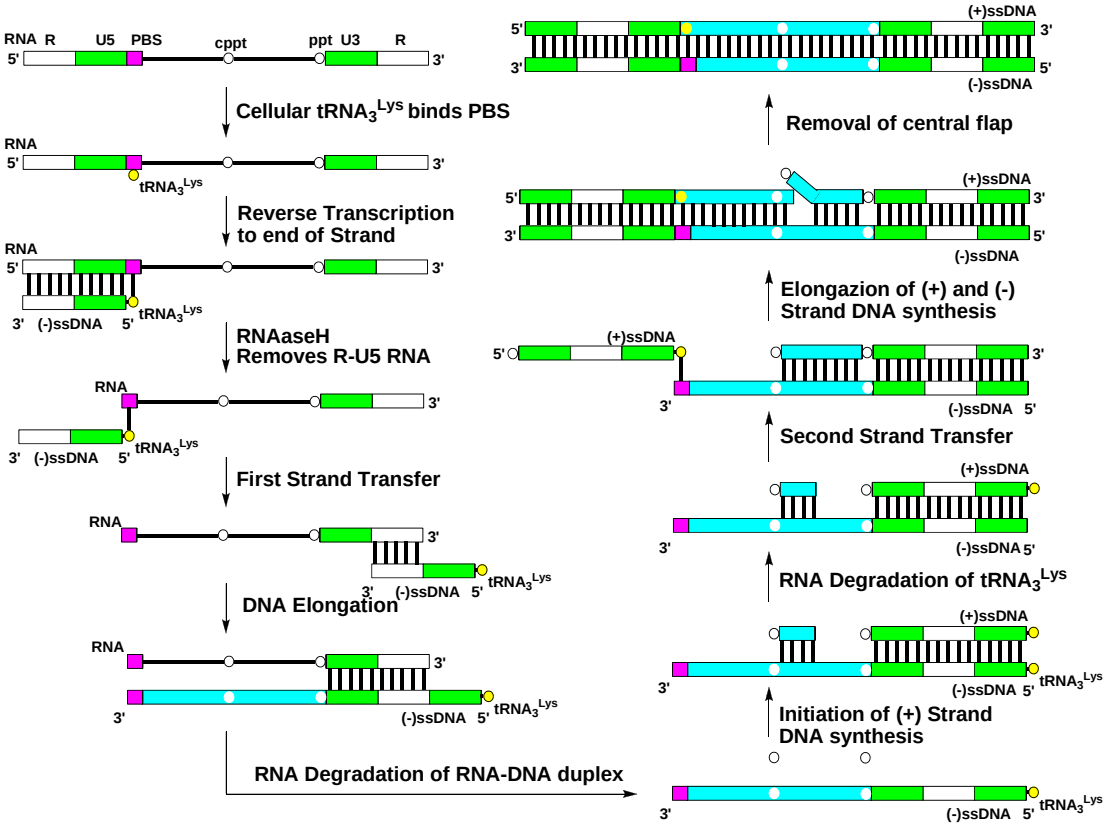

Figure 5. Mechanism of HIV-1 RT.[17] Kinetic studies of the enzymatic reaction indicate that the DNA polymerization takes place in an ordered mechanism. The reaction is initiated by the binding of the primer, in most cases the $tRNA^{Lys}$, to the free RT, which is followed by the template binding to the binary complex. Then NTP binds subsequently to the complex. The RNase H activity catalyzes the degradation of the template RNA in the RNA/DNA hybrid during the reverse transcription. Both endo- and exonuclease activities have been found with HIV RT.

six coding for *rev,* one coding for *tat-env-rev* (*tev*), and three coding for *nef* mRNA species. The late viral mRNAs consist of 4-5 kb singly spliced and 9.3 kb unspliced mRNA species. The singly spliced mRNAs include 1 *vif,* 1 *vpr,* 1 *tat* (a truncated form), and 3 *vpu/env* mRNA species. The unspliced RNAs serve as mRNA for $Pr55^{gag}$ and $Pr160^{gag\text{-}pol}$ synthesis and as genomic RNA packaged within the virus particles.

Virion assembly and release. The viral mRNA utilizes almost all the cell resources to translate its genetic information into large glycoprotein and polyproteins. These products then disintegrate into smaller building blocks of the viral membrane, enzymes, and nucleocapsid through the action of viral protease.

For the creation of new virions, the full length 9.3 kb genomic RNA must leave the nucleus, transit the cytoplasm, and be associated with the budding virions without being involved in protein synthesis. Viral genomic RNAs contain a Ψ signal located within the 5' untranslated region and the *gag* reading frame.[18] In addition, a 1.1 kb RNA sequence encompassing the Rev responsive element (RRE) has been shown to be required for efficient packaging of HIV-1 genomic RNAs.[19] DLS, through guanine and/or purine quartets, allows dimerization of viral genomic RNAs and permits them to exist in an overall parallel orientation.[20] The NC domain of $Pr55^{gag}$ and $Pr160^{gag\text{-}pol}$ [21] allows genomic RNA incorporation within the virus particles via specific zinc finger motifs.[35f]

The assembly of the viral building blocks produces new viral particles that shed off the cell surface to infect other target cells. There are now two major models for HIV-1 budding, process necessary used by the virus to exit from infected cells. One is the lipid raft budding model. Lipid rafts are regions on the plasma membrane that are enriched in sphingolipids as well as cholesterol and GPI-linked proteins. Gag and Gag/Pol precursor proteins have been shown that disruption of these membrane domains can reduce virus production. Taken together these data suggest that HIV-1 may be preferentially budding from these regions.[22] The other model for HIV-1 budding is the Trojan exosome

hypothesis.[23] This model suggests that HIV-1 hijacks the pre-existing pathway for exosomal exchange for its propagation and masquerades as an exosome. This model is largely based on the evidence that HIV-1 assembles in the multivesicular bodies or MVBs and buds into this compartment in primary macrophages. Multivesicular bodies[24] are membrane bound organelles that serve as endocytic intermediates. The MVB then moves closer to the plasma membrane where the membranes fuse releasing its contents as an exosome. There are data showing that virus produced in the macrophage does not incorporate raft-associated cellular proteins but does contain exosomal markers found in macrophage derived exosomes. Both of these models have strong evidence supporting them. Perhaps both of them are plausible models that may not be mutually exclusive. It also appears that release of HIV-1 from infected cells can be directional with virus being released to sites of cell-cell contact to facilitate infection of target cells.[25] Evidence for such a mechanism come from the long standing knowledge that infected cells can much more efficiently infect target cells compared to cell-free virus found in culture media. Evidence for directed release was recently presented with the identification of preferential accumulation of HIV-1 *Gag* and *Env* at sites of cell-cell contact.[26] This site of controlled virus release has been called the infectious synapse. Formation of these synapses has been shown to be actin-dependent and contain many cellular projections that depend on cytoskeletal rearrangement for their formation.[27] HIV-1 has been seen budding from leading pseudopods, which are actin-dependent.[28] The presence of cytoskeletal proteins inside mature virions suggests that the cellular cytoskeleton plays an important role in viral egress.[45] Clearly, HIV-1 has evolved to usurp several cellular pathways to increase the efficiency of the spread of virus between cells.

AIDS Treatment

Three years after the discovery of HIV in 1984, GlaxoSmithKline's Retrovir (zidovudine) became the first drug to be approved for the treatment of this disease. It belongs to the class of nucleoside reverse transcriptase inhibitors (NRTIs), which have been at the forefront of antiretroviral therapy ever since. However, even in combination with each other, NRTIs could only produce transient viral suppression and the necessity to administer high doses led to high levels of toxicity and resistance. With the introduction of HIV protease inhibitors (PIs) in 1995, it was found that major and prolonged reductions in viral burden could be achieved by the combination of a PI with two NRTIs known as highly active antiretroviral therapy (HAART). Similar results were later obtained by adding a member of a third class of drugs known as non-nucleoside reverse transcriptase inhibitors (NNRTIs) to two NRTIs. NNRTI based HAART regimens have quickly become the preferred choice for initial antiretroviral therapy, whereas drugs from the newest classes, such as entry and integrase inhibitors, form useful adjuncts.

Today, 25 drugs are approved by FDA for the AIDS treatment and they fall into six classes based on the specific target:

1. Nucleoside (and Nucleotide) Reverse Transcriptase Inhibitors (NRTIs and NtRTIs): abacavir, didanosine, emtricitabine, lamivudine, stavudine, tenofovir, zalcitabine, and zidovudine (Figure 6);

2. Non Nucleoside Reverse Transcriptase Inhibitors (NNRTIs): delavirdine, efavirenz, nevirapine, and etravirine (Figure 7);
3. Protease inhibitors (PI): amprenavir, atazanavir, danuravir, fosamprenavir, indinavir, lopinavir, nelfinavir, ritonavir, saquinavir, and tipranavir (Figure 8);

4. Fusion inhibitor (FI): enfuvurtide (Figure 9);

5. Integrase inhibitor (II): raltegravir (Figure 10);

6. CCR5 antagonist: maraviroc (Figure 10).

Reverse transcriptase inhibitors. Due to the essential role of the HIV RT in the viral replication, the inhibition of RT is regarded as one of the most attractive targets in the anti-HIV chemotherapy. Based on the structure and the mechanism, HIV RT inhibitors can be classified as two groups, NRTIs and NNRTIs. The NRTIs are competitive inhibitors to deoxynucleotide triphosphate (dNTP) and need to be transformed through a phosphorylation process to their corresponding nucleoside triphosphates or nucleotide diphosphates which then are incorporated into the growing viral DNA chain and subsequently to terminate the DNA elongation. They are normally active against both HIV-1 and HIV-2. The NNRTIs, on the other hand, are almost inactive on HIV-2, need no metabolic activation and they bind to the enzyme independently from dNTP and template/primer with a non-competitive kinetics to dNTP and are uncompetitive to template/primer. Different aspects on the inhibition of HIV-1 RT with NNRTIs are discussed below.

Protease inhibitors. Protease inhibitors have been developed as anti-HIV drugs. The processing of large HIV precursor proteins, such as p55 and p40 encoded by the *gag* and *gag-pol* genes of HIV, into structural proteins p17, p24, and p7 of the viral core is performed via proteolytic cleavage by a viral encoded aspartic protease and is necessary for maturation of immature viral particles into infectious virions. These drugs are synthetic analogues of the HIV protein and block the action of HIV-protease to interfere with viral replication.[29] Protease inhibitors may also function by decreasing $CD4^+$ lymphocyte apoptosis through decreased CD4 interleukin-1β-converting enzyme (ICE, or caspase 1) expression.[30]

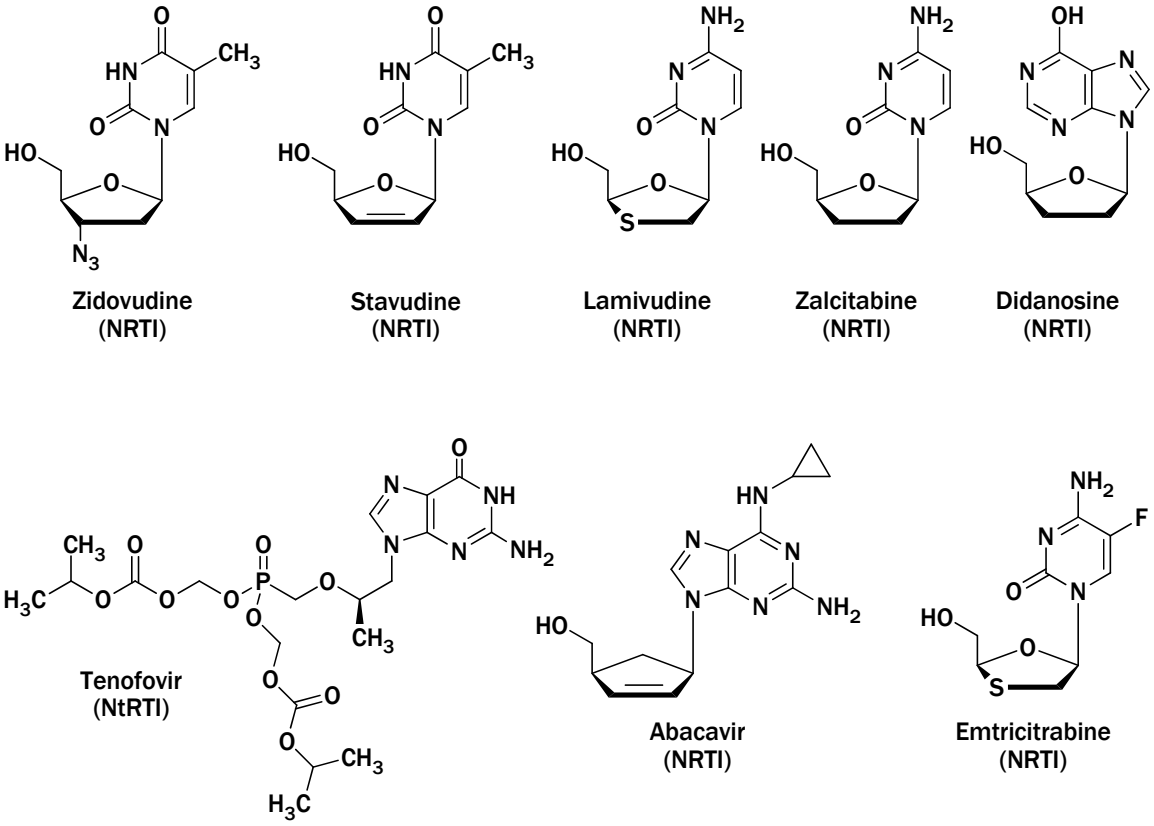

Figure 6. NRTIs and NtRTIs structures.

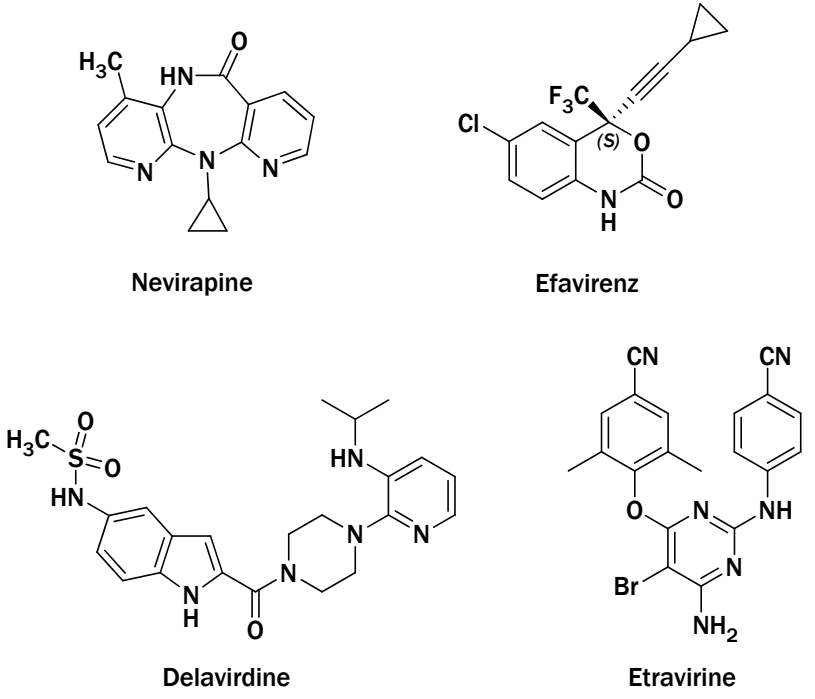

Figure 7. NNRTIs structures.

Fusion inhibitors. This compound class blocks fusion of HIV with the target cell surface. Enfuvirtide is a synthetic peptide that corresponds to 36 amino acids within the C-terminal heptad repeat region (HR2) of HIV-1 gp41 subunit of the viral envelope (Env) protein, and prevents conformational changes required for membrane fusion to target cells. The drug is delivered by subcutaneous injection.[31]

Integrase. The integrase inhibitor raltegravir appears to be as potent as any previously developed antiretroviral drug in terms of its short term 5 and 24 week anti-HIV effects.[32] It is expected to become a mainstay of second line therapy, if not an eventual candidate for first line use. The advantage of this drug target is that integrase is an essential and highly conserved enzyme. However, one disadvantage is that moderate level to high level resistance to this and other integrase inhibitors can follow after only one or two amino acid mutations.[33] A second integrase inhibitor, elvitegravir, is also in advanced clinical development. In September 2007, an independent FDA advisory committee voted for accelerated approval of raltegravir.

CCR5. The CCR5 antagonist maraviroc has excellent short term anti-HIV activity, and is associated with substantial efficacy after 24 weeks of treatment when combined with antiretroviral nucleosides in treatment experienced patients.[34] The attraction of this chemokine co-receptor target is that virtually all individuals are initially infected with the CCR5 trophic virus, and maraviroc is the first approved oral drug in the broad category of entry inhibitors. One drawback, however, is that maraviroc has little or no activity against viruses that use the chemokine (CXC motif) receptor 4 (CXCR4) as a co-receptor, or have dual/mixed tropism. Patients will need to be screened for virus co-receptor use with a commercial tropism assay before receiving this drug. A second CCR5 antagonist, vicriviroc, has efficacy in Phase II trials in treatment experienced patients, and is entering Phase III trials.

Highly active antiretroviral therapy. In the 1996 was introduced the HAART for the treatment of HIV infection. The rate of formation and accumulation of mutations was so great that monotherapy and dual-therapy were doomed to

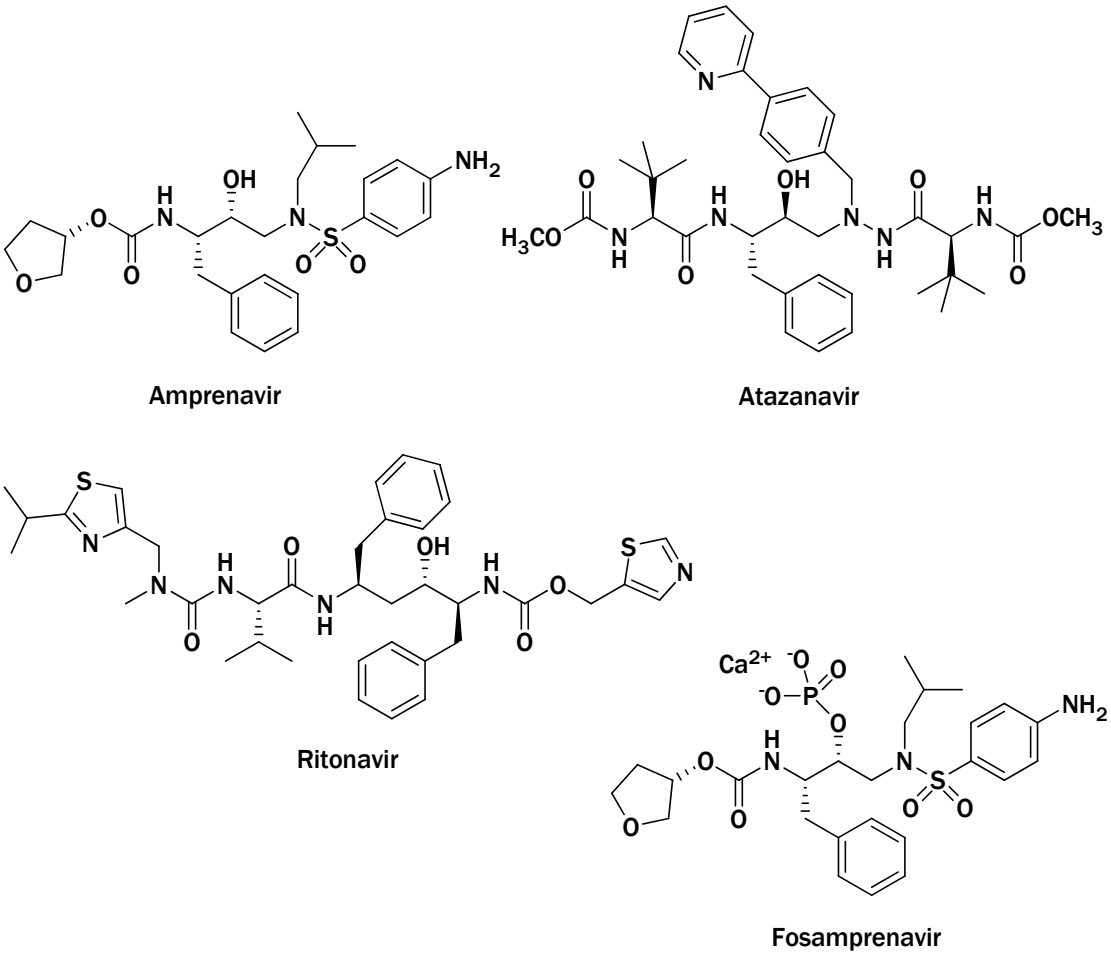

Figure 8. PIs structures.

(Continued)

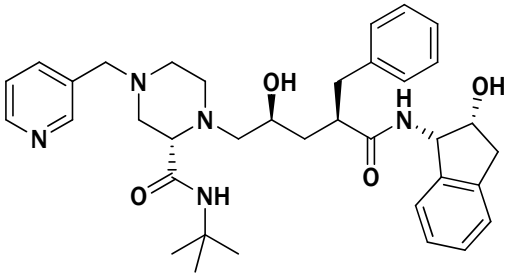

Indinavir

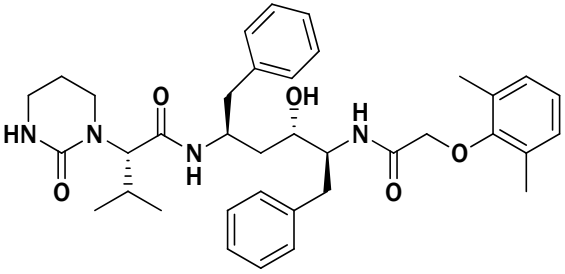

Lopinavir

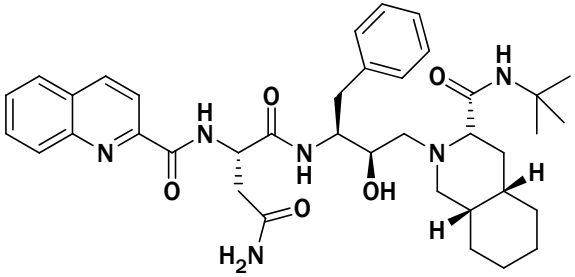

Saquinavir

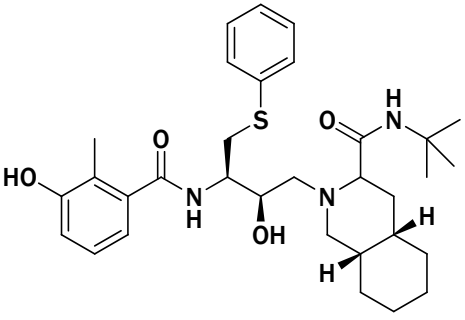

Nelfinavir

Figure 8. PIs structures.

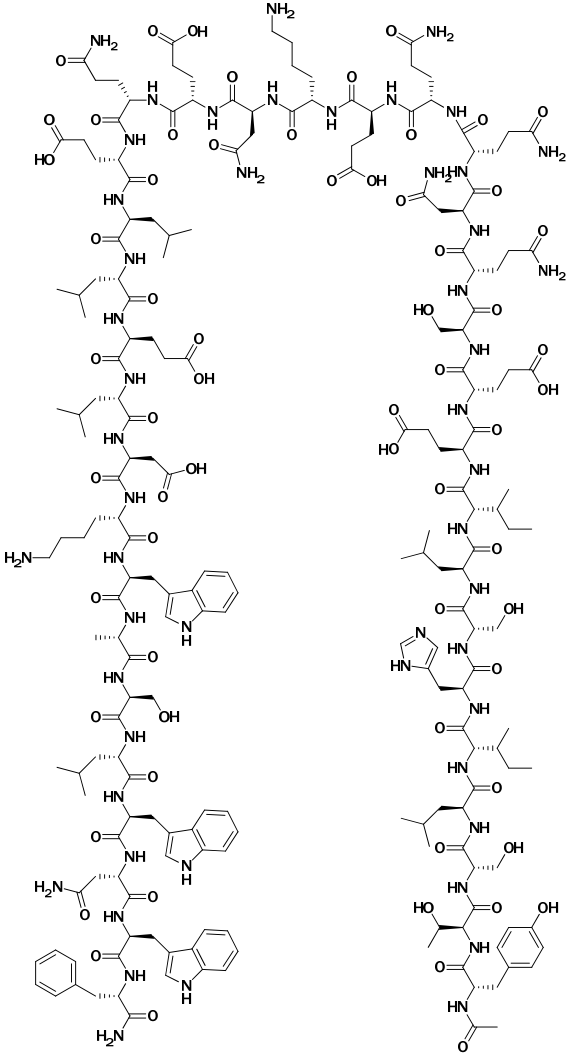

Figure 9. FI structures (Enfuvirtide).

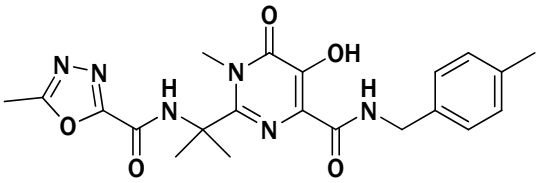

Raltegravir
Integrase Inhibitor

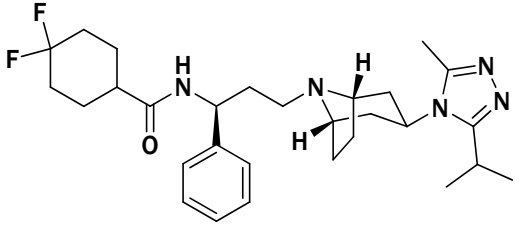

Maraviroc
CCR5 Antagonist

Figure 10. Structure of Raltegravir and Maraviroc.

fail because of the rapid emergence of drug resistance. On the other hand, the math also predicted that it was highly improbable ($<10^{-8}$ per day) for HIV-1 to mutate in ≥3 positions, simultaneously, in a single genome. This realization led clinical investigators to pursue the use of three or more drugs in combination, starting in early 1995. In 1996, it was clear that such combination antiretroviral therapy resulted in durable control of HIV-1 replication. Viremia was reduced to below the level of detection for more than a year, and significant immunological and clinical recovery was observed. Thus, 1996 marked a turning point in the AIDS pandemic. AIDS-associated mortality has since dropped by 80%–90% in the US and Europe and, conservatively, more than 3 million person-years of life have been saved. Over the past decade, HAART has gradually evolved from drug regimens with more than 20 pills daily (stavudine, lamivudine and indinavir combination) in 1996, to 3 pills daily (that is, zidovudine/lamivudine (Combivir) twice daily and efavirenz (EFV) once daily) in 2003, to 2 pills daily (that is, emtricitabine ((–)-FTC)/tenofovir disoproxil fumarate (Truvada) and EFV) in 2004, and finally one pill daily in 2006 (Atripla, which contains tenofovir disoproxil fumarate (TDF) (300 mg) plus emtricitabine (200 mg) and EFV (600 mg)).[35] Atripla (Bristol–Myers Squibb/Gilead) is the first anti-HIV pill (to be taken once daily) that contains three active ingredients belonging to three different classes of HIV inhibitors (coformulation of efavirenz (FI), tenofovir (NRTIs) and emtricitabine (NtRTIs)). The approval of Atripla in July 2006, signalled the start of a new era in antiretroviral therapy. Co-formulations greatly simplify treatment, and put HIV infection in the same class as hypercholesterolaemia, hypertension or gastroesophageal reflux disease, all chronic conditions that can be controlled with a single pill taken once daily.

In Tables 1-4 were reported the side effects and other properties of anti-HIV approved drugs.

Multi-class combination products				
Brand name (drugs)	Side Effects	Drug Interactions	Reccomandations	Approval date
Atripla (Efavirenz, emtricitabime and tenofovir disoproxil fumavate) Bristol-Mayer Squibb and Gilead Sciences				12 July 2006

Nucleoside Reverse Transcriptase Inhibitors (NRTIs)				
Brand name (drugs)	Side Effects	Drug Interactions	Reccomandations	Approval date
Retrovir (Zidovudina, azidothymidine) GlaxoSmithKline Dose: 300-600 mg/day. Approved for pedriatic use.	Nausea, vomiting, anemia, low white blood-cell counts, bone-marrow damage, headaches, rash, itching, weakness, loss of appetite, muscle loss.	**Serious**: d4T, toxic bone-marrow drugs (e.g. ganciclovir, chemotherapies, antineoplastics). **Possible**: Methadone, Dilantin, fluconazole (Diflucan), Depakene, ongoing use of Tylenol, dapsone, pentamidine, probenecid, fencytosine, alpha-interferon, Biaxin, rifabutin, rifampin, ribavirin.	AZT with food if you have stomach irritation. Take vitamin E, erythropoieitin alpha (EPO), or G-CSF to prevent possible blood-cell damage; B vitamins and manganese. **Warning**: A structural flaw in AZT may lead to HIV resistance.	19 Mar 1987
Videx (didanosine, dideoxyinosine) Bristol-Mayer Squibb Dose: 400 mg/day Approved for pedriatic use. **Videx EC** (enteric coated didanosine and dideoxyinosine)	Stomach pain, diarrhea, pancreatitis, hepatitis, seizures, headaches; neuropathy with high doses.	**Serious**: pentamidine, ethambutol. **Possible**: antineoplastics, alcohol, ganciclovir, ciprofloxacin, cimetidine (Tagamet). Coated pill causes poor absorption of Crixivan, Nizoral (ketoconazole), dapsone, tetracycline (all should be taken two hours apart from ddI.)	Avoid alcohol, which increases risk of pancreatitis. Take on empty stomach at least 30 minutes before meal.	**Videx:** 09 Oct 1991 **Videx EC:** 31 Oct 2000

Table 1. Proprieties of Atripla and NRTIs.

Continued NRTsI...

Hivid (Zalcitabine, dideoxycytidine) Hoffmann-La Roche Dose: three 0.77 mg/day. Approved for pedriatic use.	Skin rashes, canker sores, inflammation of mouth, nausea, neuropathy, upset stomach, pancreatitis, liver damage.	**Serious**: pentamidine, ddI, 3TC. Avoid other neuropathy-causing drugs (chloramphenicol, Antabuse, dapsone, isoniazid). **Possible**: Radiation therapy, amphotericin B, pyrimethamine, sulfadiazine, intravenous TMP/SMX (Bactrim), ganciclovir, acyclovir, foscarnet, probenecid.	Watch for neuropathy and pancreatitis. Avoid taking with food if possible.	19 Jun 1992
Zerit (Stavudine) Bristol-Mayer Squibb Dose: two 40 mg/day. Liquid solution for pedriatic use.	Neuropathy, pancreatitis, insomnia, hyperactivity; elevated liver enzymes and anemia at high doses.	**Serious**: AZT. **Possible:**Ganciclovir, pentamidine, other drugs that cause neuropathy.	Watch for neuropathy and pancreatitis. Take with or without food.	24 Jun 1994
Epivir (lamivudine) GlaxoSmithKline. Dose: 300 mg/day (or two 150 mg/day). Liquid solution for pedriatic use.	Headache, nausea, fatigue, low white-bloodcell count, rare hair loss, neuropathy.	**Serious:** ddC. **Possible:** Bactrim may increase 3TC levels.	Watch for anemia and neutropenia. Monitor triglycerides for pancreatitis, especially in children. Take with or without food.	17 Nov 1995
Combivir (Lamivudine 150mg and Zidovudine 300mg) GlaxoSmithKline.	See 3TC and AZT.	3TC/AZT combo can cause severe anemia.	Watch for anemia.	27 Sep 1997

Table 1. Proprieties of NRTIs (...continued).

Continued NRTIs...

Ziagen (Abacavir sul fate) GlaxoSmithKline. Dose: two 300 mg/day. Under study for pedriatic use.	Headache, fatigue; rare allergy (fever, rash, nausea, dizziness, vomiting); abdominal pain, GI and liver problems. **Warning: Stop drug immediately and don't try again if any sign of allergy.**	Alcohol increases blood level of Ziagen.	Expanded access for patients failing standard regimens. Compassionate use: adults with HIV dementia and pediatric HIV. Crosses blood-brain barrier.	17 Dec 1998
Trizivir (abacavir, Zidovudine, lamivudine) GlaxoSmithKline				14 Nov 2000
Viread (tenofovir disoproxil fumarate) Gilead				26 Oct 2001
Emtriva (Emtricitabine) Gilead Sciences				12 Jul 2003
Epzicom (abacavir and lamivudine) GlaxoSmithKline				02 Ago 2004
Truvada (Tenofovir disoproxil fumarate, and emtricitabine) Gilead Sciences, Inc.				02 Ago-2004

Table 1. Proprieties of NRTIs (...continued).

NonNucleoside Reverse Transcriptase Inhibitors (NNRTIs)				
Brand name (drugs)	Side Effects	Drug Interactions	Reccomandations	Approval date
Viramune (Nevirapine) Boehringer Ingelheim. Dose: one 200 mg/day (for 14 days than two 200 mg/day) Expanded access for pedriatic use	Fever, muscle soreness, elevated liver function, rash (possibly indicating life-threatening Stevens-Johnson syndrome in rare cases).	**Possible**: rifampin, rifabutin, oral contraceptives, protease inhibitors, triazolam and midazolam. Use with fluconazole increases risk of rash.	If rash develops, call your doctor; Benadryl or topical corticosteroids may relieve rash symptoms. Drug crosses the placenta. Take with or without food.	21 Jun 2006
Rescriptor (Delavirdine) Pfizer. Dose: three 400 mg/day. Under study for pediatric use.	Rash (possibly Indicating life threatening Stevens-Johnson syndrome in rare cases).	**Serious:** terfenadine, astemizole, alprazolam, midazolam, cisapride, rifabutin, rifampin, triazolam, ergot derivatives, amphetamines, nifedipine, anticonvulsants. **Possible:** Rescriptor increases levels of Biaxin, dapsone, quinidine, warfarin, Crixivan, Fortovase. Take an hour apart from ddI and antacids (Tagamet).	Take with or without food. Take with cranberry or orange juice if you have low stomach acid. If rash develops, call your doctor; Benadryl or topical corticosteroids may relieve rash symptoms. One study shows women may have higher blood levels of Rescriptor.	4 Apr 1997
Sustiva (Efavirenz) Bristol-Mayer Squibb. Dose: 600 mg/day. Approved for pedriatic use	Light-headedness, dizziness, body ache, rash, diarrhea, nausea, flu-like symptoms.	**Serious:** Fortovase; rifampin (untildosing is clarified). **Possible:** Drug may slightly increase Novir levels and decrease levels of Crixivan and Angenerase. Sustiva can cause a false positive THC (marijuana) reading on the CediaDau urine test.	Take before bedtime to avoid light-headedness; split dosage between a.m. and p.m. if leeplessness is a problem. **Warning**: Not for use in early pregnancy (caused birth defects in some newborn monkeys). Take with or without food.	17 Sep 1998
Intelence (Etravirine) Tibotec Therapeutics.				18 Gen 2008

Table 2. Proprieties of NNRTIs.

Protease Inhibitors (PIs)				
Brand name (drugs)	Side Effects	Drug Interactions	Reccomandations	Approval date
Invirase (Sequinavir mesylate) Hoffmann-La Roche. *See Fortovase*				6 Dec !995
Norvir (Ritonavir) Abbott Laboratories Dose: six 100 mg twice day (400 mg doses twice day with Fortovase). Currently available in formula liquid only (400 mg = 1 tps). Liquid solution for children.	Nausea, vomiting, weakness, diarrhea, rash, fatigue, numbness around mouth, changed taste in mouth, elevated liver enzymes.	**Serious**: A long list. Read package insert carefully. Poor interaction with common antihistamines and antidepressants like Prozac.	Build up to optimal dose over a few days. Take with a full, high protein meal. Yogurt may reduce side effects. See "Norvir Alert" for tips on taking liquid formulation.	1 Mar 1996
Crixivan (Indinavir) Merk Dose: three 800 mg/day Under study for pedriatic use	Kidney stones, anemia, rarely elevates liver enzymes.	**Serious**: grapefruit juice. **Potential**: Viramune, Fortovase (poor interaction in test tube studies), ergot derivatives.	Take on empty stomach with water one hour before or two hours after eating. Drink at least six glasses of water daily to avoid kidney stones. Alternative liquids: juice, skim milk, coffee, tea. Eat with fat free snacks.	13 Mar 1996
Viracept (Nelfinamvir mesylate) Agouron Pharmaceuticals Dose : three 750 mg/day. Approved for pedriatic use: 20-30 mg/Kg	Fatigue, rash, nausea, stomach cramps, diarrhea, elevated liver enzymes.	**Potential:** Increases Fortovase (under study as combo) and Crixivan in preliminary studies**.**	Take with food. Use Imodium, Lomotil to control diarrhea. Women should consult with their doctors prior to use. Monitor glucose levels to avoid risk of diabetes.	14 Mar 1997

Table 3. Proprieties of PIs.

Continued PIs...

Fortovase (Saquinavir, no longer marketed) Hoffmann-La Roche Dose: three 1200 mg/day (400-800 mg/day with Norvir) *Invirase*: old formula. Under study for pedriatic use	Diarrhea, gas, nausea, stomach cramps, heartburn, fatigue, numbness, rash; elevated liver enzymes.	**Serious:** In early studies, Sustiva reduces Fortovase. **Possible**: phenobarbital, phenytoin, dexamethasone, carbamezapine, Norvir, Viramune.	Take with food or within two hours of eating. Fortovase is more potent than nvirase. Invirase not recommended as first-line therapy due to poor absorption and resistance issues.	7 Nov 1997
Agenerase (amprenavir) GlaxoSmithKline Under study for pediatric use.	Nausea, heacache, neuropathy, rash, diarrhea, fatigue.	**Possible**: Sustiva	Expanded access for patients who have taken at least one other protease inhibitor. Can be taken with or without food.	15 Apr 1999
Kaletra (Lopinavir and Ritonavir) Abbott Laboratoires				15 Sep 2000
Reyataz (Atazanavir sulphate) Bristol-Mayer Squibb.				20 Jun 2003
Lexiva (Fosamprenavir Calcium) GlaxoSmithKline				20 Oct 2003
Aptivus (Tripanavir) Boehringer Ingelheim				22 Jun 2005
Prezista (Darunavir) Tibotec				23 Jun 2006

Table 3. Proprieties of PIs (...continued).

Fusion Inhibitor (FI)				
Brand name (drugs)	Side Effects	Drug Interactions	Reccomandations	Approval date
Fluzeon (Enfuvurtide) Hoffmann-La Roche & Trimeris				13 Mar 2003

HIV Integrase Strand Transfer Inhibitor				
Brand name (drugs)	Side Effects	Drug Interactions	Reccomandations	Approval date
Isentress (Raltegravir) Merk & Co, Inc.				12 Oct 2007

Entry Inhibitors – CCR5 co-receptor antagonist				
Brand name (drugs)	Side Effects	Drug Interactions	Reccomandations	Approval date
Selzenty (Maraviroc) Pfizer				06 Ago 2007

Table 4. Proprieties of FI, II, and CCR5 antagonist.

Reverse Transcriptase Structure

HIV reverse transcriptase is a multi-functional enzyme which has the enzymatic activities of RNA-dependent DNA polymerase, DNA-dependent DNA polymerase and RNase H. All of the three functions are essential to complete the reverse transcription (for mechanism see Figure 5). The polymerase activity of the HIV RT shares similar feature as most DNA polymerases, however, with a higher affinity to RNA as a template.

HIV-1 RT is a heterodimer, consisting of a p66 subunit with 560 amino acids and a p51 subunit with 440 amino acids. The overall structure of HIV-RT resembles a right hand as shown in Figure 11 here the subdomains of p66 are designated as finger, palm and thumb regions. Besides, there are other subdomains as RNase H and connection. The conserved residues Asp185, Asp186 and Asp110 form the polymerase active site in the palm domain.[36] Although the p51 subunit shares the same sequence as the *N*-terminal of the p66 subunit, the p51 subunit adapts a spatial arrangement totally different from the p66 subunit and the p55 subunit has no catalytic function as the corresponding Asp residues are buried in the structure. It is believed that p51 plays a role in maintaining the overall structure of the RT. The p66 finger and thumb domains are rather flexible and the nucleic acid template and primer are bound in this cleft passing between the fingers and in front of the thumb domain. When dNTP is bound to the complex, the fingers bend towards the palm forming a catalytic pocket.[37]

The NNRTI binding pocket (NNBP) exists only when an inhibitor is bound to the enzyme.[38] Upon binding of an NNRTI to RT, the side chains of Tyr181 and Tyr188, originally pointing to the hydrophobic centre of the pocket, are now pointing towards the direction of the catalytic site. This conformation change creates the NNBP and this pocket can accommodate a space of about 620-720 $Å^3$ which is approximately more than twice of the volume occupied by most of the present NNRTIs. The formation of the new pocket brings about the

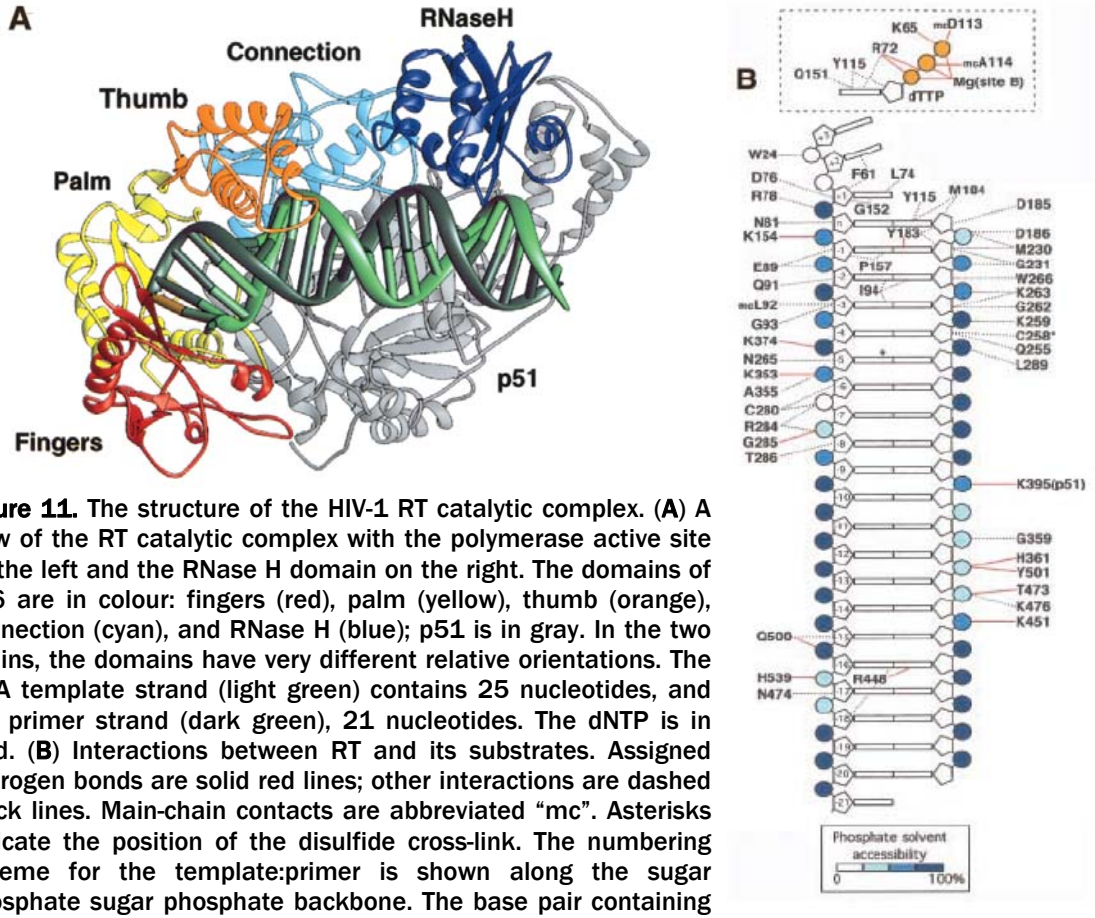

Figure 11. The structure of the HIV-1 RT catalytic complex. (**A**) A view of the RT catalytic complex with the polymerase active site on the left and the RNase H domain on the right. The domains of p66 are in colour: fingers (red), palm (yellow), thumb (orange), connection (cyan), and RNase H (blue); p51 is in gray. In the two chains, the domains have very different relative orientations. The DNA template strand (light green) contains 25 nucleotides, and the primer strand (dark green), 21 nucleotides. The dNTP is in gold. (**B**) Interactions between RT and its substrates. Assigned hydrogen bonds are solid red lines; other interactions are dashed black lines. Main-chain contacts are abbreviated "mc". Asterisks indicate the position of the disulfide cross-link. The numbering scheme for the template:primer is shown along the sugar phosphate sugar phosphate backbone. The base pair containing the 39-primer terminus is labelled n. Bases in the 5'-template extension are numbered n+1 to n+3, where n+1 is the templating nucleotide. (Template bases n+4 and n+5 are not ordered in this crystal structure.) Base pairs in the duplex are numbered from n to n-20, and there is a single-base overhang at n-21 at the 39 end of the template strand. Single-letter abbreviations for the amino acid residues are as follows: A, Ala; C, Cys; D, Asp; E, Glu; F, Phe; G, Gly; H, His; I, Ile; K, Lys; L, Leu; M, Met; N, Asn; P, Pro; Q, Gln; R, Arg; S, Ser; T, Thr; V, Val; W, Trp; and Y, Tyr.

dislocation of β-sheets where the catalytic Asp residues sit, leading to a position shift of around 2 Å for the catalytic residues.[39] The mouth for entering the pocket is flanked by Pro225 and Pro236 which are located on flexible chains. The flexibility is crucial for permitting the entrance of the NNRTI and subsequently closing the mouth after the entrance of the NNRTI. The residues in the NNRTI binding pocket contribute at a varied degree to the affinity between the inhibitor and the enzyme. Some interactions are crucial and play an important role in a majority of the NNRTIs. The aromatic residues in RT, like, Tyr181, Tyr188 and Trp229, provide very important hydrophobic π-interactions with π-electron containing components of the inhibitors. The inhibitors are also possible to increase their affinity to the enzyme through van der Waals interactions with various positions in RT. Interactions with Lys101, Lys103 and Glu1138 represent the possibility of catching electrostatic interactions. Many NNRTIs form H-bonds with the enzyme through the side chain as well as backbone amides. Loss of some key interactions will significantly reduce the potency of the inhibitor. For example, Tyr181 plays an important role in interacting with many NNRTIs and the fact that HIV-2 RT has a isoleucine in the 181 position partly explains the reason that many NNRTIs are inactive to HIV-2, although HIV-2 RT shares an similar overall folding as HIV-1 RT.[40] Three mechanism hypotheses for the inhibition of HIV-1 RT by NNRTIs have been suggested and none of them should be regarded as mutually exclusive. In fact, the nature of a particular inhibitor may dictate which mechanism is dominant. The first mechanism suggests a disposition of the catalytic Asp residues. It has been shown by kinetic studies that a NNRTI present in RT has a relatively small effect on the dNTP binding with an overall affinity reduction of around 10 fold. Meanwhile the affinity of the primer/template duplex to the enzyme is increased. Hence, the major effect of the inhibition is believed from the blocking of the chemical step, which was confirmed by the analysis of the pre-steady state burst of the DNA polymerization. The structural studies of the NNRTI bound enzyme clearly showed the disposition of the catalytic residue, which can partly explain the blockage or low efficiency of the nucleotide

transfer reaction. The second mechanism suggests a hindrance of the cooperative motion of the thumb/finger subdomains. The binding of the NNRTI can also cause a long range distortion of the RT structure. It was found that the p66 thumb subdomain is rotated by 40° relative to the finger domains compared to their relation in the NNRTI unbound enzyme. Associated with the hinge movement of the thumb, p66 connection and RNase H subdomains are also distorted from the normal position in unbound enzyme. A dynamic study of RT suggested that the NNRTI binding not suppress the mobility of the finger, thumb and palm subdomains, but it will interfere with the global hinge-bending movement that controls the cooperative motion of the subdomains.[41] The last mechanism suggestion is rather speculative, addressing the effect the NNRTI binding has on the interaction between the two subunits p66 and p51. The change of the dissociation free energy of the RT heterodimer has been observed when binding with a NNRTI, which may has an impact on the modulating of the enzymatic function, since the heterodimeric structure is essential for the RT activity.[42]

Reverse Transcriptase Inhibitors

The inhibition of HIV-1 RT is regarded as one of the most attractive targets in the chemotherapy against HIV/AIDS due to its essential role in the viral replication and NNRTIs have been proven to be important components in HIV/AIDS combination therapy, because at their efficacy is associate a low toxicity. Today four NNRTIs have been licensed for clinical use, namely nevirapine, efavirenz, delavirdine and etravirine and many structural classes are being explored.

Nevirapine. Nevirapine (Viramune®) was developed and launched by Boehringer Ingelheim for the treatment of HIV infection.[43] As the first NNRTI to be introduced into HIV treatment, it dramatically changed the strategy of HIV therapy. Nevirapine has since been widely used in the combination therapy for HIV/AIDS in various treatment regimens. It is a relatively potent inhibitor of wild type HIV-1 and has low inhibitory effect on cellular polymerases and is non cytotoxic up to a very high concentration (CC_{50} = 321000 nM). Nevirapine shows a strong synergistic effect in combination with NRTIs, hence being widely used in the combination therapy with anti-HIV nucleoside analogues. For examples, in the plague assays the IC_{50} value for AZT is 10 nM, and for nevirapine 32 nM. In the combination experiment, 50% inhibition was achieved with 0.3 nM AZT and 10nM nevirapine giving a combination index of 0.24, which indicates a strong synergistic effect.[44]

Nevirapine SAR has been extensively studied and are summarized Figure 12. Nevirapine adopts a butterfly-like conformation which is commonly seen with many NNRTIs. The molecule is fold such that the angle of the two pyridine rings is about 120°. Due to the electron delocalization, the amide bond moiety in the 7-membered ring adopts an almost planar conformation. The cyclopropyl substituent points up and away from the tricyclic system. One of the pyridine keeps a strong π-stacking with Y181, Y188 and W229, while the other has

interactions with K101, K103, V106, V179, Y318, and even possibly with the main chain atoms of H235 and P236.

Nevirapine is a relatively safe drug; the very low genetic barrier seen with nevirapine has had a great impact on the clinical use of nevirapine and is a driving force in the search of new NNRTIs. It was noticed very early that the rate of resistance development was very fast upon monotherapy with nevirapine.[45] The resistance development is still an debated issue as nevirapine is used in Africa for the prevention of HIV from mothers to infants and in a recent publication these aspects have been discussed and it was concluded that resistance after single-dose nevirapine occurs more readily than previously thought. [46]

Delavirdine. Delavirdine (Rescriptor®) was originally developed by Upjohn and launched by Pharmacia&Upjohn for the combination therapy against HIV infection.[47] The compound is now marketed by Pfizer. Delavirdine has a good activity against HIV-RT with an extremely low cytotoxicity (Selectivity Index (SI) > 10000). However, the substance loses substantially its potency against resistant strains with single mutations such Y181C, K103N, which are commonly seen with NNRTI treatment, as well as P236L which is specific for delavirdine. SAR of delavirdine has been thoroughly studied (Figure 13).[48]

Delavirdine occupies the same NNRTI binding pocket as other NNRTIs however with a very different binding mode as delavirdine is bulkier than the other NNRTI with a volume of about 380 $Å^3$ opposed to 230- 290 $Å^3$ for the others.

The compound has also an overall shape which differs dramatically from other NNRTIs. The complex between delavirdine and RT is stabilized in a unique way; when bond, delavirdine extends beyond the usual pocket and projects into the solvent.[49] The delavirdine binding pocket is connected to the solvent through a channel between well-ordered β-sheets and a highly mobile flap, and the entry of delavirdine is by means of this channel. Delavirdine also interacts with regions of NNBP inaccessible to other NNRTIs. Besides, the carbonyl oxygen in the central spacer is H-bonded to the main chain of K103.

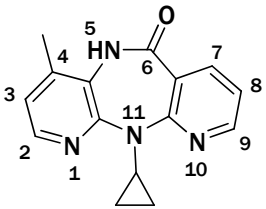

Nevirapine

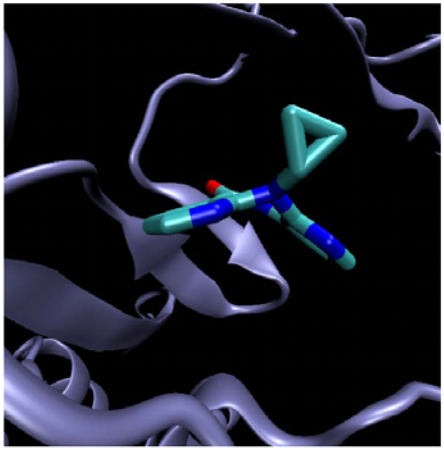

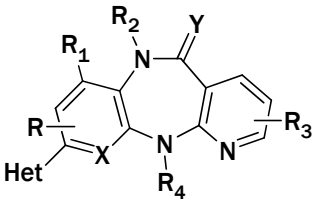

X: CH < N; CH derivatives are quickly metabolized than Nevirapine (N11 dealkylation)

Het: heterocycles in this position give good potency

R = position 2 limited effect on the activity position 3 is unfavorited

R_1 = methyl group give a good potency

R_2 = Increasing sustituent size will reduce the activity

Y = S < O; S derivatives have less metabolic stability

R_3 = Substituent in position 7, 8, 9 affect the potency negatively

R_4 = Et, Pr, cyPr = good activity
H, hydrophilic or electron-withdrawing groups diminuishpotency

Figure 12. Nevirapine SAR studies.

Delavirdine treatment can develop resistance quite rapidly and the compound loses substantially the efficacy against mutant strains of HIV virus. With relatively high and inconvenient dose regimens involving 400 mg/3 times a day, relatively low potency and an unfavourable resistance profile, the compound is not as widely clinically used as the other two launched NNRTIs.

Efavirenz. Efavirenz (Sustiva®) was developed by DuPont and later by BMS for the treatment of HIV infection in combination with other anti-HIV agents.[50] The product was first approved by FDA in 1998 for use in the triple combinations as an alternative to protease inhibitors. Due to the high potency against wild type and some mutant strains, the compound is regarded as the leading prescribed NNRTI as a safe and efficacious component of early HAART regimens. Efavirenz is a highly potent inhibitor of HIV RT and is not cytotoxic and has a CC_{50} of about 80 μM (SI = 80000). Despite with certain loss, it maintains good activities against many single mutants commonly occurred in HIV therapy such as the L100I, K101E, V106A, V179D and Y181C. However, it loses potency against double or triple mutants (for example K101D+K103N, L100I+K101D, K103N+Y181C and L100I+K103N). Efavirenz was found as the result of the optimization work as show in Figure 14.[79]

Similar to most NNRTIs, efavirenz binds to RT through strong hydrophobic interactions.[51] The cyclopropylpropynyl group points to a sub-pocket surrounded by aromatic side chains of Y181, Y188, W229 and F227, where the left pyridine ring of nevirapine binds. The benzoxazinone ring is situated between the side chains of L100 and V106 in a sandwich shape. The edge of the benzoxazinone has contact with the residues Y318 and V179. A prominent non hydrophobic contact is the H-bonding formed between the NH in benzoxazinone and the main chain carbonyl oxygen of K101. The interaction of efavirenz with the mutant RT has been a subject of great interest and the structural information shed some light to the understanding of the mechanism of the efavirenz resistance. K103N is one of the major mutations efavirenz and other NNRTIs encounter. The structure of efavirenz with K103N mutant clearly shows that the mutation causes a significant conformational change within the

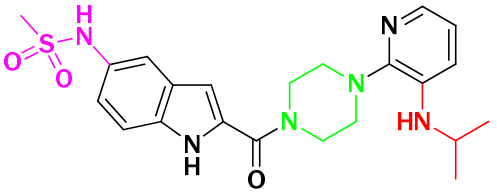

Delavirdine

The *i*-Pr substituent is important, but not essential.

Pyperidine nucleous increased the activity against wilde type and mutant HIV strains

The substituent at 5 position give a good metabolic stability and relatively good potency

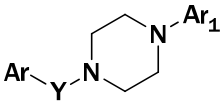

Y = CH_2, C=O; for a good activity

Ar = Indole ring give more active compounds with a less inhibitory effect to the cellular DNA polimerase

Ar_1 = Ph or substitued Ph give inactive compounds. Pyrimidine replacement will destroy the potency.

Figure 13. Delavirdine SAR studies.

binding pocket. The bigger asparagine side chain pushes efavirenz deeper into the pocket, which in turn forces the side chain of Y181 flip to opposite direction and its OH is displaced for more than 8 Å. This affects the position of E1138 and K101. The displacement of efavirenz itself is about 0.5 Å for the carbonyl oxygen and 0.7 Å for the cyclopropyl group, which is sufficient to alter some contacts between efavirenz and the enzyme. However, efavirenz loses the activity against single mutants much less than nevirapine in general. A hypothesis is forwarded from the structural study to explain the phenomenon. The overall size of efavirenz in relation to its binding size may determine its ability to adapt a mutation. A smaller inhibitor can reposition itself within the pocket whereas nevirapine's bulky ring system remains relatively rigid and no such repositioning is possible.[52]

Etravirine.[53] Etravirine (Intelence, Tibotec) is a potent second-generation NNRTIs with broad *in vitro* activity against HIV-1.

Etravirine binds to the reverse transcriptase enzyme via a horseshoe-shaped configuration with 2 "wings" capable of rotating to optimize binding. This structure allows for multiple binding conformations and may explain etravirine's potent activity against NNRTIs-resistant strains. The 50% effective concentration for etravirine against wild type HIV-1 is in the nanomolar range (1.4-4.8 nM), which is similar to that of efavirenz (1.0-3.4 nM). The majority of etravirine trials have focused on patients with NNRTI-resistant HIV-1 infections; however, etravirine has also been evaluated as a treatment for patients with wild type HIV-1 infections. In a parallel screening study involving wild-type and NNRTI-resistant HIV-1 strains, etravirine was demonstrated to inhibit 98% of all samples and 97% of NNRTI resistant strains with an EC_{50} <100 nM. The investigators concluded that etravirine has a high genetic barrier to resistance with excellent activity against NNRTI-resistant viral strains, making this agent a potential alternative treatment in patients who have developed resistance to either NNRTIs. Based on the results of clinical trials, multiple mutations in the reverse transcriptase enzyme are required for the virus to become resistant to etravirine.

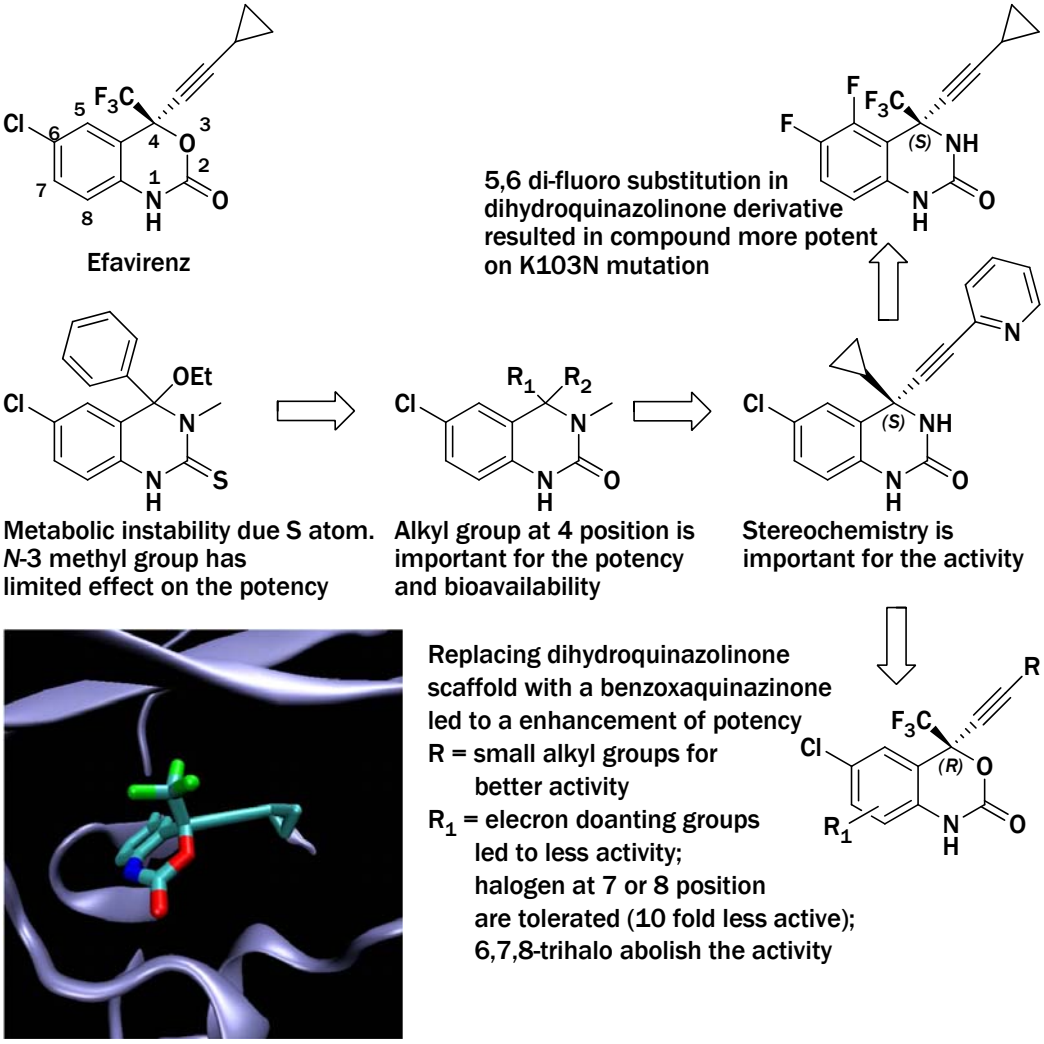

Figure 14. Efavirenz optimization.

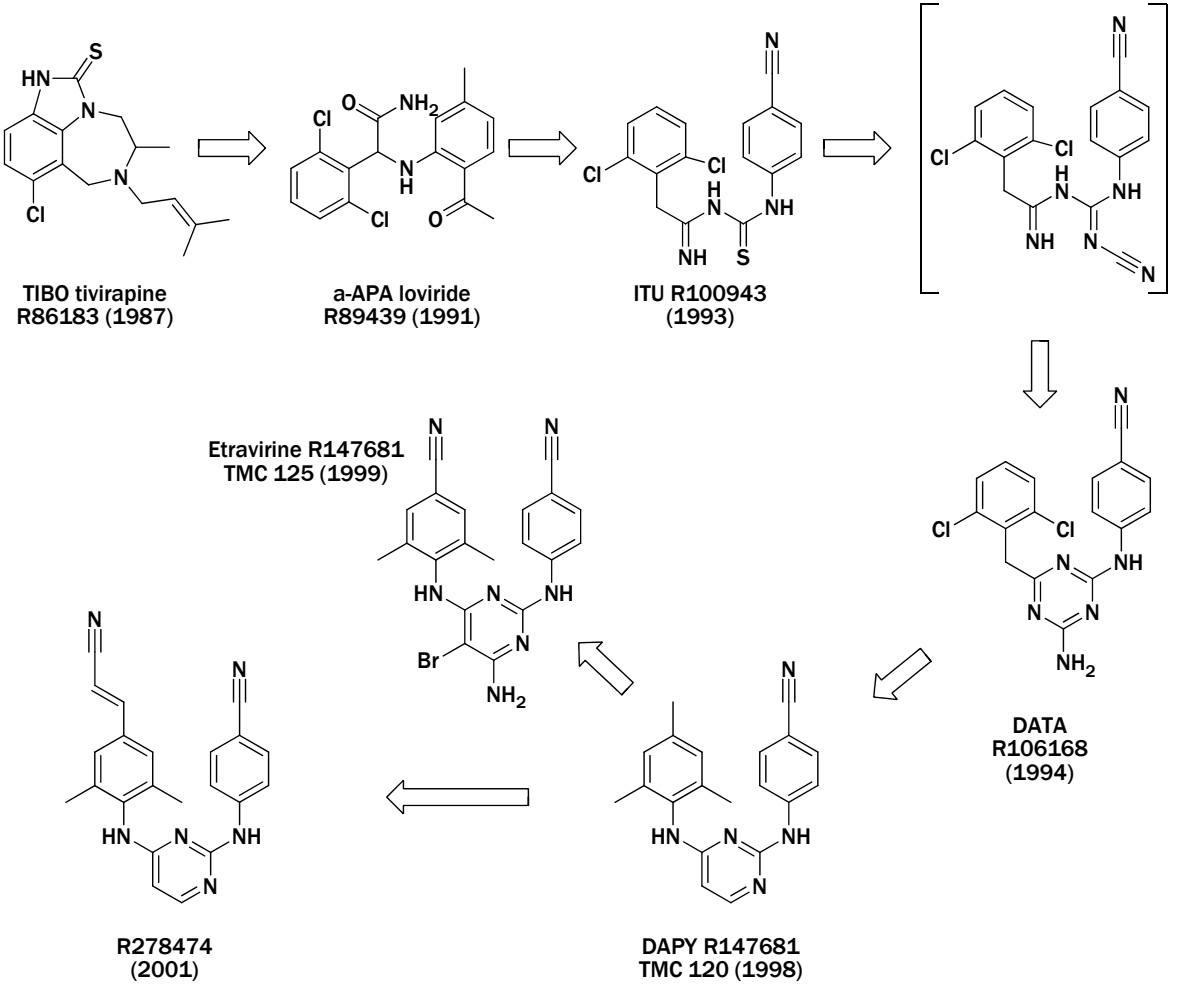

Figure 15. Chemical evolution from TIBO to Etravirine and R278474 (Rilpivirine).[54]

Indolyl Aryl Sulfones

In the 1993, Merck Research Laboratories reported the synthesis and the activity of 5-chloro-3-(benzenesulfonyl)indole-2-carboxyamide (**1** (L-737,126) Figure 16), a novel potent and selective RT inhibitor.[55] Taking into account our know-how in the pyrrole containing chemotherapeutic agents, we designed pyrryl aryl sulfones (PAS) (**2-5**, Figure 16).[56] By intramolecular cyclization of PASs were obtained pyrrolo[1,2-b][1,2,5]benzothiadiazepines (PBTDs) (**6-8**, Figure 16),[57] a novel class of NNRTIs structurally related to nevirapine. Both classes have as common feature the *para*chloroniline moiety.

The lack of SAR investigations on anti-HIV-1 indolyl aryl sulfones (IASs) motivated our laboratory to address further research towards discovery of novel indole sulfones related to the potent Merck derivative **1**. First we used SARs taken from the already described PAS family in order to plan the synthesis of novel IASs: (i) by replacing the phenyl ring of **1** with the *para*-chloroanilino pharmacophore; (ii) by shifting the benzenesulfonyl moiety of **1** from position 3 to position 1 of the indole ring; (iii) by modifying the carboxyamide side-chain and changing its position from C2 to C3.[58] In general 1-benzenesulfonylindoles were totally devoid of anti-HIV-1 activity. Indoles **9-12** characterized by the presence of carboxyethyl or carboxyamide groups at position 3 of indole, were totally inactive. 3-benzenesulfonyl indoles carrying a carbethoxy group at positon 2 of indole proved weakly active (data not shown). Substitution of the ester group of the last compounds with a carboxyamide function led to a very significant increase of both potency and selectivity (**13-16**).

Introduction of methyl groups in the phenyl ring of benzenesulfonyl moiety led to derivatives as potent as **1** (see compounds **17-19**), but much less cytotoxic with consequent increasing of selectivity; on the contrary, 2,4- and 3,5-dimethyl derivatives **20** and **21**, although endowed with high potency, were more cytotoxic than the related mono-methyl derivatives.

When tested against a panel of HIV-1 strains carrying clinically relevant

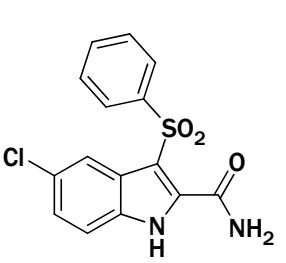

1, (L737,126)
EC_{50} = 0.001*

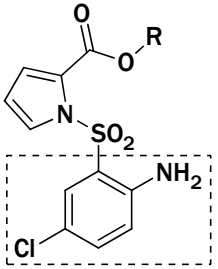

Amino-PASs	EC_{50}*
2 R = CH_3	0.18
3 R = C_2H_5	0.14
4 R = *n*-C_3H_7	0.22
5 R = *iso*-C_3H_7	0.14

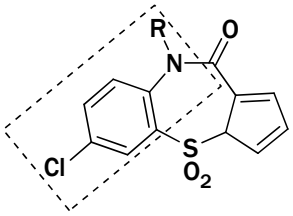

PBTDs	EC_{50}*
6 R = H	1.0
7 R = CH_3	0.5
8 R = C_2H_5	2.4

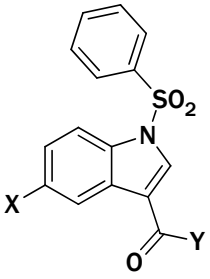

		EC_{50}*
9 X = H;	Y = OC_2H_5	> 32
10 X = H;	Y = NH_2	> 32
11 X = Cl;	Y = OC_2H_5	> 42
12 X = Cl;	Y = NH_2	66

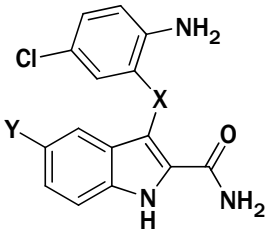

		EC_{50}*
13 X = S;	Y = H	9
14 X = SO_2;	Y = H	0.5
15 X = S;	Y = Cl	1.6
16 X = SO_2;	Y = Cl	0.04

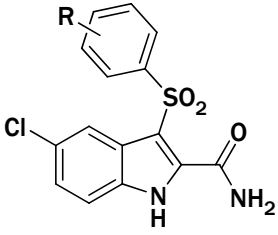

	EC_{50}*	CC_{50}*
17 R = 2-CH_3	0.001	> 100
18 R = 3-CH_3	0.001	> 100
19 R = 4-CH_3	0.003	> 100
20 R = 2,4-$(CH_3)_2$	0.004	37
21 R = 3,5-$(CH_3)_2$	0.004	15

*All values are reported as μM concentration

Figure 16. Structure and anti-HIV activity (EC_{50}) of compounds **1-21**. For compounds 17-21 are reported also cytotoxic concentration (CC_{50}). All values are reported as μM concentration.

NNRTI resistance mutations, monomethyl derivatives **17**-**19** were inhibitory to the Y181C mutant at submicromolar concentrations (Table 5). However, these compounds were less effective against the K103N-Y181C double mutant and the EFV^R (K103R-V179D-P225H) triple mutant highly resistant to efavirenz. In fact, the *meta* derivative (**18**) showed high inhibitory activity against Y181C mutant, appreciable activity against EFV^R, and moderately inhibited the double mutant K103N-Y181C, whereas the *para* (**19**) and *ortho* (**17**) analogues were clearly less active against these mutants. A high inhibitory activity against Y181C, K103N-Y181C and EFV^R mutants was exhibited by the 3,5-Me_2 derivative **21**, which proved 10-fold more potent than **1** against the two HIV-1 strains carrying mutations at 103 position of the RT gene. When compared to efavirenz, **21** turned out to be a 4-fold less efficient inhibitor of the double mutant K103-Y181C, but a 22-fold better inhibitor of the triple mutant K103R-V179D-P225H. A determinant structural requirement for a potent activity against mutant strains was the 3,5-Me_2 substitution on the phenyl ring. In fact, compound **21** turned out as active as **1** and efavirenz against WT HIV-1 RT and Y181C mutant, about 10- and 20- fold more potent against EFV^R than **1** and efavirenz, and about 10-fold more potent than **1** and only 4-times less potent than efavirenz against the double mutant K103N-Y181C.

Subsequently we studied the importance of substituent at 5 position of indole nucleus. Replacement of 5-chloro with 5-bromo in the 3,5-dimethylbenzenesulfonyl series did not alter potency and selectivity. We also synthesized novel IAS derivatives with a nitro group at position 5 of the indole ring. 5-nitro-IASs were highly active against wild-type HIV-1 at nanomolar concentrations with low cytotoxicity. When tested against resistant mutants, all nitroderivatives showed antiviral activities at submicromolar concentrations against both Y181C and EFV^R mutant strains. Continuing our efforts to develop IASs with improved activity against the viral mutants, we planned the synthesis of new derivatives **22**-**33** bearing two halogen atoms at the indole ring. Cytotoxicity (TC_{50}) and antiretroviral activity (ED_{50}) of these compounds were evaluated against the HIV-1 WT (Figure 17) and NNRTI-resistant strains Y181C

and K103N-Y181C. IASs **1** and **21**, NVP, and EFV were used as reference compounds. The compounds obtained by the introduction of a second halogen atom at indole nucleus (dihalo-IASs) were generally highly active against the HIV-1 WT and not cytotoxic up to 20000 nM. The ED_{50} ranged from 0.5 nM (**32** in MT-4 cells) to 100 nM (**22** in C8166 cells), and selectivity indexes (TC_{50}/ED_{50} ratio) (SI) ranged from >40000 (**32** in MT-4 cells) to >200 (**22** in C8166 cells). As a rule, derivatives bearing two halogen atoms at positions 4 and 5 of the indole and the 3-(3,5-dimethylphenyl)sulfonyl moiety were more potent than the corresponding 5,6- or 5,7-dihalo-IAS counterparts in both cell lines. The 4,5-difluoro-IAS (**26**) and 5-chloro-4-fluoro-IAS (**32**) (ED_{50}) 1 and 0.5 nM, respectively, in MT-4 cells) were the most potent and selective HIV-1 WT inhibitors within the series.

The 4,5-dihaloindole was an optimal substitution pattern for the antiviral activity of IASs. The antiviral potency was particularly correlated to the presence of the fluorine atom at position 4.

Against the Y181C mutant strain, derivatives IASs **22** and **33** were as active as the reference compounds **1** and **21**. The most potent derivative **32** (ED_{50}) 4 nM) was as active as EFV in inhibiting the Y181C mutant strain (Table 6). Compounds **26** (ED_{50} = 1200 nM) and **32** (ED_{50} = 300 nM) effectively inhibited the K103N-Y181C double-mutant strain, which is highly resistant to NVP. Against this strain, **32** was as active as EFV and >667-fold more active than NVP. The most potent derivatives **26** and **32** were evaluated in lymphocytes against HIV-1 WT (IIIB) and primary isolates HIV-112 and HIV-AB1 obtained from two HIV-1-Ab seropositive individuals who had experienced therapeutic failure after treatment with HAART regimens (Table 7). The 112 strain was selected after treatment with NRTIs and NNRTIs and carried mutations at K103N-V108I-M184V positions that showed >99% resistance to NVP and EFV. The AB1 strain was selected after treatment with NRTIs, NNRTIs, and at least one PI and carried L100I-V108I mutations that were >90% and >85% resistant to NVP and EFV, respectively. Compounds **26** and **32** inhibited the 112 and the AB1 strains in lymphocytes and the multiplication of the

Table 5. Activity of compounds **1**, **17**-**21** against clinically relevant HIV-1 mutant strains.

	EC_{50}[b] (μM)			EFV^R
Compd	Wt-III_B	Y181C	K103N-Y181C	EC_{90}[c] (μM)
17	0.001	0.16	10	2.6
18	0.001	0.006	7	0.26
19	0.003	0.02	> 100	93
20	0.004	0.15	10	5.3
21	0.004	0.03	0.65	0.08
1	0.001	0.02	8	0.9
EFV[d]	0.004	0.025	0.15	1.8

[a]Data represent mean values for three separate experiments. [b]Compound concentration (μM) required to achieve 50% protection of MT-4 cells from the indicated strain HIV-1 induced cytopathogenicity as determined by the MTT method. [c]Compound concentration (μM) required to reduce the amount of p24 by 90% in C8166 cells infected with an efavirenz resistant strain carrying mutations K103R, V179D and P225H. [d]EFV, efavirenz.

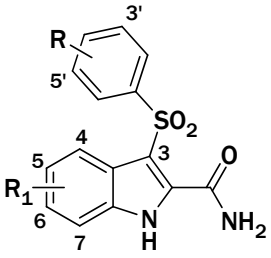

Cmpd			ED_{50} (nM) MT-4	ED_{50} (nM) C8166	TC_{50} (nM) MT-4
22	R = H	R_1 = 5,6-Cl_2	80	100	>20000
23	R = 3',5'-Me_2	R_1 = 5,6-Cl_2	10	15	>20000
24	R = 3',5'-Me_2	R_1 = 5,7-Cl_2	21	12	>20000
25	R = H	R_1 = 4,5-F_2	8	10	>20000
26	R = 3',5'-Me_2	R_1 = 4,5-F_2	1	3	>20000
27	R = H	R_1 = 5,6-F_2	16	20	>20000
28	R = 3',5'-Me_2	R_1 = 5,6-F_2	20	30	>20000
29	R = 3',5'-Me_2	R_1 = 5,7-F_2	7	25	>20000
30	R = H	R_1 = 4-Cl,5-F	8	9	>20000
31	R = 3',5'-Me_2	R_1 = 6-Cl,5-F	50	50	18000
32	R = 3',5'-Me_2	R_1 = 5-Cl,4-F	0.5	0.8	>20000
33	R = H	R_1 = 4-Cl,6-F	12	10	>20000
1	R = H	R_1 = 5-Cl	2	3	>20000
21	R = 3',5'-Me_2	R_1 = 5-Cl	6	10	12000

Figure 17. Structure of dihalo IASs.

IIIBBa-L strain in macrophages at nanomolar concentrations. Derivatives **26** and **32** were tested against RT WT and RTs containing the K103N, Y181I, and L100I single amino acid mutations responsible for resistance to NNRTIs (Table 8). Against RT WT, **26** and **32** were more potent than NVP (235 and 133 times, respectively) and EFV (47 and 27 times, respectively). Compound **32** proved to be an exceptionally potent inhibitor of the RTs carrying the K103N, Y181I, and L199I mutations (K103N, 1167 and >3333 times more potent than NVP and EVF, respectively; Y181I, >690 and 14 times more potent than NVP and EVF, respectively; L100I, 4500 times more potent than NVP). The recombinant HIV-1 RT carrying the Y181I mutation was absolutely comparable to the Y181C substitution in terms of drug resistance, as we previously characterized in our laboratory from an enzymological point of view.

Table 6. Antiviral Activity of IASs **22**-**33** and Reference Compounds **1**, **21**, NVP, and EFV against the HIV-1 WT (IIIB) and the Y181C and the K103N-Y181C Resistant Strains in MT-4 Cells.[a]

	ED_{50}[b] (nM)		
Compd	wt-III_B	Y181C	K103N-Y181C
22	80	1700	> 20000
23	10	1000	> 20000
24	21	4200	> 20000
25	8	600	18000
26	1	50	1200
27	16	8200	> 20000
28	20	400	> 20000
29	7	1500	> 20000
30	8	2200	> 20000
31	50	700	12000
32	0.5	4	300
33	12	50	> 20000
1	2	30	10000
21	6	50	800
NVP	50	14000	> 20000
EFV	3	10	200

[a]Data are mean values of two experiments performed in triplicate. [b]Compound concentration (nM) required to achieve 50% protection of MT-4 cells from HIV-1 WT (IIIB), Y181C, and K103N-Y181C resistant strains cytopathogenicity as monitored by MTT method.

Table 7. Activities of Derivatives **26** and **32** and Reference Compounds **1**, **21**, **NVP**, and **EFV** against the HIV-1 WT (IIIB) and the Primary Isolates HIV-112 and HIV-AB1 in Lymphocytes.[a]

		ED_{50}[b] (nM)			Si[c]		
Compd	TC_{50} (nM)	IIIB	112	AB1	IIIB	112	AB1
26	>20000	20	130	84	>1000	>154	>238
32	>20000	8	10	12	>2500	>2000	>1667
1	>20000	160	2300	2500	>125	>9	>8
21	18000	200	300	220	90	60	82
NVP	>20000	90	>20000	>20000	>222		
EFV	>20000	7	>20000	>20000	>2857		

[a]Data are mean values of two experiments performed in triplicate. [b]Compound concentration (nM) required to reduce the amount of p24 by 50% in the indicated strain. HIV-p24 antigen production in control HIV-1 infected lymphocytes was 118 900 and 247 200 pg/mL in HIV-112 and HIV-AB1 infected lymphocytes, respectively. [c]Selectivity index: TC_{50}/ ED_{50} ratio.

Table 8. Activities of Derivatives **26** and **32** and Reference Compounds **1** and **21** against the HIV-1 WT (IIIBBa-L) in Macrophages[a] and against the WT and Mutant Enzymes Carrying Single Amino Acid Substitutions.[b]

			ID_{50}[e] (nM)			
Compd	ED_{50}[c] (nM)	Si[d]	Wt	K103N	Y181I	L100I
26	23	>870	1.7	1000	2050	90
32	10	>2000	3	6	29	2
1	2000	>10	400	7000	>20000	9000
21	115	174	80	>20000	400	nd[f]

[a]Data are mean values of two experiments performed in triplicate. [b]Data represent mean values of at least three separate experiments. [c]Compound concentration (nM) required to reduce the amount of p24 by 50% in the indicated strain. HIV-p24 antigen production in control HIV-1 infected lymphocytes was 118 900 and 247 200 pg/mL in HIV-112 and HIV-AB1 infected lymphocytes, respectively. [d]Selectivity index: TC_{50}/ ED_{50} ratio.[e]Compound dose (*K*i, nM) required to inhibit by 50% the RT activity of the indicated strain. [f] nd, no data.

Aim of the Work

The obtained results from IASs **9-33** are enough to make some study of structure-analysis relationship. By the analysis of results of compounds **9-12** is obvious that the carboxyamide derivatives are more potent than correspondent esters. Comparing the activity of compounds **14** and **16** with **13** and **15**, respectively, it is evident as the sulfonyl derivatives are more active than corresponding sulfur against wild-type HIV-1. The introduction of two methyl groups at position 3 and 5 of phenyl ring gave compounds with more cytotoxicity, but they retained the antiviral-activity against clinically relevant HIV-1 mutant strains as Y181C single mutant and Y181C-K103N double mutant strains, and in particularly against EFV^R mutant highly resistant at the treatment with nevirapine and efavirenz. The substitution of chorine atom at 5 position of indole nucleus with bromine or nitro groups gave compound with a good activity associated with a low cytotoxicity; moreover the nitroderivatives are active at submicromolar concentration against HIV-1 mutant strains. The introduction of second halogen at indole nucleus gave compounds with inhibitory activity of HIV-1 wild-type reproduction at nanomolar and submicromolar concentrations. Particularly, the introduction of a fluorine atom at position 4 of indole nucleus of **21** (4-fluoro, 5-chloro substitution) gave compound **32** that was active against HIV-1 wild-type at subnanomolar concentration, and active against HIV-1 mutant strains at nanomolar concentration and it was more potent than reference compounds in cellular and enzymatic assays.

On these results, we design new indolyl aryl sulfones to investigate the role of the carboxyamide function introducing different groups at carboxyamide function at position 2 of indole ring. Already was reported IASs carrying amino acids (mono-, di-, tripeptide derivatives) at this carboxyamide function with a good anti-HIV activity. We planned to prepare different IASs bearing different

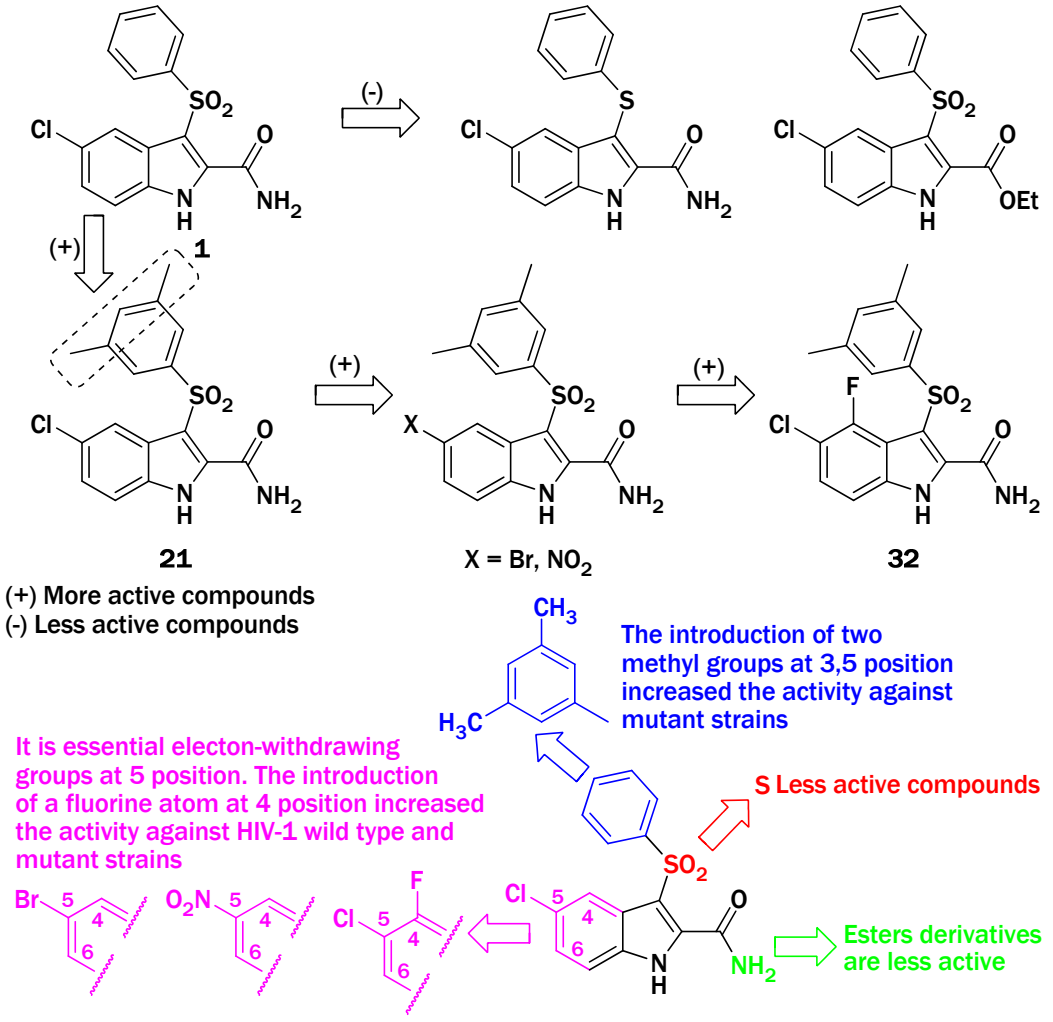

Figure 18. Development of IASs and structure-activity relationship study.

amino acids unit (Figure 19). They consist in natural and unnatural amino acids, branched and not including taurinamide and β-methyltaurinamide.

Moreover we prepared and evaluated many different amide derivatives with heterocyclic groups bond at nitrogen amide atom by a different length linker (Figure 20).

All new synthesized IASs are characterized by the presence of (3,5-dimethylphenyl)sulfonyl groups at position 3 of indole nucleus, while it was substituted at position 5 with the chlorine and bromine atoms, nitro groups; moreover was prepared derivatives of **32** characterized by 4-fluoro-5-chloroindole scaffold.

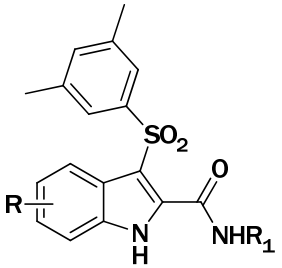

34-57

Compd	R	R_1	Compd	R	R_1
34	5-Cl	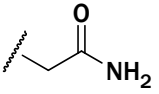	**46**	5-Cl	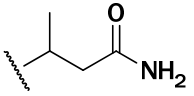
35	5-Br		**47**	5-Br	
36	5-NO_2		**48**	5-NO_2	
37	4-F,5-Cl		**49**	4-F,5-Cl	
38	5-Cl	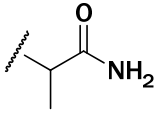	**50**	5-Cl	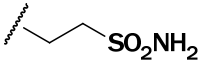
39	5-Br		**51**	5-Br	
40	5-NO_2		**52**	5-NO_2	
41	4-F,5-Cl		**53**	4-F,5-Cl	
42	5-Cl	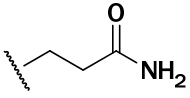	**54**	5-Cl	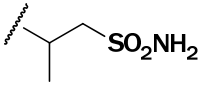
43	5-Br		**55**	5-Br	
44	5-NO_2		**56**	5-NO_2	
45	4-F,5-Cl		**57**	4-F,5-Cl	

Figure 19. New Amino acid IASs derivatives.

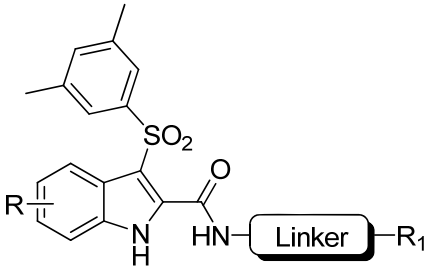

58-93

Compd	R	Linker-R_1
90	5-Cl	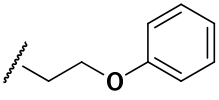
91	5-Br	
92	5-NO_2	
93	4-F-5Cl	

Compd	R	Linker-R_1	Compd	R	Linker-R_1
58	5-Cl	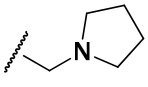	**74**	5-Cl	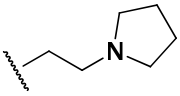
59	5-Br		**75**	5-Br	
60	5-NO_2		**76**	5-NO_2	
61	4-F,5-Cl		**77**	4-F,5-Cl	
62	5-Cl	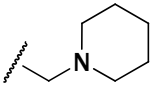	**78**	5-Cl	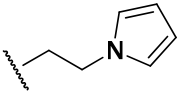
63	5-Br		**79**	5-Br	
64	5-NO_2		**80**	5-NO_2	
65	4-F,5-Cl		**81**	4-F,5-Cl	
66	5-Cl	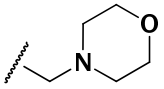	**82**	5-Cl	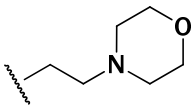
67	5-Br		**83**	5-Br	
68	5-NO_2		**84**	5-NO_2	
69	4-F,5-Cl		**85**	4-F,5-Cl	
70	5-Cl	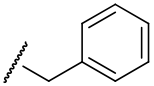	**86**	5-Cl	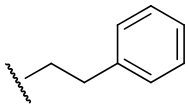
71	5-Br		**87**	5-Br	
72	5-NO_2		**88**	5-NO_2	
73	4-F,5-Cl		**89**	4-F,5-Cl	

Figure 20. New Mannich/Amides IASs derivatives.

Chemistry

A general pathway for preparation of described compounds is showed in Scheme 1. The 3-arylsulfonyl derivatives (**b**) were prepared from the appropriate indoles (**a**), and then, the ester function was converted in amide to give the final desired compounds.

For the preparation of amino acid derivatives, ester (**b**) hydrolysis gave the correspondent acids that were reacted with appropriate ester amino acid using BOP as coupling agents. The menaced esters (**e**) were converted in the desired compounds (**g**) by treatment with ammonium hydroxide. Other amide derivatives (**d**) may be prepared by reaction between correspondent acids and amine or by direct microwave assisted reaction between ester and amine. Finally, the derivatives **f** were prepared by Mannich reaction between amide **3**, formaldehyde and appropriate amine.

The ethyl 5-chloro-1*H*-indole-2-carboxylate and ethyl 5-nitro-1*H*-indole-2-carboxylate were commercially available, while ethyl 5-bromo-1*H*-indole-2-carboxylate and ethyl 5-chloro-4-fluoro-1*H*-indole-2-carboxylare were synthesized.

Fore the preparation of ethyl 5-bromo-1*H*-indole-2-carboxylate was used the Fischer indole synthesis strategy (Scheme 2). Reaction between commercially available 4-bromophenyl hydrazine hydrochloride (**94**) and ethyl pyruvate in ethanol at reflux temperature gave hydrazone **95** that was converted in the desired indole (**96**) by the treatment with hot polyphosphoric acid. This synthetic pathway is very simple, and the both reactions have a good yield. The same procedure was used for the preparation of indole **105**.

For this purpose was prepared hydrazono **103** using two different pathways (Scheme 3). The former strategy consist in the protection of 3-fluroaniline (**97**) as pivalamide (**98**) that was chlorinated with *N*-chlorosuccinimide (NCS) (**99**) and then deprotected to give aniline **100** that was converted in hydrazono **103** using Jaap-Kinglemann reaction. This procedure consist in the initial conversion

Scheme 1. General pathways for IASs synthesis.

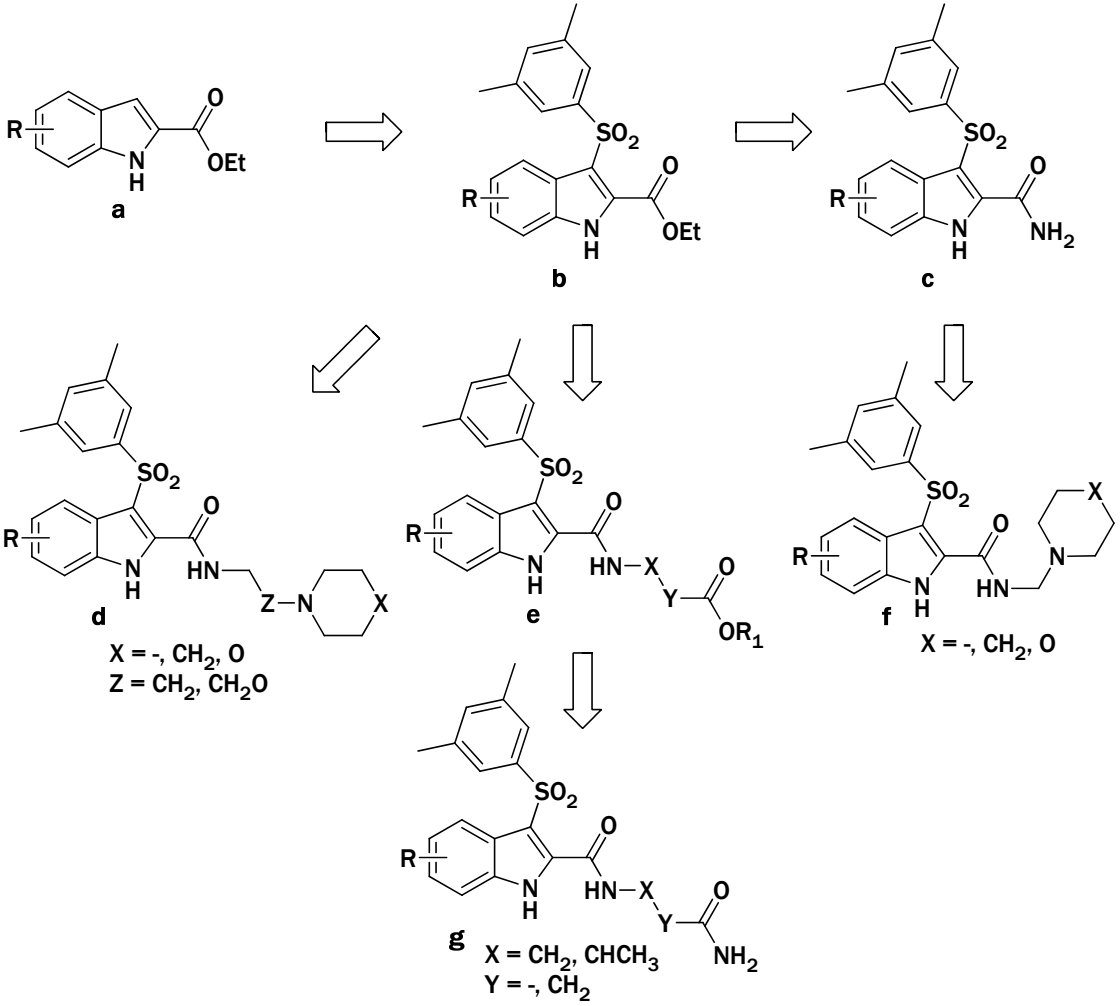

Scheme 2. Synthesis of ethyl 5-bromo-1*H*-indole-2-carboxylate.

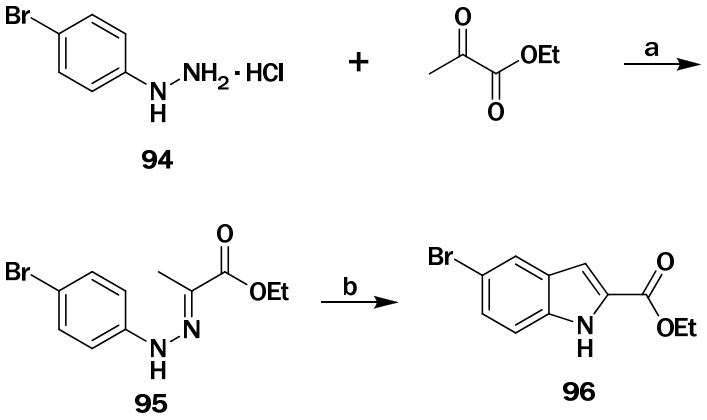

Reagents and Reaction Conditions: a) CH_3COOH, EtOH, reflux, 2 h; b) Polyphosphoric acid, 110 °C, 1 h.

of the aniline in the correspondent diazonium salt, that was coupled with ethyl 2-methylacetoacetate and successive hydrolysis of addition product to give the desired hydrazono **103**.

Alternatively, the reaction between 3-fluorophenylhyrazine hydrochloride **101** and ethyl pyruvate gave hydrazono **102** that was chlorinated with *N*-chlorosuccinimide to give **103**.The chlorination reactions from **98** to **99** and from **102** to **103** were performed in different conditions. Compound **99** was obtained by the treatment of **98** with *N*-chlorosuccinimide in *N*,*N*-dimethylformamide at 80°C for 30 min.; the same conditions for preparation of **103** from **102** gave a mixture of chlorination products. It was performed in the same solvent but at room temperature for overnight to give the desired product with a yield of 60%.

The treatment of **103** with hot polyphosphoric acid gave two indole isomers: ethyl 5-chloro-6-fluoro-1*H*-indole-2-carboxylate (**104**) and ethyl 5-chloro-4-fluoro-1*H*-indole-2-carboxylate (**105**) that could be separated by repeated chromatography columns. Moreover, indole **104** is the major isomer and the best yield for preparation of indole **105** using this pathways is minor than 5%.

Due the low yield and the difficult to separate both isomers, and the its importance because of high anti-HIV potency of **36**, it was necessary to investigate for a more convenient synthesis of this indole.

Different possible pathways were planned, and our aim was to obtain it as single isomer. In a first attempt we converted aniline **106** in amide **107** by the treatment with ethyl oxalyl chloride in the presence of triethylamine. Chlorination of **107** was performed as already describe for the preparation of **99** to obtain **108**. Both attempt used to convert **108** in the indole **105** was unsuccessfully. For this purpose **105** was initially treated with *n*-, *t*-butyl lithium and lithium di-*i*-propylamide, and then it was converted in the correspondent chloro imminium derivative **109** that was treated with sodium ethoxide.

In a second attempt, aniline **106** was protected as *N*-pivalamide (**110**) and then chlorinated with *N*-chlorosuccinimide to give *N*-(4-chloro-3-fluoro-2-

Scheme 3. Synthesis of indole **102** using Fischer indole synthesis strategy.

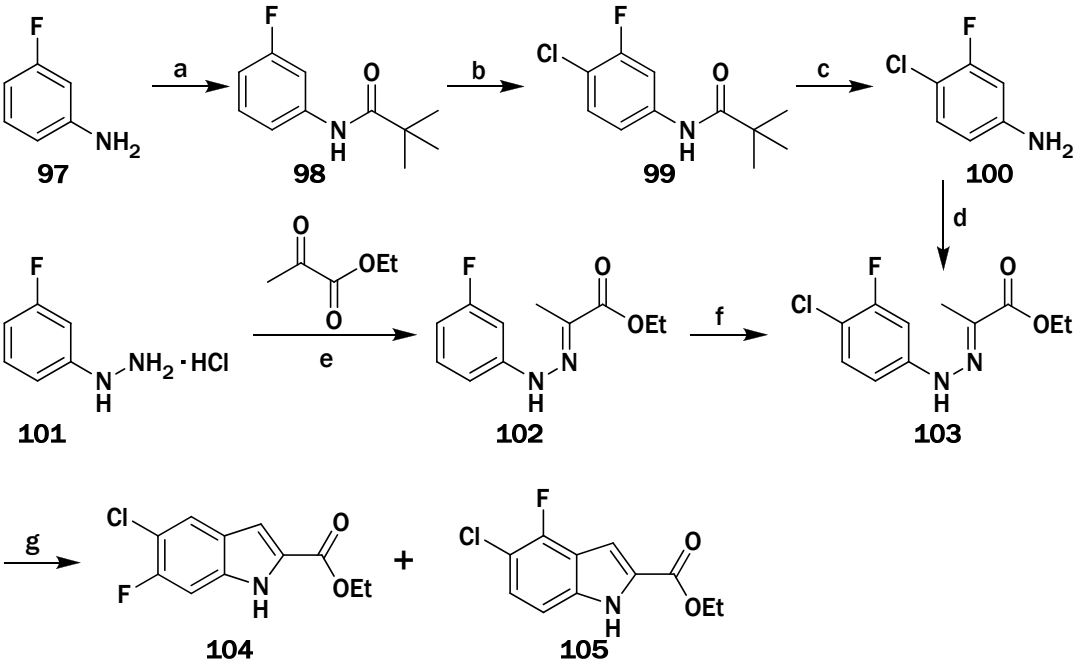

Reagents and Reaction Conditions: a) Pivaloyl chloride, Et_3N, THF, rt, 1h; b) NCS, DMF, 80 °C, 30 min.; c) 6N HCl, dioxane, riflux, overnight, 98%; d) (i) $NaNO_2$, HCl, H_2O-EtOH, 0 °C, 10 min.; (ii) Ethyl 2-methylacetoacetate, CH_3COOK (until pH ~ 5), H_2O-EtOH, 0 °C, 4 h; (iii) EtOH, rt, overnight; e) CH_3COOH, EtOH, reflux, 2 h;; f) NCS, DMF, rt, overnight, 63 %; g) Polyphosphoric acid, 110 °C, 1 h, YIELD.

methylphenyl)pivalamide (**111**). The elongation of methyl group with diethyloxalate in the presence of *n*-butyl lithium from **111** and **112** was

unsuccessful, so we performed acid deprotection of **112** to afforded 4-chloro-3-fluoro-2-methylaniline (**113**) which was oxidized to the corresponding nitro derivative **114** with 3-chloroperoxybenzoic acid (*m*-CPBA); for a good reaction yield it was necessary to use 5 equivalent of *m*-CPBA; the same reaction was performed with hydrogen peroxide with a low yield. Reaction of **114** with diethyl oxalate in the presence of sodium ethoxide gave ethyl 3-(3-chloro-2-fluoro-6-nitrophenyl)-2-oxopropanoate (**115**), that for reduction nitro group with iron powder by heating at 60 °C in acetic acid and subsequent intramolecular cyclization of the intermediate amino derivative provided the indole ester **105** as single isomer (Scheme 5). The latter six-step procedure provided **105** in 37% overall yield starting from the commercially available aniline **106** (the overall yield with the older procedure showed in scheme 3 was only 5%). In addition, it is faster because it avoids tedious repeated chromatographies needed for the separation of the isomers.

The reaction between ethyl indole-2-carboxylate **96**, **105**, **117** and **118** with *N*-(3,5-dimethylphenylthio)succinimide (**116**) in the presence of the borontrifluoride diethyl etherate gave the correspondent ethyl 3-(3,5-dimethylphenyl)thio-indole-2-carboxylate **119-122** (Scheme 6); the reaction was performed in dichloromethane, and it was stirred at room temperature for two hours and at reflux temperature for the same time.

In the case of ethyl 5-nitro-1*H*-indole-2-carboxylate the yield of reaction was only about 53%, with recovery of starting material. To improve the yield, the reaction was performed to varying reaction time, the reactant and reagent ratio and increasing the reaction temperature using chloroform or 1-bromo-3-chloropropane as solvent and performed the reaction using microwaves irradiation. The many attempts were unsuccessfully to improve significantly the yield of reaction, probably due to the degradation of **116** in more drastic conditions.

Scheme 4. First synthetic attempt to prepare **105** as single isomers.

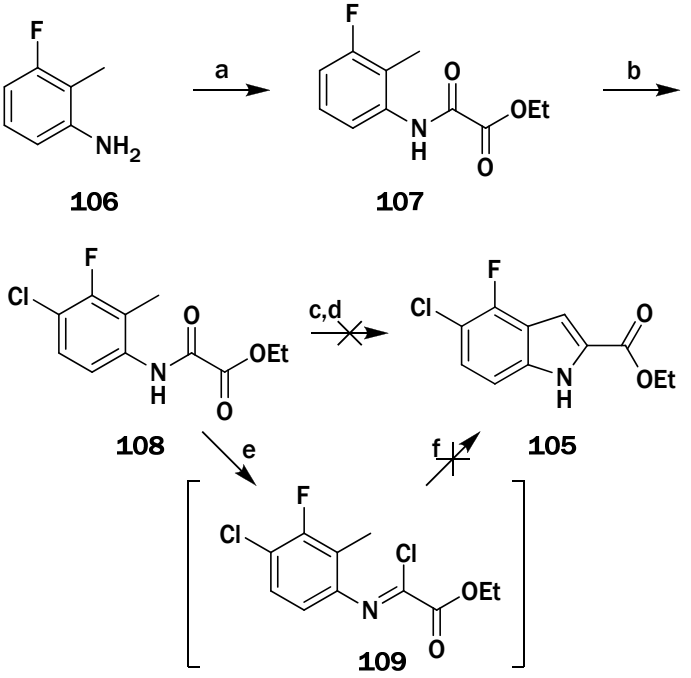

Reagents and Reaction Conditions: a) Ethyl oxalyl chloride, Et_3N, THF, 0 °C, 1h; b) *N*-Chlorosuccinimide, DMF, 80 °C, 45 min.; c) *n*-BuLi (or *t*-BuLi), THF, from -78 °C to rt.; d) *n*-BuLi, *i*-Pr_2NH, THF, -78 °C, than **108**, from -78 °C to rt; e) $SOCl_2$, reflux, 2h; f) EtONa, EtOH, from rt to reflux, overnight.

Scheme 5. Synthesis of indole **102** as single isomer.

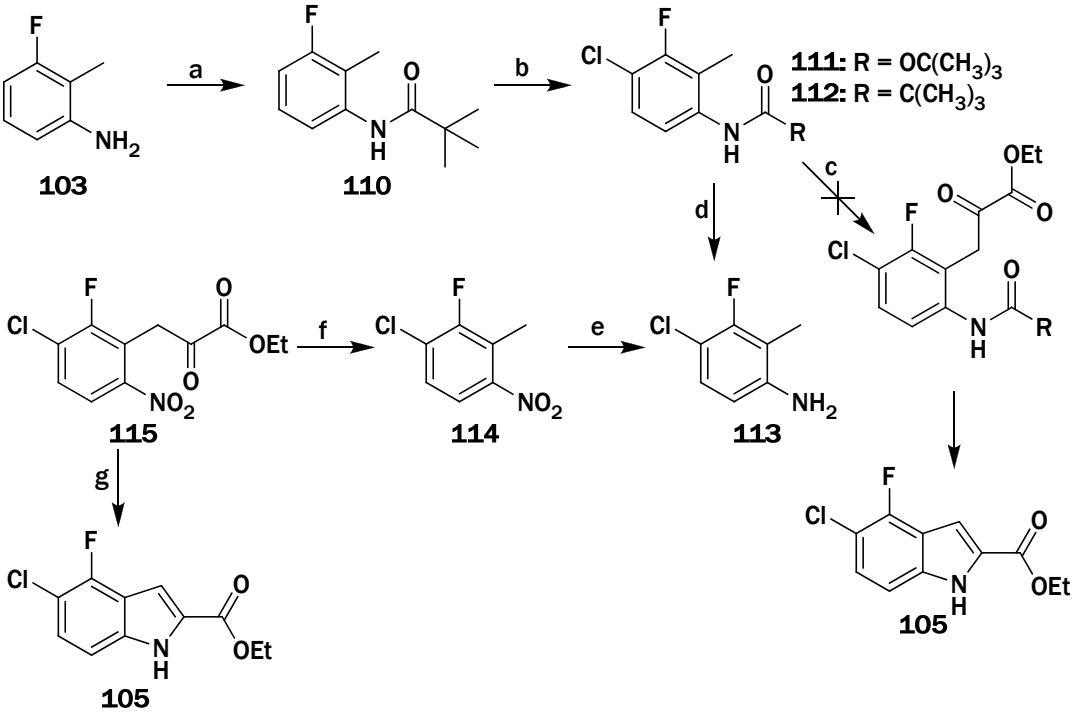

Reagents and Reaction Conditions: a) Pivaloyl chloride, Et_3N, THF, from 0°C to rt, 2h; b) *N*-Chlorosuccinimide, DMF, 80 °C, 45 min.; c) *n*-BuLi, diethyl oxalate, THF, from -78 °C to rt, overnight; d) (from **112**) 6N HCl, dioxane, reflux, overnight; e) *m*-CPBA, toluene, 80 °C, 3 h; f) EtONa, EtOH, diethyl oxalate, rt, overnight; g) Fe, CH_3COOH, 60 °C, overnight.

The sulfonyl derivatives **123-126** were obtained by the oxidation of **119-122** using two equivalent of *m*-CPBA in chloroform at 0 °C. Finally, the esters hydrolysis was performed with three equivalent of lithium hydroxide monohydrate in a mixture of tetrahydrofuran and water at room temperature with a variable time of reaction from 1 to 3 days. The hydrolysis was also performed with the same solvent and base, but using reflux temperature for 5 hours with the same reaction yield.

Thiosuccinimide **116** was obtained from the reaction between 3,5-dimethylthiophenol and *N*-chlorosuccinimmide in dichloromethane at 0°C as already reported.[59] In this reaction is necessary to monitor accurately the temperature otherwise could give *N*-(4-chloro-3,5-dimethylphenyl)thiosuccinimide as by-product.

Coupling reaction between acids **127-130** with the appropriate ethyl or methyl amino acids ester hydrochloride gave the correspondent ethyl or methyl amino acids IASs (**131-146**) that was converted in the desired compounds **34-49** by treatment with ammonium hydroxide (Scheme 7). This reaction was performed in oil bath at the temperature of 60 °C, with a variable time of reaction and, in many cases, low yield with branch amino acids. The same reaction was performed using microwave reactor with a better reaction yield. In the last case the reaction conditions were accurately monitored otherwise could give the correspondent 2-indolecarboxyamide as by product.

Sulphonamides **50-57** were obtained by reaction of **127-130** with 2-aminoethanesulfonamide hydrochloride[60] or 2-aminopropanesulfonamide hydrochloride in the presence of BOP reagent as coupling agent and triethylamine (Scheme 7).

2-Aminopropanesulfonamide hydrochloride (**152**) was synthesized by reaction of mesylate **147**[61] with potassium thioacetate in DMF to afford **148**, which was oxidized with hydrogen peroxide to give the sulfonic acid **149** (Scheme 8). Treatment of **149** with phosgene gave the corresponding sulfonyl chloride **150** which was transformed into sulfonamide **151** with gaseous ammonia and then deprotected by hydrogenation to provide **160**.

Scheme 6. Synthetic pathways for preparation of acid **127-130**.

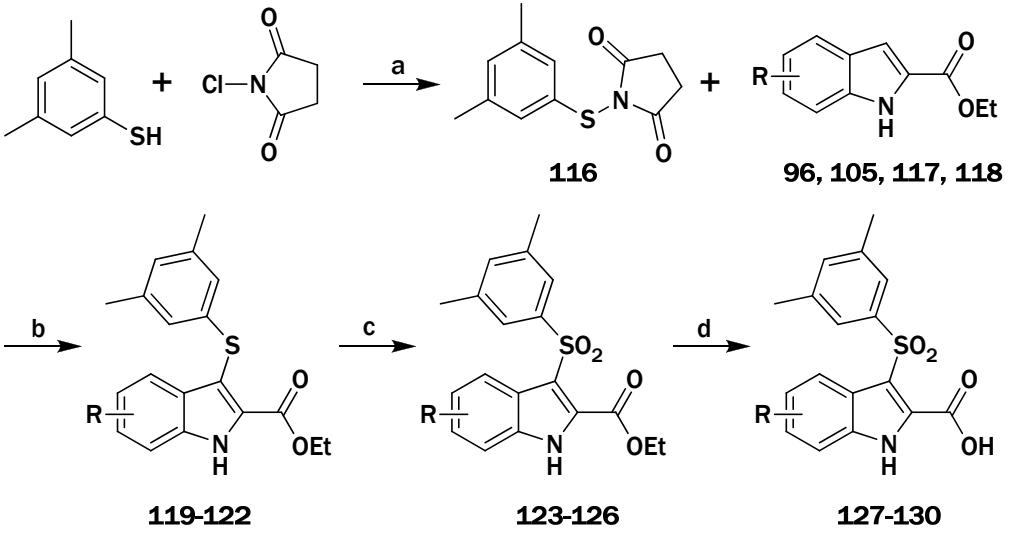

116

96, 105, 117, 118

119-122

123-126

127-130

117,119,123,127: R = 5-Cl
96,120,124,128: R = 5-Br
118,121,125,129: R = 5-NO_2
105,122,126,130: R = 5-Cl.4-F

Reagents and Reaction Conditions: a) Dichloromethane, Et_3N, 0°C, 2.5 h; b) $BF_3 \cdot Et_2O$ diethyl etherate, dichloromethane, 2 h at rt then 2 h at reflux temperature; c) *m*-CPBA, chloroform, 0°C, 1 h; d) $LiOH \cdot H_2O$, tetrahydrofuran, water, rt, overnight.

Derivatives **58-69** were obtained by Mannich reaction between carboxyamide **21**, **32**, **153**, **154** and the appropriate amine (pyrrolidine, piperidine and morpholine) in the presence of formaldheyde (Scheme 9). This reaction was performed using two different procedures. In the first attempt *t*-butanol was used as solvent. The desired product was recovery as precipitate. It was necessary a week and/or the addition of *n*-hexane to form the precipitate and it was difficulty to have a high purity product.

Due the acid instability of Mannich product, they couldn't purified by silica gel column chromatography. An improved synthesis for the preparation of Mannich base was developed. Benzene was used as solvent, and the reaction was performed using Dean-Stark apparatus. Paraformaldehyde was used instead of aqueous formaldehyde. In this case it is necessary to use a very high purity starting material (**21**, **32**, **153**, **154**) (purified by silica gel column chromatography and then by crystallization (only first precipitate)) to obtained a high purity reaction product. The reaction was monitored by TLC, and it was complete in 2-3 h. After cooling the immediately formed precipitate was collected to give a high purity desired product with a good yield.

The Mannich product stability weren't evaluated in the assay's conditions, but they were stable as pure product and in dimethylsulfoxyde at room temperature for a week.

The amide **21**, **32**, **153** and **154** were obtained by direct conversion of esters **123-126**, or from the correspondent acid derivatives **127-130**. The direct conversion of the esters was performed using ammonium hydroxide and ethanol as solvent in the sealed tube at the temperature of 110 °C. The same reaction was performed using microwave reactor, with reduced time of reaction and an increased yield (the best yield was about 60%). In both cases the acid **127-130** were formed as reaction by-product. The reaction of acid **127-130** with 1,1'-carbonyl-diimidazole to give the correspondent imidazole amide that was converted in the desired product by the treatment with ammonium hydroxide with high yield (more of 90%).

Scheme 7. Synthetic pathways for preparation of amino acids IASs derivatives **38-57**.

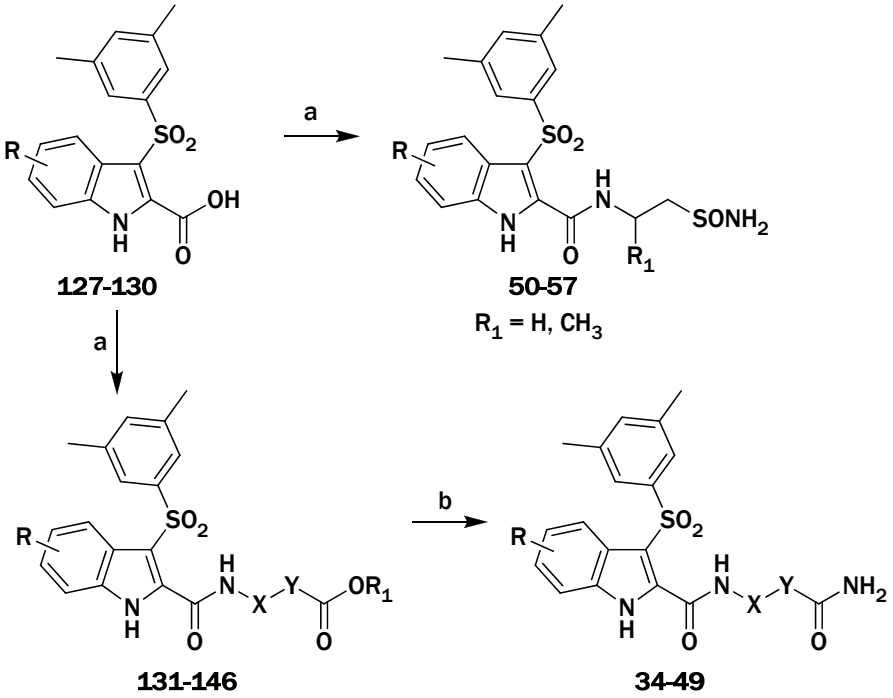

131: R = 5-Cl; X = CH_2; Y = -; R_1 = Et
132: R = 5-Br; X = CH_2; Y = -; R_1 = Et
133: R = 5-NO_2; X = CH_2; Y = -; R_1 = Et
134: R = 5-Cl,4-F; X =CH_2; Y = -; R_1 = Et
135: R = 5-Cl; X = $CH(CH_3)_2$; Y = -; R_1 = Et
136: R = 5-Br; X = $CH(CH_3)_2$; Y = -; R_1 = Et
137: R = 5-NO_2; X = $CH(CH_3)_2$; Y = -; R_1 = Et
138: R = 5-Cl,4-F; X = $CH(CH_3)_2$; Y = -; R_1 = Et

139: R = 5-Cl; X = CH_2; Y = CH_2; R_1 = Me
140: R = 5-Br; X = CH_2; Y = CH_2; R_1 = Me
141: R = 5-NO_2; X = CH_2; Y = CH_2; R_1 = Me
142: R = 5-Cl,4-F; X =CH_2; Y = CH_2; R_1 = Me
143: R = 5-Cl; X = $CH(CH_3)_2$; Y = CH_2; R_1 = Et
144: R = 5-Br; X = $CH(CH_3)_2$; Y = CH_2; R_1 = Et
145: R = 5-NO_2; X = $CH(CH_3)_2$; Y = CH_2; R_1 = Et
146: R = 5-Cl,4-F; X = $CH(CH_3)_2$; Y = CH_2; R_1 = Et

Reagents and Reaction Conditions: a) Appropriate amino acids, BOP, Et_3N, rt, overnight; b) NH_4OH, EtOH, 60 °C, 2h.

Scheme 8. Synthetic pathway for preparation of **152**.

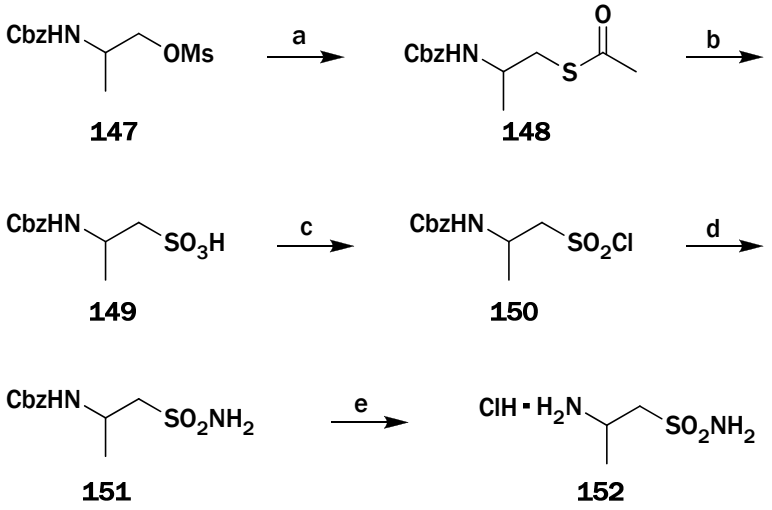

Reagents and Reaction Conditions: a) Potassium thioacetate, DMF, room temp., overnight; b) Hydrogen peroxide, acetic acid, room temp., overnight; c) Phosgene, DMF, dichloromethane, 2 h, overnight, nitrogen atmosphere; d) Gaseous NH_3, benzene, 60 °C, 2 h; e) Hydrogen, palladium over carbon, aqueous methanol, 37% HCl, room temp, 3 h.

Scheme 9. Synthetic pathway for preparation of derivatives **58-69**.

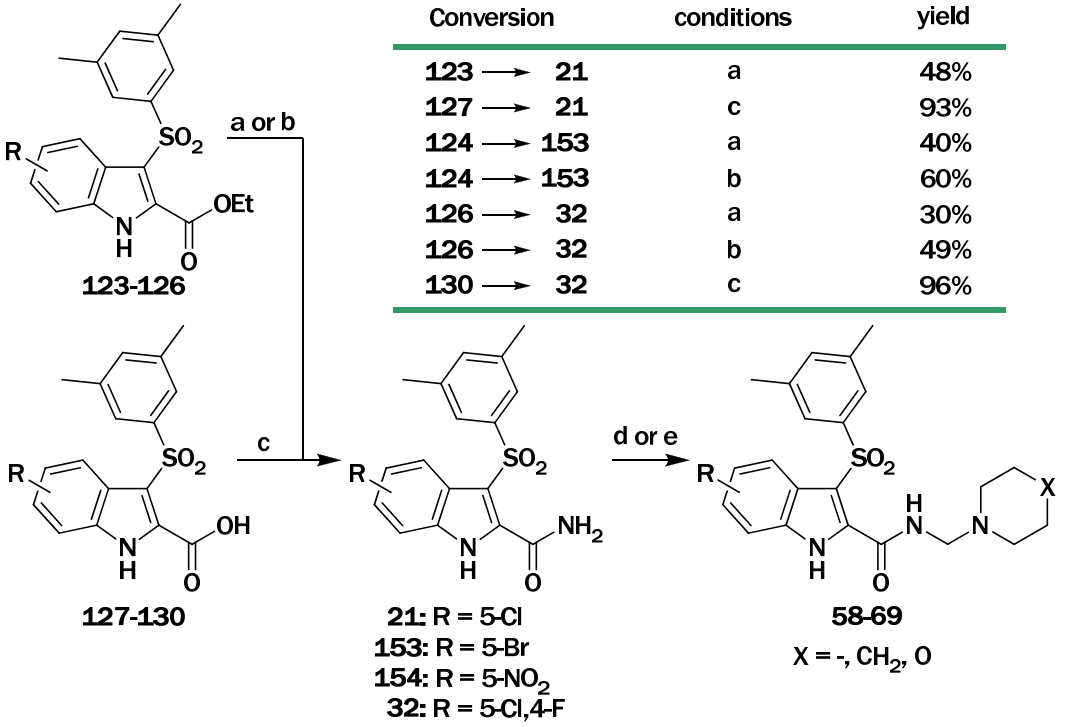

Conversion	Reaction conditions	Reaction yield
123 → **21**	a	48%
127 → **21**	c	93%
124 → **153**	a	40%
124 → **153**	b	60%
126 → **32**	a	30%
126 → **32**	b	49%
130 → **32**	c	96%

Reagents and Reaction Conditions: a) NH_4OH, ethanol, 110 °C, 2h; b) NH_4OH, ethanol, 120 °C, MW, 15 min. c) (i) CDI, tetrahydrofuran, rt, 4h; (ii) NH_4OH, 30 min.; d) Appropriate amine, CH_2Oaq, *t*-butanol, overnight; e) Appropriate amine, *p*-CH_2O, benzene, Dean-Stark apparatus, 3 h.

Scheme 10. Synthetic pathways for the preparation of compounds **70-93**.

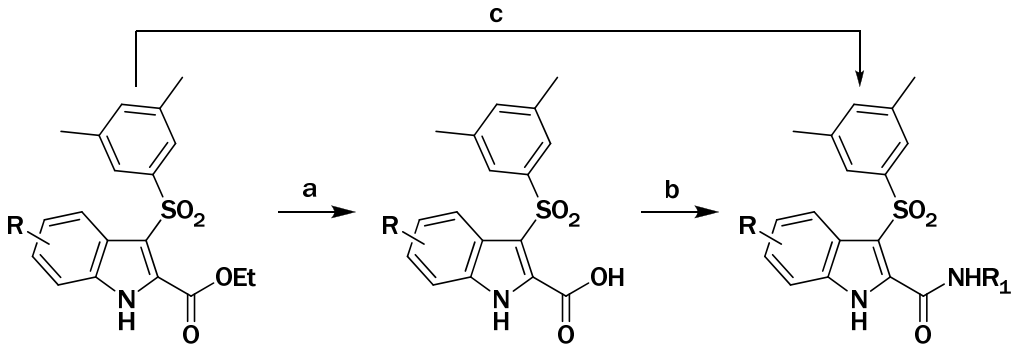

Reagents and Reaction Conditions: a) $LiOH \cdot H_2O$, tetrahydrofuran, water, rt, 2 days; b) Appropriate amine, BOP, Et_3N, *N*,*N*-dimethylformamide, rt, overnight; c) Appropriate amine (3 eq.), EtOH, MW, 120 °C, 15 min.

Also preparation of compounds **70-93** was performed using two different synthetic pathways. They can be prepared from acids acid **127-130** using BOP coupling reagent, or by microwave assisted reaction between the esters **123-126** and the appropriate amine (Scheme 10). The last reaction conditions were more advantageous:

1. only one step of reactions (instead of two);
2. less time of reactions;
3. more yield of reactions (single and overall);
4. reaction product was collected with high purity

For the microwave assisted reaction was used ethanol as solvent and it was optimized using different amine equivalent, temperature and time of reaction. 3 amine equivalents at temperature of 120 °C is the optimal reaction condition, and generally the starting material was totally converted in the desired product in about 15 minutes (as monitored by TLC). The least quantity of ethanol was used (generally 0.5 mL for 300 mg of ester), and the product was collected as precipitate with a high purity and yield and it don't request successive purification.

Biological Activity

The antiretroviral activity (EC_{50} values) of IAS derivatives **34-57** was evaluated against the HIV-1 WT in human T-lymphocyte (CEM) cells, using IASs **21** and **32** as reference compounds. The data are mean values of two experiments performed in triplicate. Antiviral activity is reported as EC_{50} values (effective concentration (nM) or concentration required to protect CEM cells against the cythopathicity of HIV by 50%, as monitored by giant cell formation). All compounds proved to be highly potent against HIV-1 in human T-lymphocyte (CEM) cells, and showed inhibitory potencies in low/sub-nanomolar range of concentrations which were comparable with the previously reported lead compounds **21** and **32**.[16] Against HIV-1 WT, the inhibitory activity was only marginally affected by the substituent introduced on the indole nucleus, and with only one exception (**46**), 5-chloro-IASs were the most potent inhibitors (Table 9). Only all compounds bearing β-alanine units, indipendently from other substituent, were high active with a concentration less of 2 nM. In Table 9 are also reported the inhibitory effects of compounds on the proliferation of Murine Leukemia Cells (L1210) and Human T-Lymphocyte Cells (Molt4/C8, CEM) and the activity are reported as IC_{50} values at μM concentration. Generally, the IASs inhibited the cell proliferation in the micromolar range, that is at compound concentrations that are usually 3 to 4 orders of magnitude higher than their antivirally active concentrations. 5-Nitro-IASs bearing an unbranched aminoacid unit were often devoid of any significant cytostatic effect at 500 μM (i.e. **36**, **44**, **52**). On the contrary, the bromine atom at position 5 of the indole had the tendency to rather strengthen the cytotoxicity.

A selection of active compounds **34**, **38**, **42**, **50**, and **54** have been evaluated against mutant HIV-1 strains that harbour the L100I, K103N, Y181C, Y181I and Y188L mutations in their RT (Table 10), and Nevirapine (NVP) and Efavirenz (EFV) were used as reference compounds. The compounds lost antiviral potency against all the mutant virus strains, but they were more potent

Table 9. Antiviral activity and cytotoxicity of derivatives **34**-**57**.

Compd	HIV-1 (III_B) EC_{50}[b] (nM)	HIV-2 (ROD) EC_{50}[b] (nM)	L1210 (IC_{50} μM)	Molt4C8 (IC_{50} μM)	CEM (IC_{50} μM)
34	1.9 ± 1.3	>50000	220 ± 2	15 ± 7	92 ± 13
35	2.6 ± 2.0	43000 ± 9900	40 ± 5	17 ± 0	31 ± 15
36	2.4 ± 1.8	>50000[c]	>500	>500	≥500
37	3.1 ± 1.9	>10000	53 ± 3	34 ± 1	31 ± 19
38	1.6 ± 1.3	>10000[c]	12 ± 1	3.8 ± 1.3	11 ± 1
39	1.9 ± 1.1	>10000[c]	10 ± 0	8.7 ± 1.4	10 ± 0
40	3.8 ± 0.98	>10000[c]	96 ± 4	44 ± 13	66 ± 17
41	3.7 ± 1.7	>10000	30 ± 10	22 ± 11	21 ± 3
42	1.0 ± 0.6	>10000[v]	26 ± 2	9 ± 1	16 ± 2
43	1.1 ± 0.21	23000 ± 8500	46 ± 4	25 ± 12	36 ± 1
44	1.6 ± 1.4	>10000[c]	>500	>500	≥500
45	2.0 ± 1.0	>10000	42 ± 3	33 ± 0	30 ± 2
46	26 ± 8.7	30000 ± 3500	48 ± 1	36 ± 1	32 ± 1
47	1.5 ± 0.57	>10000[c]	16 ± 4	16 ± 11	18 ± 9
48	5.1 ± 0.81	>10000[c]	37 ± 13	41 ± 1	36 ± 11
49	4.6 ± 2.2	>10000[c]	42 ± 3	25 ± 0	27 ± 4
50	1.4 ± 1.5	>10000[c]	20 ± 7	12 ± 2	14 ± 5
51	1.0 ± 0.14	>10000[c]	17 ± 2	11 ± 0	14 ± 1
52	2.7 ± 1.3	>10000[c]	408 ± 131	244 ± 1	200 ± 73
53	2.3 ± 2.3	>10000[c]	42 ± 3	36 ± 3	31 ± 0
54	2.3 ± 1.1	>10000[c]	15 ± 0	8.8 ± 0.7	13 ± 3
55	2.3 ± 5.9	>10000[c]	11 ± 1	9.3 ± 0.5	12 ± 1
56	4.2 ± 0.89	≥10000	20 ± 3	11 ± 0	15 ± 1
57	3.9 ± 2.4	>10000[c]	18 ± 6	12 ± 1	16 ± 1
21	1.1 ± 0.0	>2000[c]	≥ 500	20 ± 2	301 ± 211
32	1.0 ± 0.0	>10000	46 ± 27	14 ± 6	>28 ± 18

than Nevirapine in all valued mutant strain. All tested IASs were more active than Efavirenz against L100I and K103N RT HIV-1 strains, but lost quite the antiviral potency against the mutant Y181I RT HIV-1 strain. Against Y181C RT HIV-1 strain compounds **34**, **38**, **42** were more active than Efavirenz, and compounds **50** and **54** are less active. Against Y188L, only **34** and **38** showed a comparable activity with Efavirenz. These results were in agreement with the inhibitory effects of the compounds against the corresponding mutant enzyme.
Many new IASs were potent inhibitors of the RT of HIV-1 wild type, and they were always superior to Nevirapine and often comparable of EFV (Table 11). Against the RT wild type, the sulphonamides **50** and **54** showed inhibitory concentrations comparable to the reference compound **21**, and 7.5, 1000 and 200 times superior to **32**, Nevirapine and Efavirenz, respectively. Seventeen compounds inhibited in the submicromolar range the mutant K103N RT HIV-1, which is the major mutation emerging in patients treated with Efavirenz, whose viral loads rebounds after an initial response to the drug. Against the K103N RT HIV-1 strain, the most active compounds **34**, **38**, **42**, **50** and **54** were notably more active than Nevirapine and Efavirenz, albeit less active than the references **21** and **31**. Both 5-chloro and 5-bromo-IASs were potent inhibitors of the L100I RT mutant, and compound **54** was exceptionally effective against this mutant. Against the recombinant HIV-1 RT carrying the Y181I mutation, compounds **39** and **54** as active as **34**, and >10 times more potent than Nevirapine, but about 4 times less potent than Efavirenz. Compound **54**, containing the 2-aminopropane-1-sulfonamide motif, was identified as a potent inhibitor of RT WT and RTs bearing commonly emerging single amino acid substitution.

To evaluate the influence of the chiral center at the amino acid unit, the racemates **38**, **39** and **46** were separated by chiral HPLC. Against HIV-1 WT RT, the enantiomers **38a** and **38b**, **39a** and **39b**, and **46a** and **46b** obtained from the corresponding racemic mixtures **38**, **39** and **46**, respectively, showed negligible differences of activity (Table 12). Against the K103N mutation, the (*D*)-enantiomers **38b** and **39b** were about five times more potent than the

Table 10. Antiviral activity against HIV-1 strain carring L100I, K103N, Y181C, Y181L, and Y188L mutation of compounds **34**, **38**, **42**, **50**, and **54**.

	IC_{50} (nM)				
Compd	L100I	K103N	Y181C	Y188L	Y181L
34	8 ± 7	29 ± 18	74 ± 18	690 ± 440	>1000
38	9 ± 7	14 ± 6	96 ± 34	660 ± 480	>1000
42	7 ± 2	19 ± 9	78 ± 23	≥1000	>1000
50	1.2 ± 1	40 ± 32	230 ± 190	>1000	>1000
54	2.0 ± 8	36 ± 32	390 ± 120	>1000	>1000
NVP	60 ± 4	2900 ± 1320	11000 ± 4100	>10000	>10000
EFV	22 ± 14	130 ± 180	160 ± 180	760 ± 630	12 ± 14

Data are mean values of two to three independent experiments.

corresponding (*L*)-enantiomers **38a** and **39a**, and the enantiomers **46a** and **46b** did not show significant difference of activity.

In Table 13 is reported the activity of some compounds **58-73** against wild type HIV-1; for some of this derivatives is also reported the activity against Y181C, Y181C-K103N, and EFV^R mutant strains. Nevirapine and Efavirenz were used as reference compounds, and they were tested using the same assay conditions. Compounds **58-73** are characterized by the presence of a one carbon atom between the carboxyamide function and the specific amine of phenyl group. The 5-chloroindole derivatives **58**, **62**, and **66** were active against wild type HIV-1 with at nanomolar concentrations as well as 5-bromo derivatives **71**. These four compounds were more potent of both reference compounds. The introduction of nitro group in the same position led to less potent activity (**60**, **64**, **68**, and **72**), but derivative **60** was less cytotoxic.

The presence of the nitrogen atom in the radical seem important for the activity, in fact derivatives **58**, **62**, and **66** were more potent than compound **70** bearing phenyl group at carboxyamide function.

Derivatives **58**, **62**, and **66** were also valued against mutant strains. Against Y181C RT HIV-1 mutant strains they retain the activity at nanomolar concentrations, and were more active against reference compounds, as well as against the EFV^R mutant strain. These compounds were active against the double mutant strain (Y181C-K103N) at submicromolar concentration, and they were more potent than Nevirapine and less potent than Efavirenz.

In Table 14 is reported the activity of compounds **74-89** bearing a two carbons atom linker. 5-Chloroindole derivatives **74**, **78**, and **72** and 5-nitroindole derivatives **76**, **80** were active at nanomolar concentrations and more active than Nevirapine, but only **74** and **76** were more potent than Efavirenz, and **82** was equipotent. Compounds **74** and **82** were 2 times less potent than the corresponding **58** and **66** bearing one carbon linker. The introduction of bromine atom at position 5 of indole gave compounds with low activity. Derivative **82** was more cytotoxic of syntesized compound with a CC_{50} = 2 μM.

Table 11. Enzymatic activity of compounds **34**-**57** against HIV-1 RT of wild type and mutant strains.

Compd	IC_{50} (nM)			
	WT	L100I	K103N	Y181I
34	26	161	280	1645
35	26	199	782	2211
36	34	206	417	2909
37	25	319	1042	2459
38	20	112	447	2493
39	16	41	555	1810
40	22	209	362	4211
41	62	270	1522	6277
42	27	143	351	5055
43	86	169	420	8566
44	27	204	474	5534
45	34	130	783	7165
46	490	252	1690	4137
47	81	296	321	15830
48	33	191	1088	11920
49	359	390	3387	>40000
50	0.4	25	584	>40000
51	2	13	529	>40000
52	61	388	787	>40000
53	-	-	-	-
54	0.4	4	233	1944
55	3	125	1328	8550
56	28	364	3277	26220
57	36	267	3	>40000
21	0.3	60	3	140
32	3	2	6	29
NVP	400	9000	7000	>20000
EFV	80	-	>20000	400

Table 12. Inhibitory Activity of Racemates **38**, **39** and **46**, and Enantiomers **38a**, **38b**, **39a**, **29b**, **46a** and **46b** against HIV-1 RT WT and RTs Carrying Single Amino Acid Substitutions.[a]

Compd	IC_{50}[b](nM)		
	Chirality	WT	K103N
38	*D,L*	20	477
38a	*L*	26	1005
38b	*D*	17	253
39	*D,L*	16	555
39a	*L*	13	1504
39b	*D*	16	324
46	*D,L*	490	1690
46a	*L*	315	1340
46b	*D*	147	1417

[a]Data represent mean values of at least three separate experiments. [b]Compound dose (IC_{50}, nM) required to inhibit by 50% the RT activity of the indicated strain.

Table 13. Biological Activity of Derivatives **58-73** (Mannich bases) against HIV-1 wild type. For some is also reported the activity against some single, double, and EFV^R mutant strains.

Compd	HIV-1 (III_B) $EC_{50}{}^b$ (nM)	Y181C $EC_{50}{}^b$ (nM)	K103N-Y181C $EC_{50}{}^b$ (nM)	EFV^R $EC_{90}{}^b$ (nM)	CC_{50} (μM)
58	1.0	2.0	300	50	5
59	-	-	-	-	-
60	21	-	-	-	104
61	-	-	-	-	-
62	2.0	7.0	500	40	5
63	-	-	-	-	-
64	85	-	-	-	>20
65	-	-	-	-	-
66	2.0	6.0	300	20	7
67	-	-	-	-	-
68	5.4	-	-	-	>20
69	-	-	-	-	-
70	270	-	-	-	>20
71	3.8	-	-	-	>20
72	79	-	-	-	>20
73	-	-	-	-	-
NVP	37	>30000	>30000	>30000	>100
EFV	4	25	150	1800	35

Against mutant strains all valued compounds were more active than Nevirapine. Compounds **78** and **86** were less potent than Efavirenz aganist Y181C single mutant and K103N-Y181C double mutant, and more potent against EFV^R mutant strain.

Finally, compounds **90-93** were active against HIV-1 wild type at submicromolar concentrations and they were less active than both reference compounds.

Table 14. Biological Activity of Derivatives **74**-**89** against HIV-1 wild type. For some is also reported the activity against some single, double, and EFV^R mutant strains.

Compd	HIV-1 (III_B) $EC_{50}{}^b$ (nM)	Y181C $EC_{50}{}^b$ (nM)	K103N-Y181C $EC_{50}{}^b$ (nM)	EFV^R $EC_{90}{}^b$ (nM)	CC_{50} (μM)
74	3.0	-	-	-	12
75	63	-	-	-	>20
76	2.1	-	-	-	>20
77	-	-	-	-	-
78	6	60	500	60	44
79	41	-	-	-	>20
80	8.8	-	-	-	>20
81	-	-	-	-	-
82	4	-	-	-	2
83	860	-	-	-	>20
84	19	-	-	-	>20
85	-	-	-	-	-
86	20	430	>11000	60	>20
87	36	-	-	-	>20
88	1200	-	-	-	>20
89	-	-	-	-	-
NVP	37	>30000	>30000	>30000	>100
EFV	4	25	150	1800	35

Table 15. Biological Activity of Derivatives **74-77** against HIV-1 wild type. For some is also reported the activity against some single, double, and EFV^R mutant strains.

Compd	HIV-1 (III_B) $EC_{50}{}^b$ (nM)	Y181C $EC_{50}{}^b$ (nM)	K103N-Y181C $EC_{50}{}^b$ (nM)	EFV^R $EC_{90}{}^b$ (nM)	CC_{50} (μM)
90	**200**	-	-	-	**>20**
91	**100**	-	-	-	**>20**
92	**160**	-	-	-	**>20**
93	**110**	-	-	-	**59**
NVP	**37**	**>30000**	**>30000**	**>30000**	**>100**
EFV	**4**	**25**	**150**	**1800**	**35**

Molecular Modelling Studies

The binding mode of the IASs was extensively studied by means of docking experiments into the non-nucleoside binding site (NNBS) of the RT. The latest available **153**/RT co-crystal structure (PDB code 2rf2) solved by Merck[62] was used as a new starting point for docking studies, because of the high structural correlation between the co-crystallized inhibitor **153** (Figure 21) and IASs. In our previous studies,[63] we used Autodock 3.0[64] software to generate IASs docking poses. However, Autodock 3.0[65] software consistently yielded two different clusters of poses, and the crystallographic conformation was often the lower scoring pose. To obtain more accurate docking results and also to validate the generated poses with crystallographic information, we decided to test the docking softwares PLANTS,[65] FlexX[65] and MOE[66] docking algorithm.

We selected seven PDB structures of inhibitors co-crystallized with either HIV-1 WT RT or mutated RTs (2rf2,[63] 1vrt,[38] 2zd1,[67] 1fk0,[53] 1s1t,[68] 2opq,[69] and 1jkh[70]). The best scoring poses predicted by the different algorithms were compared with the crystallographic conformations obtained from each complex in terms of the RMSD. Our experiments showed that only PLANTS was able to correctly dock each molecule with a RMSD <1. The other docking software always achieves bigger RMSD values than PLANTS on the whole test set (Table 16). Therefore, we decided to use PLANTS to dock the new IAS series. Interestingly, the best scoring conformation obtained by PLANTS clustering algorithm was always superimposed to Merck's crystal.

In order to investigate the possible binding mode of the new IASs, we selected the highly potent compound **42** (IC_{50} = 26 nM; EC_{50} = 1.0 ± 0.6 nM) for docking studies into the NNBS of the HIV-1 WT RT. From docking, feature interactions of **42** into the NNBS were: (i) the H-bond between the indole NH and the carbonyl oxygen of Lys101 (in stick in the Figure 22); (ii) the interactions of the *N*-(3-amino-3-oxopropyl)carboxamide moiety with the residues Lys101 and Glu138B at the bottom of the binding pocket (they

Table 16. RMSD values for co-crystallized inhibitors by PLANTS, FlexX and MOE.

PDB code	RMSD Values		
	PLANTS 1.0	FlexX 3.0	MOE 2007/09
1vrt	0.23	1.18	1.53
2rf2	0.80	1.59	1.20
2zd1	0.40	2.01	>5
1fk0	0.85	1.28	1.47
1s1t	0.26	1.04	4.60
20pq	0.48	0.90	2.10

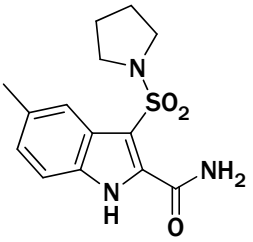

153

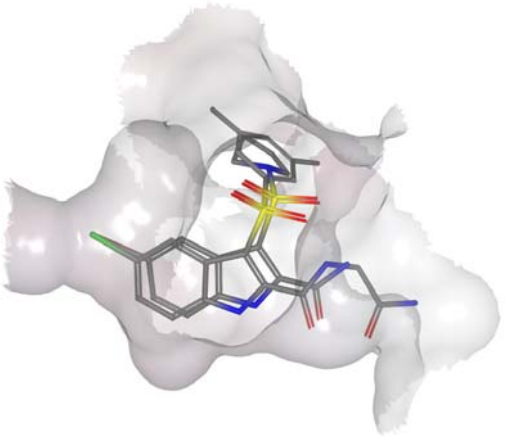

Figure 21. Structure of Merck compound **153** and superimposed structure with derivative **42**.

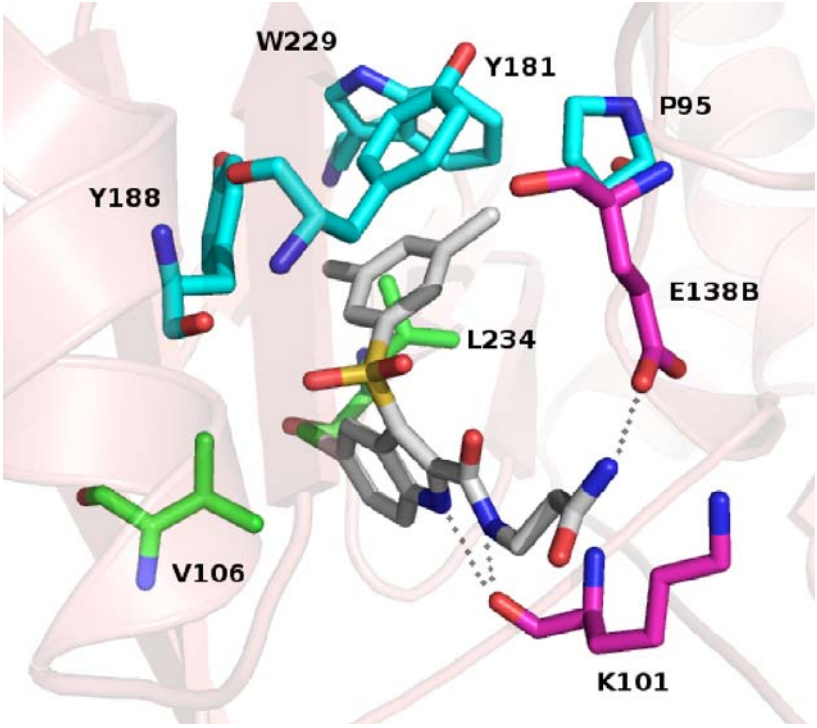

Figure 22. Binding conformation of **42** in the NNBS of HIV-1 WT RT.

seemed to be particularly important for the anti-HIV activity); (iii) the sulfone group allowed **42** to assume a butterfly-like conformation that is common to many other NNRTIs; (iv) the chlorine atom at position 5 of the indole occupied a hydrophobic pocket formed by Val106 and Leu234, and formed steric rather than electrostatic interaction; (v) the 3,5-dimethylphenyl moiety formed hydrophobic interactions with an aromatic cleft formed by the side chains of Tyr181, Tyr188, Trp229, and Pro95 residues (Figure 21).

Worthy to note, a superimposition of PLANTS docked conformations of **42** and the highly active derivative **32**[71] (IC_{50} = 3 nM; EC_{50} = 1.0 nM) showed different hydrophobic interactions of the 3,5-dimethylphenyl group, for which a stacking interaction with the Tyr181 aromatic side chain was observed (Figure 23).

The IASs binding mode was extensively studied also in mutated RTs. The results obtained by docking the IASs analogues with PLANTS in L100I mutated RT (pdb code: 1s1t, 2opq), showed that the mutation of leucine to isoleucine does not affect the binding mode confirming all the interactions reported for the WT strain. Furthermore, all compounds show a similar binding mode, consistent with the low EC_{50}'s (Figure 24).

We have also repeated the docking simulations on the K103N and Y181I mutated RTs and the results obtained did not show significant differences with the IASs binding mode observed with the wild-type. However, the lower anti-viral activity of the IASs against these mutants could be the consequence of the reduced interaction between **42** and the mutated residues. In particular, for the Y181I RT HIV-1 strain, the limited anti-HIV efficiency could be caused by the loss of the favourable protein-ligand π-π interactions, while in the mutant K103N RT, the loss of the favourable hydrophobic interaction between the ligand and the side chain of the lysine 103 might be responsible for the reduced activity (Figure 25). In both cases the geometry of the H-bonds between the carbonyl oxygen of the E138 with unsubstituted amidic nitrogen of **42** are worst than the wild type.

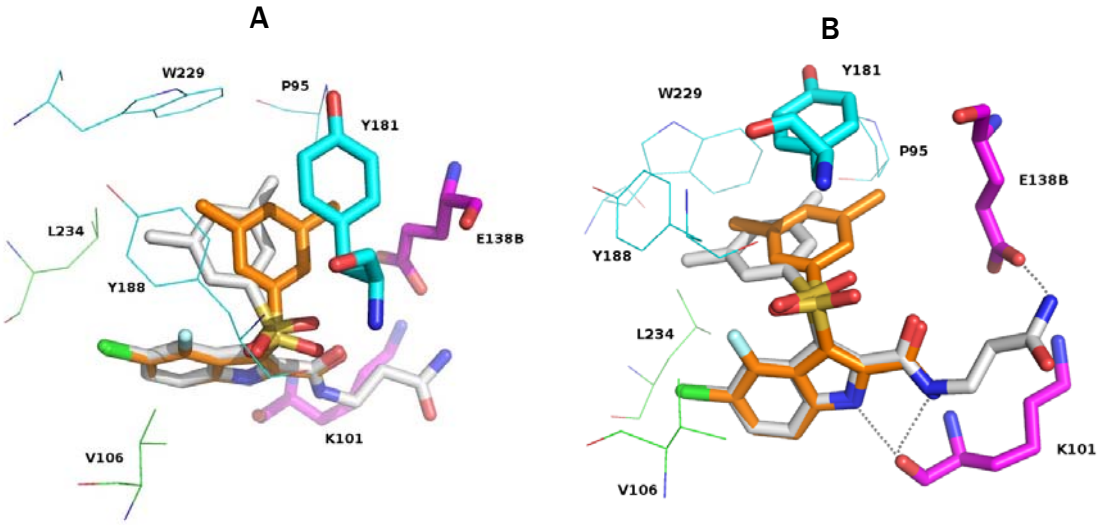

Figure 23. Binding conformation of **42** (white stick) and **32** (orange stick) are reported. Are also reported, in stick, the residues involved in hydrogen bonding (dot lines) and the **Y181**. The superimposition of compounds shows the better alignment between phenyl ring of **32** and aromatic side chain of **Y181** to give stronger stacking interaction. Some relevant key residues are also reported.

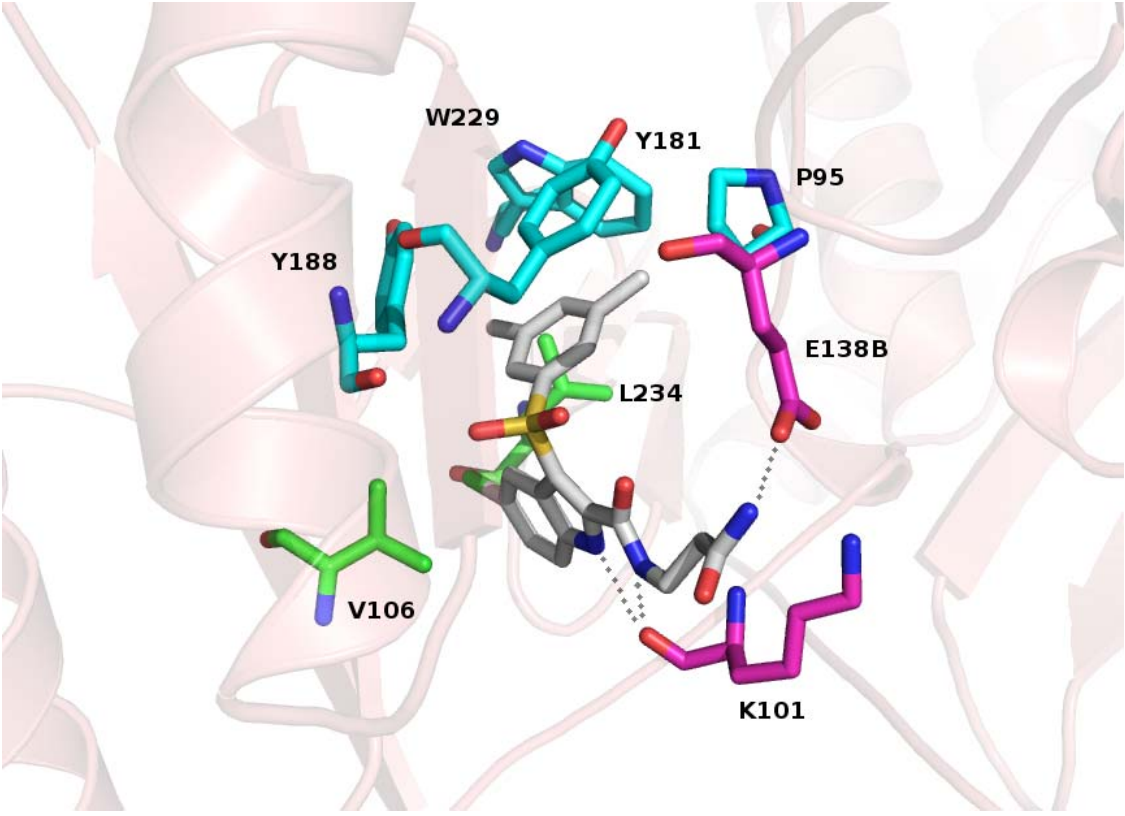

Figure 24. Binding conformation of **42** in the NNBS of HIV-1 L100I RT.

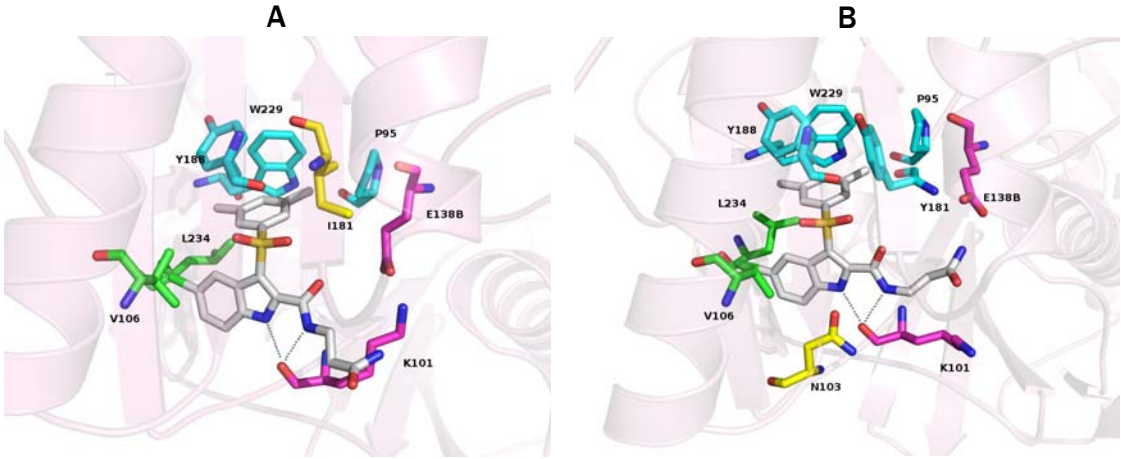

Figure 25. Figures show 4.5 Å core of RT (figure B pdb code 1fk0, figure A pdb code 1vrt). The residue 103 is reported in stick for WT (left) as well for the mutated (right) form. All hydrogens are hidden for clarity. The lipophilic maps analysis for the WT form (left) shows a hydrophobic interaction between the indole of **42** and the side chain of Lys103. For K103N RT (right) there is not any hydrophobic interaction between indole moiety and Asn103.

Kinetic Studies About IASs-RT Complex and Inhibition Mechanism (*di-halo*-IASs 32, 37, 81 and 93)

NNRTI interaction with HIV-1 reverse transcriptase (RT) is a highly dynamic process. Upon complexation, the NNBS hydrophobic pocket changes its own conformation, leading to the inactivation of the enzyme itself. NNBS adopts different conformations depending on the 3-D features of the inhibitors and the amino acids side chain flexibility. Moreover, mutations of some amino acids cause structural variations of the NNBS, which ultimately result in reduced affinities of most of the inhibitors.[72] In particular, the NNRTI resistance mutations Y188L and Y181I/C reduce $\pi-\pi$ interactions; the G190A mutation leads to a smaller active site space because of a steric conflict between the methyl side chain and the inhibitor and the formation of an additional hydrogen bond; when amino acid 103 is mutated from Lys to Asn it reduces inhibitor entrance into the NNBS. In addition, HIV-1 RT itself also undergoes a conformational reorganization upon interaction with its substrates template-primer (TP) and deoxynucleoside triphosphate (dNTP), so that three structurally distinct mechanistic forms can be recognized in the reaction pathway catalyzed by HIV-1 RT: the free enzyme, the binary complex of RT with the template primer (RT/TP), and the catalytically competent ternary complex of RT with both nucleic acid and dNTP (RT/TP/dNTP) (Figure 26A). This means that, in principle, the NNBS might not be identical in these three mechanistic forms.[73] Several kinetic studies have shown that this is indeed the case, so that some NNRTIs selectively target one or a few of the different enzymatic forms along the reaction pathway. This observation likely reflects the different spatial rearrangements not only of the NNBS itself but also of the adjacent nucleotide binding site. Indeed, it has been shown that a "communication" exists between the NNBS and the nucleotide binding site, so that some NRTI resistance mutations can influence NNRTI binding and vice versa. In view of their extremely potent activities, especially towards NNRTI-resistant mutants, we

sought to investigate in detail the mechanism of action of some selected IAS derivatives. IASs are highly flexible molecules, whose mode of interaction, and hence the mechanism of RT inhibition, can be modulated by the nature of the different substituents, so that from compounds endowed with a classical fully non-competitive mechanism, a series of inhibitors showing mixed-non-competitive and even partially competitive mechanism of action can be derived. This high flexibility was exploited to synthesise novel IAS derivatives able to better accommodate into the NNBS of drug resistant mutants.

Kinetic model. The mechanism of action of the examined *di-halo*-IASs was found to be either fully non-competitive or partially mixed. A schematic drawing of the different equilibria is depicted in Figure 26. According to the ordered mechanism of the polymerization reaction, whereby template-primer (TP) binds first followed by the addition of dNTP, HIV-1 RT can be present in three different catalytic forms as reported in Figure 26A: as a free enzyme, in a binary complex with the TP, and in a ternary complex with TP and dNTP. The resulting rate equation for such a system is very complex and impractical to use. For these reasons, the general steady-state kinetic analysis was simplified by varying one of the substrates (either TP or dNTP) while the other was kept constant. When the TP substrate was held constant at saturating concentration and the inhibition at various concentrations of dNTPs was analyzed, at the steady-state all of the input RT was in the form of the RT/TP binary complex and only two forms of the enzyme (the binary complex and the ternary complex with dNTP) could react with the inhibitor, as shown in the left part of Fig. 26. Similarly, when the dNTP concentrationwas kept constant at saturating levels and the inhibition at various TP concentrations was analyzed, RT was present either as a free enzyme or in the ternary complex with TP and dNTP, as shown in the right part of Fig. 26.

The steady-state rate equation used for the partially mixed inhibition was the one describing a reaction involving only two mechanistic forms of the enzyme (according to the simplified pathways in Fig. 26B).

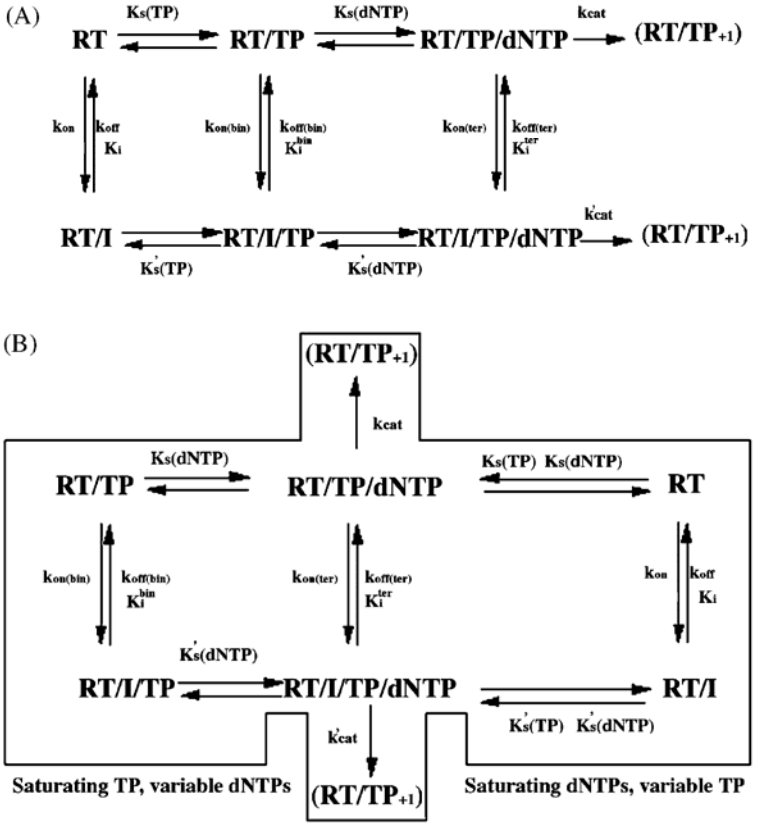

Figure 26. Simplified kinetic pathway for the reaction catalysed by HIV-1 RT and its interaction with inhibitors. (A) Schematic representation of the different equilibria in the reaction catalysed by HIV-1 RT in the absence or in the presence of an inhibitor. TP, template/primer; dNTP, nucleoside triphosphate; I, inhibitor; K_m, Michelis constant relative to the different substrates; k_{cat}, apparent catalytic rate; k_{off}, dissociation rate; k_{on}, association rate; K_i, equilibrium dissociation constant of the inhibitor; bin, binary complex of the enzyme with the TP substrate; ter, ternary complex of the enzyme with the TP and dNTP substrates. (B) Simplified reaction pathway under the reaction conditions used in this study.

Di-halo-IAS are mixed-type inhibitors of HIV-1 RT, with higher affinity for the enzyme–substrate complexe. In order to determine the exact mechanism of action of these compounds, the RNA dependent DNA polymerase activity of HIV-1 RT, either wild type or mutated (K103N, L100I and Y181I) was measured in the absence or in the presence of fixed concentrations of the inhibitors and variable concentrations of either the nucleic acid (template/primer) and/or nucleotide substrate, respectively, while the other was maintained at saturating concentrations. Data were interpolated and the K_m, and V_{max} values (Table 17) were calculated according as described in the Experimental Section. Interestingly, we found that both the K_m and the V_{max} values obtained varying the nucleic acid substrate concentrations were significantly decreased as the inhibitor concentration increased (Figure 27A and B). On the other hand, when the nucleotide substrate concentration was varied, only the V_{max} showed a dose dependent reduction by the tested IAS derivatives (Figure 27C), whereas the K_m did not change (Figure 3D). The equilibrium dissociation constants for the inhibitors (K_i) from the different enzymatic forms along the reaction pathway (free enzyme, binary complex with the nucleic acid (template/primer) and ternary complex with both the nucleic acid (template/primer) and the nucleotide substrate) were calculated from the variations of the V_m and K_m values (see Experimental Section) according to the simplified kinetic pathway shown in Fig. 26. The corresponding values are listed in Table 16. Thus, the IAS derivatives behaved as mixed-type inhibitors, showing higher affinity for the binary RT/TP and ternary RT/TP/dNTP complexes than for the free enzyme ($K_i^{free} > K_i^{bin} \approx K_i^{ter}$). The true inhibition constant (K_i) was then considered as the one corresponding to the equilibrium dissociation constant from the ternary complex (Ki^{ter}).

Effect of NNRTI resistance mutations on di-halo-IAS inhibition activity. In order to elucidate the influence of the Lys103Asn, Leu100Ile and Tyr181Ile mutations on the activity of each *di-halo*-IAS examined, we calculated the ratio between the inhibitory potencies against the mutated RT forms (K_i^{ter} mut) and against the RT wild type (K_i^{ter} wt) (Table 16). This ratio (K_i^{ter} mut/K_i^{ter} wt),

Table 17. Equilibrium dissociation constants (K_i) values of the IAS compounds, along with nevirapine and efavirenz, with respect to the different eznymatic forms of HIV-1 RT wild type and mutants.

Compd	WT		K103N	
	K_i^{free} (μM)[a]	$K_i^{bin/ter}$ (μM)	K_i^{free} (μM)	$K_i^{bin/ter}$ (μM)
37	0.031 (±0.003)	0.025 (±0.002)	3.5 (±0.3)	1.42 (±0.12)
81	0.04 (±0.005)	0.018 (±0.002)	0.7 (±0.04)	0.17 (±0.017)
93	0.07 (±0.008)	0.006 (±0.001)	1.2 (±0.2)	0.36 (±0.036)
32	0.058 (±0.006)	0.003 (±0.0005)	0.07 (±0.01)	0.006 (±0.001)
NVP	0.4 (±0.05)	0.4 (±0.04)	3.3 (±0.3)	5 (±0.05)
EFV	0.03 (±0.006)	0.004 (±0.001)	1.5 (±0.2)	0.2 (±0.03)

Compd	L100I		Y181I	
	K_i^{free} (μM)[a]	K_i^{free} (μM)[a]	K_i^{free} (μM)	K_i^{free} (μM)[a]
37	1.5 (±0.1)	0.55 (±0.055)	3.6 (±0. 3)	2.6 (±0.26)
81	0.1 (±0.01)	0.03 (±0.003)	7.5 (±0.5)	3.7 (±0.37)
93	0.2 (±0.03)	0.03 (±0.003)	15 (±1)	8.4 (±0.84)
32	0.01 (±0.002)	0.002 (±0.0003)	0.2 (±0.03)	0.029 (±0.003)
NVP	7 (±0.05)	9 (±0.9)	34 (±2)	36 (±2)
EFV	0.15 (±0.01)	0.02 (±0.003)	0.9 (±0.1)	0.12 (±0.02)

Variable NA

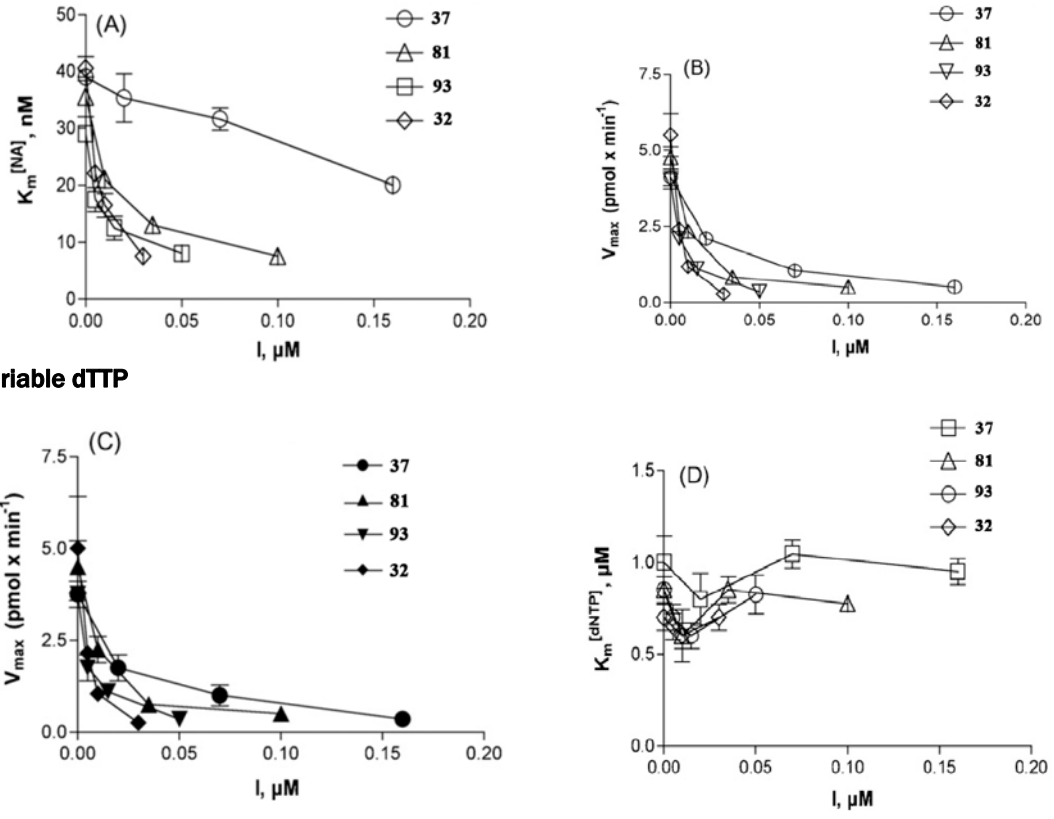

Variable dTTP

Figure 27. IAS are mixed-type inhibitors of HIV-1 RT wild type. All values are the mean of three independent estimates. Error bars are ± S. D. (A) Variation of the apparent affinity (K_m) for the nucleic acid (NA) substrate as a function of the inhibitor concentration. (B) Variation of the apparent maximal velocity (V_{max}) of the reaction as a function of the inhibitor concentration at variable nucleic acid concentrations. (C) Variation of the apparent maximal velocity (V_{max}) of the reaction as a function of the inhibitor concentration at variable dTTP concentrations. (D) Variation of the apparent affinity (K_m) for the nucleotide (dNTP) substrate as a function of the inhibitor concentration.

referred as relative resistance index (RRI), measures the degree at which the selected mutation reduced the affinity of the enzyme for the inhibitor, the higher the RRI value, the lower the affinity for the mutant with respect to the wild type enzyme. RRI comparison for all the inhibitors tested is shown in Figure 28. It can be seen that the Tyr181Ile mutation caused the highest decrease in the inhibitory potencies for all the compounds tested (Figure 28A), whereas the mutation Leu100Ile only marginally affected the affinity of the enzyme for the IAS derivatives (Figure 28B). Compound **32** was the least affected by all the mutations, showing a 9.7-fold decrease in potency against the Tyr181Ile mutant (Figure 28B), and only a 2-fold decrease against the Lys103Asn mutant (Figure 28C), whereas it was unaffected by the Leu100Ile mutant (RRI≈1, Figure 28B). The activity of the other compounds, on the other hand, was found to be dependent on both the nature of the substituents and the particular mutation analyzed. For example, compounds **37** and **93**, showed a comparable (≈60 fold) loss of potency towards the Lys103Asn mutant (Figure 28C). However, **37** was 5-fold more affected than **93** by the Leu100Ile mutation (Fig. 28B), whereas **93** showed a 12-fold higher reduction of activity than **37** against the Tyr181Ile mutant (Figure 28A). However, when compared to the clinically used compounds nevirapine (NVP) and efavirenz (EFV), the IAS derivative **32** showed a significantly improved resistance profile towards all the tested mutants (Figure 28A–C).

The higher affinity of the IAS derivatives to the complex of RT with its substrates is driven by a faster association rate. In order to clarify the molecular mechanisms for observed mixed-type inhibition exhibited by the IAS inhibitors towards the RT mutants, we evaluated, for the most active compounds 32 and 81, the corresponding association (k_{on}) and dissociation (k_{off}) rates for the three forms of the HIV-1 RT along the reaction pathway, namely the free enzyme, the binary complex of RT with the nucleic acid substrate and the ternary complex of RT with both the nucleic acid and the

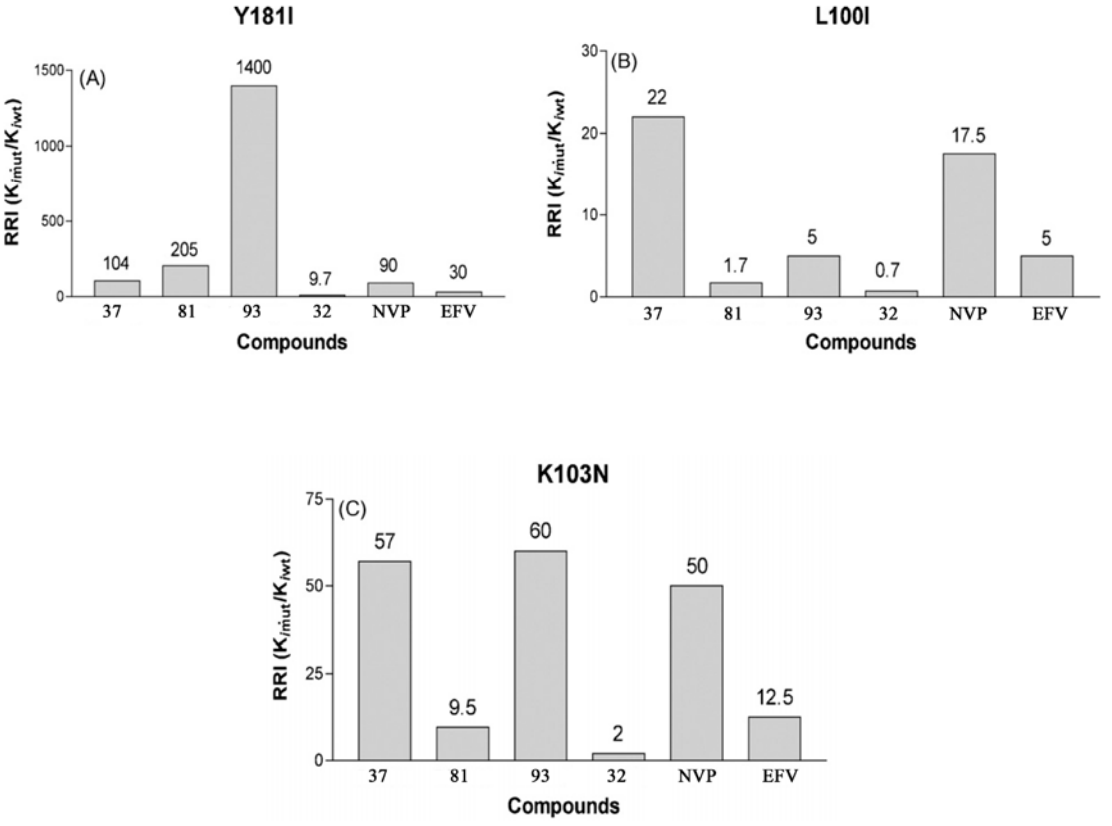

Figure 28. 81 and **32** show high levels of activity towards drug resistant mutants and faster association rates to the binary/ternary complex of HIV-1 RT than to the free enzyme. (A) Relative resistance indexes of the different compounds towards the mutant Tyr181Ile (Y181I). (B) Relative resistance indexes of the different compounds towards the mutant Leu100Ile (L100I). C. Relative resistance indexes of the different compounds towards the mutant Lys103Asn (K103N).

nucleotide substrates. The calculated values are summarized in Table 18. Fig. 29A shows a comparison of the k_{on} and k_{off} values of both compounds for the different enzymatic forms of HIV-1 RT wild type. It can be seen that both compounds showed significantly higher association rates for the binary and ternary complex with respect to the free enzyme, whereas k_{off} values were only slightly different among the different enzymatic forms. These data indicate that the NNBS of HIV-1 RT is more accessible to the IAS derivatives when the enzyme is in complex with its template/primer and substrate, thus explaining the mixed-type mechanism of inhibition observed with these analogs.

***32** shows tighter binding to RT carrying NNRTI-resistance mutations than to the wild type enzyme.* Since the equilibrium dissociation constant K_i is related to these velocities by the relationship $K_i = k_{off}/k_{on}$, a reduced affinity (corresponding to an increase of the K_i value) may be associated to a decrease in k_{on} (slower association) or to an increase in k_{off} (faster dissociation). The association and dissociation rates for the ternary complexes (k^{ter}_{on} and k^{ter}_{off}) were used to calculate the relative association index (RAI = k^{ter}_{on} wt/k^{ter}_{on} mut) and the relative dissociation index (RDI = k^{ter}_{off} mut/k^{ter}_{off} wt) for the most active compounds **32** and **81**. With RAI or RDI values >1, the inhibitor either shows a lower association rate to the mutated enzyme than to the wild type or dissociates more rapidly, the complex formed by the mutant and the inhibitor being unstable. In the case of RAI or RDI values <1, the opposite reasoning holds, revealing a selectivity of the inhibitor to the mutant enzymes. The results are shown in Figure 29. Both the Tyr181Ile and the Lys103Asn mutations significantly decreased the association rates of the compounds to the mutated enzymes (Figure 29B). The clinically relevant compounds EFV and NVP, also showed similar reductions in their association rates with the Lys103Asn mutant. On the other hand, interesting data emerged from RDI value analysis: **32** showed RDI < 1 towards both K103N and Y181I, indicating a significantly (≈10-fold) slower dissociation rate from both the mutant enzymes than from wild type RT (Figure 29C). As a result, the compound **32** dissociated from the Lys103Asn mutant 75-fold and 10-fold more slowly than the reference

Table 18. Kinetic parameters for the interaction of IAS derivatives with HIV-1 RT wild type and drug resistant mutants.

Compd	RT	[*E*][a]		
	WT	K_i^{free} (μM)[b]	K_{on} (s^{-1} μM^{-1}) x 10^2	K_{off} (s^{-1}) x10^2
81		0.04 (±0.004)	9.8 (±0.8)	0.39 (±0.038)
32		0.058 (±0.001)	14.3 (±0.7)	0.83 (±0.08)
NVP[c]		0.4 (±0.06)	0.4 (±0.1)	0.16 (±0.01)
EFV		0.03 (±0.008)	1 (±0.1)	0.03 (±0.01)
	K103N	K_i^{free} (μM)	K_{on} (s^{-1} μM^{-1}) x 10^2	K_{off} (s^{-1}) x10^2
81		0.7 (±0.034)	0.4 (±0.07)	0.28 (±0.022)
32		0.07 (±0.001)	7.5 (±0.87)	0.52 (±0.005)
NVP		3.3 (±0.2)	0.03 (±0.005)	0.1 (±0.02)
EFV		1.5 (±0.2)	0.2 (±0.03)	0.3 (±0.03)
	Y181I	K_i^{free} (μM)	K_{on} (s^{-1} μM^{-1}) x 10^2	K_{off} (s^{-1}) x10^2
81		7.5 (±0.7)	0.05 (±0.01)	0.37 (±0.037)
32		0.2 (±0.03)	0.1 (±0.01)	0.02 (±0.002)

[a][*E*], free enzyme; [b]Values are the means of three independent replicates ±S.D. [c]EFV, efavirenz,; NVP, nevirapine.

Table 18. Kinetic parameters for the interaction of IAS derivatives with HIV-1 RT wild type and drug resistant mutants (*Continued…*).

Compd	RT	[*E*:NA][a]		
	WT	K_i^{bin} (μM)	K_{on} (s^{-1} μM^{-1}) x 10^2	K_{off} (s^{-1}) x10^2
81		0.018 (±0.002)	13.7 (±0.8)	0.23 (±0.023)
32		0.003 (±0.0005)	79 (±7)	0.24 (±0.024)
NVP		0.5 (±0.1)	0.3 (±0.02)	0.15 (±0.01)
EFV		0.03 (±0.007)	1 (±0.1)	0.03 (±1)
	K103N	K_i^{bin} (μM)	K_{on} (s^{-1} μM^{-1}) x 10^2	K_{off} (s^{-1}) x10^2
81		0.17 (±0.017)	3.2 (±0.3)	0.54 (±0.054)
32		0.006 (±0.001)	84 (±8)	0.51 (±0.05)
NVP		3.3 (±0.2)	0.03 (±0.005)	0.1 (±0.02)
EFV		1.6 (±0.3)	0.25 (±0.05)	0.4 (±0.05)
	Y181I	K_i^{bin} (μM)	K_{on} (s^{-1} μM^{-1}) x 10^2	K_{off} (s^{-1}) x10^2
81		3.7 (±0.37)	0.87 (±0.09)	3.2 (±0. 3)
32		0.029 (±0.003)	0.38 (±0.04)	0.011 (±0.001)

[a][*E*:NA], binary complex with nucleic acid; [b]Values are the means of three independent replicates ±S.D. [c]EFV, efavirenz,; NVP, nevirapine.

Table 18. Kinetic parameters for the interaction of IAS derivatives with HIV-1 RT wild type and drug resistant mutants (*Continued…*).

Compd	RT	[*E*:DNA:dTTP][a]		
	WT	K_i^{free} (μM)[a]	K_{on} (s^{-1} μM^{-1}) x 10^2	K_{off} (s^{-1}) x10^2
81		0.018 (±0.002)	27.2 (±0.7)	0.45 (±0.045)
32		0.003 (±0.0005)	176 (±17)	0.53 (±0.053)
NVP		0.4 (±0.08)	0.4 (±0.1)	0.16 (±0.01)
EFV		0.004 (±0.001)	4 (±0.2)	0.016 (±0.3)
	K103N	K_i^{free} (μM)[a]	K_{on} (s^{-1} μM^{-1}) x 10^2	K_{off} (s^{-1}) x10^2
81		0.17 (±0.017)	3.91 (±0.39)	0.66 (±0.067)
32		0.006 (±0.001)	9.4 (±0.94)	0.057 (±0.006)
NVP		5 (±0.5)	0.03 (±0.005)	0.1 (±0.02)
EFV		0.2 (±0.01)	0.6 (±0.01)	0.3 (±0.03)
	Y181I	K_i^{free} (μM)[a]	K_{on} (s^{-1} μM^{-1}) x 10^2	K_{off} (s^{-1}) x10^2
81		3.7 (±0.37)	0.12 (±0.01)	0.44 (±0.044)
32		0.029 (±0.003)	2.1 (±0.2)	0.061 (±0.006)

[a][*E*:NA:dNTP], ternary complex with nucleic acid and nucleotide. [b]Values are the means of three independent replicates ±S.D. [c]EFV, efavirenz,; NVP, nevirapine.

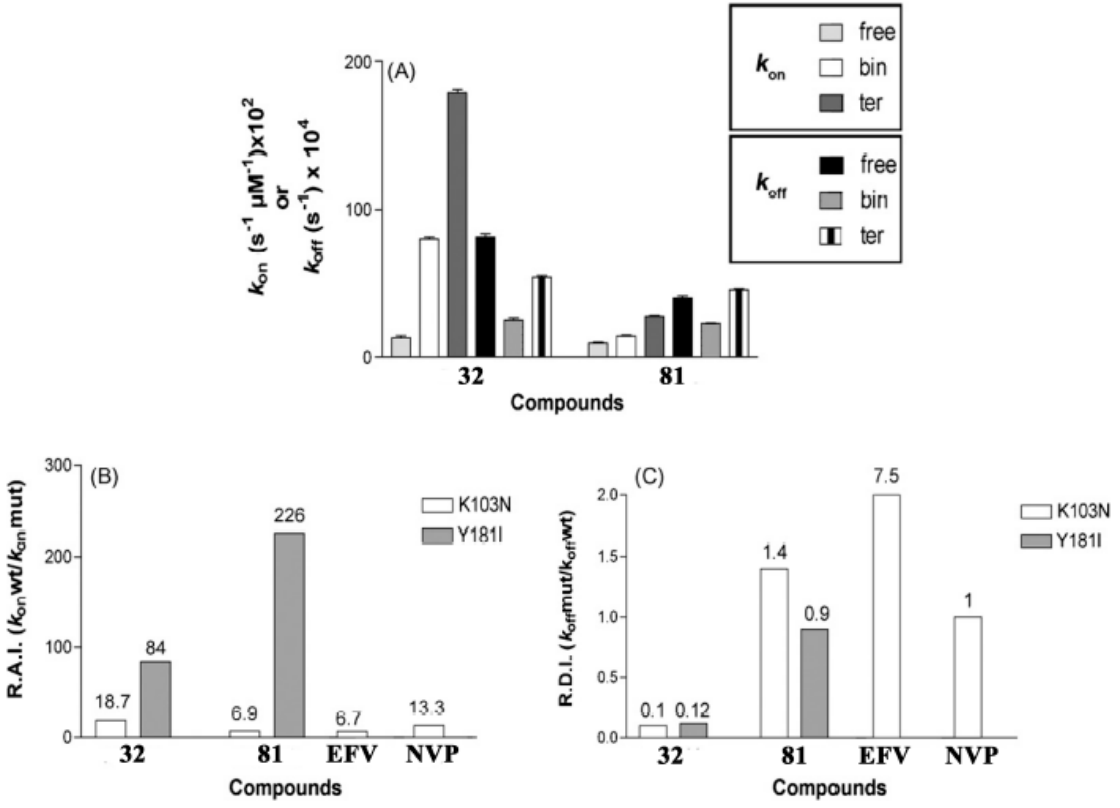

Fig. 5. Compound **32** dissociates from the drug resistant mutant RT enzymes at a slower rate than from the wild type enzyme. (A) Comparison of the association (k_{on}) and dissociation (k_{off}) rates of compounds **32** and **81** for the free enzyme, the binary complex and the ternary complex of HIV-1 RT wild type. (B) Relative association indexes of compounds **32**, **81**, nevirapine (NVP) and efavirenz (EFV) for the Lys103Asn (K103N) mutant (white bars) and of compounds **32**, **81** for the Tyr181Ile (Y181I) mutant (grey bars) RT. (C) Relative dissociation indexes of compounds **32**, **81**, nevirapine (NVP) and efavirenz (EFV) for the Lys103Asn (K103N) mutant (white bars) and of compounds **32**, **81** for the Tyr181Ile (Y181I) mutant (grey bars) RT.

compounds EFV and NVP, respectively. With **32**, the k_{off} for Lys103Asn was only 1.5-fold higher than the k_{off} for RT wt, whereas this compound disassociated from both the mutant Tyr181Ile and RT wild type at the same rate, the corresponding RDI value being ≈1.

The results of kinetic analysis showed that all these compounds have higher association rates (k_{on}) to the binary and ternary complexes than to the free enzyme. One compound, **32**, retained high inhibitory activity towards all the mutants tested, with K_i values ranging between 0.003 and 0.03 μM. This high activity is reflected by the very low resistance indexes, which ranged from 0.7 to 9.7. and it showed a much better activity profile than the reference compounds NVP and EFV towards all the clinically relevant mutants analysed. It has already shown that **32** displayed subnanomolar activities against HIV-1 virus wild type or carrying the Tyr181Cys mutation, and submicromolar activity against the double Tyr181Cys/Lys103Asn mutant virus. The kinetic analysis presented here elucidates the molecular basis for the high activity of **32**. In fact, comparison of the association and dissociation rates between RT wild type and the mutant forms, demonstrated that this compound displayed the highest association and the slowest dissociation rates to the mutated RT forms. The data further indicate that IAS compounds are very flexible molecules, which are able to adapt their conformation in order to achieve an optimal interaction with the NNBS even in the presence of mutations such as Lys103Asn and Tyr181Ile, which are invariably associated with high level resistance to all the clinically used NNRTIs. Our kinetic data suggest that the affinity of the *di-halo*-IAS inhibitors to HIV-1 RT is dictated by the nature of the functional group at position 2 of the indole ring. The reduced binding and/or faster dissociation relative to the mutated forms, especially Tyr181Ile, which was observed for those inhibitors with bulkier substituents at that position with respect to **32**, might be due to steric clashes which obstruct the entrance of the inhibitor into the NNBS pocket and/or reduce the stability of the complex formed.

Conclusion

All reported compounds proved to be highly potent against HIV-1 replication in human T-lymphocyte (CEM) cells, and some showed inhibitory potencies in low nanomolar range which were comparable with the previously reported lead compounds **21** and **32**. For compounds **34**-**57** carrying natural and unnatural amino acids the inhibitory activity against HIV-1 WT seemed only marginally affected by the substituent introduced on the indole nucleus, while it was more important in derivatives **58**-**93**. In general, none of the IASs proved to be markedly cytostatic. Against mutant strains all derivatives were always more potent than Nevirapine and against the L100I and K103N RT HIV-1 strains, many derivatives were superior to EFV. Thus, these new IASs may be potentially useful in EFV-based HIV-1 therapies. The (*D*)-enantiomers **38b** and **39b** were about five times more potent than the corresponding (*L*)-enantiomers **38a** and **39a** against RT.

Derivatives **58**-**93** were also showed a high anti-HIV activity. Particularly the more active compounds were the Mannich derivatives, and the activity decreased when was used a two or three units linker.

Superimposition of PLANTS docked conformations of **42** and the highly active derivative **32** revealed different hydrophobic interactions of the 3,5-dimethylphenyl group, for which a staking interaction with Tyr181 aromatic side chain was observed. In L100I mutated RT the mutation of leucine to isoleucine does not affect the binding mode confirming all the interactions reported for the WT strain. The lower anti-viral activity against the mutant K103N and Y181I RT HIV-1 strains could be the consequence of the reduced interaction between **42** and the mutated residues; for the Y181I RT HIV-1 strain, the limited anti-HIV efficiency could also be caused by the loss of the favourable protein-ligand π-π interactions, while in the K103N mutant, the loss of the hydrophobic interaction between the ligand and the side chain of the lysine 103 might be responsible for the reduced activity.

In kinetic study, IAS **32** showed much slower dissociation rates from both mutant enzymes with respect to HIV-1 RT wild type and showed a superior activity profile towards the Lys103Asn, Leu100Ile and Tyr181Ile mutants with respect to the reference compounds Nevirapine and Efavirenz. The results obtained by this study, as well as the excellent activity demonstrated by these inhibitors in blocking the viral replication in infected cells, suggest a possible use of these compounds for the therapy of HIV. Therefore, further toxicity and pharmacokinetics studies are warranted.

Experimental Section

Chemistry. Microwave-assisted reactions were performed on Discover LabMate (CEM), setting temperature, irradiation power, maximum pressure (Pmax), PowerMAX (simultaneous cooling while heating), ramp and hold times, and open and closed vessel modes as indicated. Melting points (mp) were determined on a Büchi 510 apparatus and are uncorrected. Infrared spectra (IR) were run on Perkin-Elmer 1310 and SpectrumOne spectrophotometers. Band position and absorption ranges are given in cm^{-1}. Proton nuclear magnetic resonance (^1H NMR) spectra were recorded on Bruker AM-200 (200 MHz) and Bruker Avance 400 MHz FT spectrometers in the indicated solvent. Chemical shifts are expressed in δ units (ppm) from tetramethylsilane. Column chromatographies were packed with alumina (Merck, 70-230 mesh) and silica gel (Merck, 70-230 mesh). Aluminium oxide TLC cards (Fluka, aluminium oxide precoated aluminium cards with fluorescent indicator at 254 nm) and silica gel TLC cards (Fluka, silica gel precoated aluminium cards with fluorescent indicator at 254 nm) were used for thin layer chromatography (TLC). Developed plates were visualized with a Spectroline ENF 260C/F UV apparatus. Organic solutions were dried over anhydrous sodium sulphate. Evaporation of the solvents was carried out on a Büchi Rotavapor R-210 equipped with a Büchi V-850 vacuum controller and Büchi V-700 (~ 5 mbar) and V-710 vacuum (~ 2 mbar) pumps. Elemental analyses were found within ±0.4% of the theoretical values.

General Procedure for the Synthesis of Derivatives 34-49. Example. *N*-(3-Amino-3-oxopropyl)-5-chloro-3-[(3,5-dimethylphenyl)sulfonyl]-1*H*-indole-2-carboxamide (42). 28% Ammonium hydroxide (28 mL) was added to a mixture of **139** (0.48 g, 0.001 mol) in ethanol (48 mL). Reaction mixture was stirred at 60 °C for 3 h. After cooling, water was added and the mixture was extracted with ethyl acetate. The organic layer was washed with brine, dried, and

evaporated to furnish a residue which was purified by silica gel column chromatography (ethyl acetate as eluent) to give 19, yield 40%, mp >290 °C (from ethanol). ^{1}H NMR (DMSO-d_6): δ 2.30 (s, 6H), 2.42 (t, *J* = 7.1 Hz, 2H), 3.52 (t, *J* = 6.4 Hz, 2H), 6.90 (broad s, 1H, disappeared on treatment with D_2O), 7.24 (s, 1H), 7.32 (dd, *J* = 8.7 and 1.9 Hz, 1H), 7.41 (broad s, 1H, disappeared on treatment with D_2O) 7.51 (d, *J* = 8.7 Hz, 1H), 7.62 (s, 2H), 7.93 (d, *J* = 1.7 Hz, 1H), 9.03 (broad s, 1H, disappeared with treatment with D_2O), 12.92 ppm (broad s, 1H, disappeared on treatment with D_2O). IR: ν 1637, 3222 cm^{-1}. Anal. ($C_{20}H_{20}ClN_3O_4S$ (433.91)) C H N Cl S.

***N*-(2-Amino-2-oxoethyl)-5-chloro-3-[(3,5-dimethylphenyl)sulfonyl]-1*H*-indole-2-carboxamide (34).** Was synthesized as **42** from **131**. Yield 48%, mp 265-267 °C (from ethanol). ^{1}H NMR (DMSO-d_6): δ 2.31 (s, 6H), 4.01 (m, 2H), 7.27 (s, 1H), 7.30-7.41 (m, 2H, on treatment with D_2O showed dd, *J* = 1.8 and 8.8 Hz, 1H), 7.47 (broad s, 1H, disappeared on treatment with D_2O), 7.57 (d, *J* = 8.8 Hz, 1H), 7.74 (s, 2H), 8.00 (d, *J* = 1.8 Hz, 1H), 9.39 (broad t, *J* = 5.5 Hz, 1H, disappeared on treatment with D_2O), 13.06 ppm (broad s, 1H, disappeared on treatment with D_2O). IR (Nujol): ν 1640, 1680, 3280, 3300, 3400 cm^{-1}. Anal. ($C_{19}H_{18}ClN_3O_4S$ (419.88)), C, H, N, Cl, S.

***N*-(2-Amino-2-oxoethyl)-5-bromo-3-[(3,5-dimethylphenyl)sulfonyl]-1*H*-indole-2-carboxamide (35).** Was synthesized as **42** using **132**. Yield 57%, mp 274-276 °C (from ethanol). ^{1}H NMR (DMSO-d_6): δ 2.32 (s, 6H), 4.01 (s, 2H), 7.27 (s, 1H), 7.33 (broad s, 1H, disappeared on treatment with D_2O), 7.47-7.49 (m, 2H), 7.52 (d, *J* = 8.2 Hz, 1H), 7.73 (s, 2H), 8.17 (s, 1H), 9.39 (broad s, 1H, disappeared on treatment with D_2O), 13.08 ppm (s, 1H, disappeared on treatment with D_2O). IR: ν 1639, 1693, 3243, 3445 cm^{-1}. Anal. ($C_{19}H_{18}BrN_3O_4S$ (464.33)) C H Br N S.

***N*-(2-Amino-2-oxoethyl)-3-[(3,5-dimethylphenyl)sulfonyl]-5-nitro-1*H*-indole-2-carboxamide (36).** Was synthesized as **42** using **133**. Yield 42%, mp 259-261 °C (from ethanol). ^{1}H NMR (DMSO-d_6): δ 2.29 (s, 6H), 4.00 (s, 2H), 7.26 (s, 1H), 7.31 (s, 1H, disappeared on treatment with D_2O), 7.46 (s, 1H, disappeared on

treatment with D_2O), 7.70-7.71 (m, 3H), 8.16 (d, *J* = 8,3 Hz, 1H), 8.89 (s, 1H), 9.33 (s, 1H, disappeared on treatment with D_2O), 13,42 ppm (s, 1H, disappeared on treatment with D_2O). IR: ν 1681, 3291 cm^{-1}. Anal. ($C_{19}H_{18}N_4O_6S$ (430.43)) C, H, N, S.

***N*-(2-Amino-2-oxoethyl)-5-chloro-3-[(3,5-dimethylphenyl)sulfonyl]-4-fluoro-1*H*-indole-2-carboxamide (37).** Was synthesized as **42** using **134**. Yield 95%, mp 255-257 °C (from ethanol). ^1H NMR (DMSO-d_6): δ 2.32 (m, 6H), 3.92 (s, 2H), 7.26 (s, 1H), 7.28-7.42 (m, 4H), 7.66 (s, 2H), 9.47 (broad s, 1H, disappeared on treatment with D_2O), 13.27 (broad s, 1H, disappeared on treatment with D_2O). IR: ν 1662, 1703, 3280 cm^{-1}. Anal. ($C_{19}H_{17}ClFN_3O_4S$ (437.87)) C H Cl F N S.

***N*-(1-Amino-1-oxopropan-2-yl)-5-chloro-3-[(3,5-dimethylphenyl)sulfonyl]-1*H*-indole-2-carboxamide (38).** Was synthesized as **42** from **135**. Yield 42%, mp 238-240 °C (from ethanol). ^1H NMR (DMSO-d_6): δ 1.40 (d, *J* = 6.9 Hz, 3H), 2.30 (s, 6H), 4.53 (m, 1H), 7.21-7.41 (m, 3H), 7.56 (m, 2H), 7.70 (s, 2H), 8.05 (m, 1H), 9.36 (d, *J* = 7.0, 1H, disappeared on treatment with D_2O, 13.10 ppm (very broad, 1H, disappeared on treatment with D_2O). IR (nujol): ν 1635, 3190 cm^{-1}. Anal. ($C_{20}H_{20}ClN_3O_4S$ (433.90)), C, H, N, Cl, S.

***N*-(1-Amino-1-oxopropan-2-yl)-5-bromo-3-[(3,5-dimethylphenyl)sulfonyl]-1*H*-indole-2-carboxamide (39).** Was synthesized as **42** using **136**. Yield 43%, mp 248-251 °C (from ethanol). ^1H NMR (DMSO-d_6): δ 1.37 (d, *J* = 7.1 Hz, 3H), 2.29 (s, 6H), 4.46-4.54 (qn, *J* = 7.1 Hz, 1H), 7.26 (s, 2H), 7.46 (dd, *J* = 8.7 and 1.7 Hz, 1H), 7.49-7.52 (m, 2H), 7.68 (s, 2H), 8.15 (d, *J* = 1.7 Hz, 1H), 9.32 (s, 1H, disappeared on treatment with D_2O), 13.05 ppm (s, 1H, disappeared on treatment with D_2O). IR: ν 1662, 1672, 3254, 3465 cm^{-1}. Anal. ($C_{20}H_{20}BrN_3O_4S$ (478.36)) C H Br N S.

***N*-(1-Amino-1-oxopropan-2-yl)-3-[(3,5-dimethylphenyl)sulfonyl]-5-nitro-1*H*-indole-2-carboxamide (40).** Was synthesized as **42** using **137**. Yield 99%, mp 245-250 °C (from ethanol). ^1H NMR (DMSO-d_6): δ 1.37 (d, *J* = 7.0 Hz, 3H), 2.29 (s, 6H), 4.46-4.54 (qn, *J* = 7.1 Hz, 1H), 7.27 (s, 1H), 7.50 (s, 1H, disappeared on

treatment with D_2O), 7.66 (s, 1H, disappeared on treatment with D_2O), 7.68 (s, 2H), 7.71 (d, *J* = 9.1 Hz, 1H), 8.17 (dd, *J* = 9.0 and 2.0 Hz, 1H), 8.90 (d, *J* = 1.9 Hz, 1H), 9.29 (s, 1H, disappeared on treatment with D_2O), 12.95 ppm (s, 1H, disappeared on treatment with D_2O). IR: ν 1673, 3275, 3409 cm^{-1}. Anal. ($C_{20}H_{20}N_4O_6S$ (444.46)) C, H, N, S.

***N*-(1-Amino-1-oxopropan-2-yl)-5-chloro-3-[(3,5-dimethylphenyl)sulfonyl]-4-fluoro-1*H*-indole-2-carboxamide (41).** Was synthesized as **42** using **138**. Yield 79%, mp 249-250 °C (from ethanol). ^1H NMR (DMSO-d_6): δ 1.39 (d, *J* = 7.1 Hz, 3H), 2.32 (m, 6H), 4.44 (q, *J* = 7.2 Hz, 1H), 7.26 (s, 1H), 7.29 (broad s, 1H, disappeared on treatment with D_2O), 7.35 (broad s, 1H, disappeared on treatment with D_2O), 7.36-7.40 (m, 2H), 7.68 (s, 2H), 9.37 (broad s, 1H, disappeared on treatment with D_2O), 13.26 (broad s, 1H, disappeared on treatment with D_2O). IR: ν 1655, 1698, 3245 cm^{-1}. Anal. ($C_{20}H_{19}ClFN_3O_4S$ (451.90)) C H Cl F N S.

***N*-(3-Amino-3-oxopropyl)-5-bromo-3-[(3,5-dimethylphenyl)sulfonyl]-1*H*-indole-2-carboxamide (43).** Was synthesized as **42** using **140**. Yield 99%, mp 258-260 °C (from ethanol). ^1H NMR (DMSO-d_6): δ 2.32 (s, 6H), 2.47 (t, *J* = 7.1 Hz, 2H), 3.58 (t, *J* = 7.1 Hz, 2H), 6.98 (broad s, 1H, disappeared on treatment with D_2O), 7.26 (s, 1H), 7.44-7.49 (m, 3H), 7.64 (s, 2H), 8.10 (s, 1H), 9.03 (s, 1H, disappeared on treatment with D_2O), 13.07 ppm (s, 1H, disappeared on treatment with D_2O). IR: ν 1635, 1665, 3212, 3273, 3473 cm^{-1}. Anal. ($C_{20}H_{20}BrN_3O_4S$ (478.36)) C H Br N S.

***N*-(3-Amino-3-oxopropyl)-3-[(3,5-dimethylphenyl)sulfonyl]-5-nitro-1*H*-indole-2-carboxamide (44).** Was synthesized as **42** using **141**. Yield: 99%, mp 260 °C (from ethanol). ^1H NMR (DMSO-d_6): δ 2.29 (s, 6H), 2.44 (t, *J* = 7.1 Hz, 2H), 3.54 (q, *J* = 6.6 Hz, 2H), 6.69 (broad s, 1H, disappeared on treatment with D_2O), 7.25 (s, 1H), 7.45 (broad s, 1H, disappeared on treatment with D_2O), 7.64 (s, 2H), 7.68 (d, *J* = 9.1 Hz, 1H), 8.16 (dd, *J* = 9.1 and 2.3 Hz, 1H), 8.84 (d, *J* = 2.2 Hz, 1H), 9.06 (broad s, 1H, disappeared on treatment with D_2O), 13.44 ppm (broad

s, 1H, disappeared on treatment with D_2O). IR: ν 1639, 11656, 3190, 3288, 3436 cm^{-1}. Anal. ($C_{20}H_{20}N_4O_6S$ (444.46)) C, H, N, S.

***N*-(3-amino-3-oxopropyl)-5-chloro-3-[(3,5-dimethylphenyl)sulfonyl]-4-fluoro-1*H*-indole-2-carboxamide (45).** Was synthesized as **42** using **142**. Yield 94%, mp 240-242 °C (from ethanol). ^1H NMR (DMSO-d_6): δ 2.32 (m, 6H), 2.43 (t, *J* = 7.3 Hz, 2H), 3.49 (t, *J* = 7.1 Hz, 2H), 6.88 (broad s, 1H, disappeared on treatment with D_2O), 7.25 (s, 1H), 7.31-7.39 (m, 3H), 7.65 (s, 2H), 9.05 (broad s, 1H, disappeared on treatment with D_2O), 13.13 (broad s, 1H, disappeared on treatment with D_2O). IR: ν 1649, 1704, 3267, 3496 cm^{-1}. Anal. ($C_{20}H_{19}ClFN_3O_4S$ (451.90)) C H Cl F N S.

***N*-(4-Amino-4-oxobutan-3-yl)-5-chloro-3-[(3,5-dimethylphenyl)sulfonyl]-1*H*-indole-2-carboxamide (46).** Was synthesized as **42** staring from **143**. Yield 43%, mp 237-240 °C (from ethanol). ^1H NMR (DMSO-d_6): δ 1.26 (d, *J* = 6.6 Hz, 3H), 2.32 (s, 6H), 2.44 (dd, *J* = 15.7 and 7.9 Hz, 1H), 2.67 (dd, *J* = 15.8 and 5.0 Hz, 1H), 4.33-4.40 (m, 1H), 7.26 (s, 1H), 7.31 (broad s, 1H disappeared on treatment with D_2O), 7.34 (d, *J* = 8.7 Hz, 1H), 7.51 (broad s, 1H, disappeared on treatment with D_2O), 7.54 (d, *J* = 8.6 Hz, 1H), 7.64 (s, 2H), 7.95 (s, 1H), 9.02 (broad s, 1H, disappeared with treatment with D_2O), 12.72 ppm (broad s, 1H, disappeared on treatment with D_2O). IR: ν 1647, 1711, 3204, cm^{-1}. Anal. ($C_{21}H_{22}ClN_3O_4S$ (447.94)) C H N Cl S.

***N*-(4-Amino-4-oxobutan-3-yl)-5-bromo-3-(3,5-dimethylphenylsulfonyl)-1*H*-indole-2-carboxamide (47).** Was synthesized as **42** using **144**. Yield: 8%, mp 225-228 °C (from ethanol). ^1H NMR (DMSO-d_6): δ 1.22 (d, *J* = 6.6 Hz, 3H), 2.29-2.32 (m, 7H), 2.45-2.49 (m, 1H), 4.27-4.32 (m, 1H), 6.90 (broad s, 1H, disappeared on treatment with D_2O), 7.26 (s, 1H), 7.41-7.46 (m, 2H), 7.48 (d, *J* = 8.7 Hz, 1H), 7.62 (s, 2H), 8.08 (d, *J* = 1.5 Hz, 1H), 8.9 (broad s, 1H, disappeared on treatment with D_2O), 13.00 ppm (s, 1H, disappeared on treatment with D_2O). IR: ν 1610, 1644, 3299, 3425 cm^{-1}. Anal. ($C_{21}H_{22}BrN_3O_4S$ (492.39)) C H Br N S.

***N*-(4-Amino-4-oxobutan-3-yl)-3-[(3,5-dimethylphenyl)sulfonyl]-5-nitro-1*H*-indole-2-carboxamide (48).** A mixture of **145** (0.30 g, 0.0006 mol) and 28% ammonium hydroxide (2 mL) was treated with microwave irradiation at 150 W, while the temperature ramped from 25 °C to 130 °C in about 3 min. The reaction mixture was maintained at 130 °C for 10 min under stirring (press max 250 psi). The reaction mixture was neutralized with 1N HCl and extracted with ethyl acetate. The organic layer was washed with brine, dried and evaporated. The residue was purified by silica gel column chromatography (ethyl acetate-ethanol 9:1 as eluent) to give 25. Yield 65%, mp 264-268 °C (from ethanol). ^{1}H NMR (DMSO-d_6): δ 1.25 (d, J = 6.6 Hz, 3H), 2.29-234 (m, 8H), 4.32-4.44 (m, 1H), 6.94 (broad s, 1H, disappeared on treatment with D_2O), 7.29 (s, 1H), 7.47 (broad s, 1H, disappeared on treatment with D_2O), 7.66 (s, 2H), 7.71 (d, J = 9.1 Hz, 1H), 8.19 (dd, J = 9.0 and 2.0 Hz, 1H), 8.85 (d, J = 1.4 Hz, 1H), 9.00 (broad s, 1H, disappeared with treatment with D_2O), 13.46 ppm (broad s, 1H, disappeared on treatment with D_2O). IR: ν 1639, 1657, 3232, 3437 cm^{-1}. Anal. ($C_{21}H_{22}N_4O_6S$ (458.49)) C H N S.

***N*-(4-Amino-4-oxobutan-2-yl)-5-chloro-3-[(3,5-dimethylphenyl)sulfonyl]-4-fluoro-1*H*-indole-2-carboxamide (49).** Was synthesized as **42** from **146**. Yield: 22%, mp 217-219 °C (from ethanol). ^{1}H NMR (DMSO-d_6): δ 1.19 (d, J = 6.7 Hz, 3H), 2.17-2.20 (m, 1H), 2.31 (s, 6H), 2.44-2.49 (m, 1H), 4.29-4.37 (m, 1H), 6.89 (broad s, 1H, disappeared on treatment with D_2O), 7.24 (s, 1H), 7.31-7.38 (m, 2H), 7.43 (broad s, 1H, disappeared on treatment with D_2O), 7.66 (s, 2H), 8.96 (broad s, 1H, disappeared on treatment with D_2O), 13.22 (broad s, 1H, disappeared on treatment with D_2O). IR: ν 1625, 1691, 3194 cm^{-1}. Anal. ($C_{21}H_{21}ClFN_3O_4S$ (465.93)) C H Cl F N S.

General Procedure for the Synthesis of Derivatives 50-57, 70-72, 75, 76, 78-80, 82-84, 86-88, 90-92 and 131-146. Example. Methyl 3-[*N*-[5-chloro-3-[(3,5-dimethylphenyl)sulfonyl]-1*H*-indole-2-carboxamido]]propanoate (139). A mixture of **127**[73] (0.70 g, 0.0019 mol), methyl β-alanine hydrochloride (0.52 g, 0.0037 mol), triethylamine (0.57 g, 0.79 mL, 0.0056 mol) and BOP (0.80 g,

0.0019 mol) in DMF (10 mL) was stirred at room temperature overnight. Water was added and the mixture was extracted with ethyl acetate. The organic layer was washed with brine, dried, and evaporated to dryness. The residue was purified by silica gel column chromatography (ethyl acetate as eluent) to give 59, yield 81%, mp 197-200 °C (from ethanol). ^{1}H NMR (DMSO-d_6): δ 2.29 (s, 6H), 2.65 (t, *J* = 6.7 Hz, 2H), 3.58 (t, *J* = 6.3 Hz, 2H), 3.61 (s, 3H), 7.24 (s, 1H), 7.31 (dd, *J* = 8.8 and 1.9 Hz, 1H), 7.51 (d, *J* = 8.8 Hz, 1H), 7.60 (s, 2H), 7.90 (d, *J* = 2.0 Hz, 1H), 9.08 (broad s, 1H, disappeared with treatment with D_2O), 13.00 ppm (broad s, 1H, disappeared on treatment with D_2O). IR: ν 1738, 3204 cm^{-1}. Anal. ($C_{21}H_{21}ClN_2O_5S$ (448.92)) C H N Cl S.

5-Chloro-3-[(3,5-dimethylphenyl)sulfonyl]-*N*-(2-sulfamoylethyl)-1*H*-indole-2-carboxamide (50). Was synthesized as **139** using 2-aminoethanesulfonamide hydrochloride.[20] Yield 21%, mp 245-247 °C (from ethanol). ^{1}H NMR (DMSO-d_6): δ 2.32 (s, 6H), 3.27-3.35 (m, 2H), 3.72-3.77 (m, 2H), 7.05 (broad s, 2H, disappeared on treatment with D_2O), 7.26 (s, 1H), 7.35 (dd, *J* = 8.8 and 2.1 Hz, 1H), 7.55 (d, *J* = 8.8 Hz, 1H), 7.67 (s, 2H), 7.92 (d, *J* = 2.1 Hz, 1H), 9.19 (broad s, 1H, disappeared with treatment with D_2O), 13.05 ppm (broad s, 1H, disappeared on treatment with D_2O). IR: ν 1641, 3228 cm^{-1}. Anal. ($C_{19}H_{20}ClN_3O_5S_2$ (469.96)) C H N Cl S.

5-Bromo-3-[(3,5-dimethylphenyl)sulfonyl]-*N*-(2-sulfamoylethyl)-1*H*-indole-2-carboxamide (51). Was synthesized as **139** using **128** and 2-aminoethanesulfonamide hydrochloride. Yield 32%, mp 260 °C (from ethanol). ^{1}H NMR (DMSO-d_6): δ 2.32 (s, 6H), 3.31 (t, *J* = 7.5 Hz, 2H), 3.73 (t, *J* = 6.8 Hz, 2H), 7.06 (broad s, 2H, disappeared on treatment with D_2O), 7.26 (s, 1H), 7.45 (dd, *J* = 8.7 and 1.7 Hz, 1H), 7.50 (d, *J* = 8.7 Hz, 1H), 7.67 (s, 2H), 8.06 (d, *J* = 1.7 Hz, 1H), 9.19 (broad s, 1H, disappeared with treatment with D_2O), 13.08 ppm (broad s, 1H, disappeared on treatment with D_2O). IR: ν 1646, 3226 cm^{-1}. Anal. ($C_{19}H_{20}BrN_3O_5S_2$ (514.41)) C H N Br S.

3-[(3,5-Dimethylphenyl)sulfonyl]-5-nitro-*N*-(2-sulfamoylethyl)-1*H*-indole-2-carboxamide (52). Was synthesized as **139** using **129** and 2-

aminoethanesulfonamide hydrochloride. Yield 14%, mp 265-268 °C (from ethanol). ^{1}H NMR (DMSO-d_6): δ 1.06 (t, J = 7.0 Hz, 2H), 2.32 (s, 6H), 3.72-3.76 (m, 2H), 7.06 (broad s, 2H, disappeared on treatment with D_2O), 7.28 (s, 1H), 7.68 (s, 2H), 7.73 (d, J = 9.1 Hz, 1H), 8.19 (dd, J = 9.1 and 2.2 Hz, 1H), 8.82 (d, J =1.8 Hz, 1H), 9.24 (broad s, 1H, disappeared on treatment with D_2O), 13.48 ppm (broad s, 1H, disappeared on treatment with D_2O). IR: ν 3205, 1637 cm^{-1}. Anal. ($C_{19}H_{20}N_3O_5S_2$ (514.41)) C H N S.

5-Chloro-3-[(3,5-dimethylphenyl)sulfonyl]-4-fluoro-*N*-(2-sulfamoylethyl)-1*H*-indole-2-carboxamide (53). Was synthesized as **139** using **130** and 2-aminoethanesulfonamide hydrochloride. Yield 28%, mp 238-240 °C (from ethanol). ^{1}H NMR (DMSO-d_6): δ 2.32 (s, 6H), 3.30 (t, J = 7.8 Hz, 2H), 3.69 (t, J = 6.8 Hz, 2H), 7.03 (broad s, 2H, disappeared on treatment with D_2O), 7.26 (s, 1H), 7.33-7.41 (m, 2H), 7.65 (s, 2H), 9.25 (broad s, 1H, disappeared with treatment with D_2O), 13.22 ppm (broad s, 1H, disappeared on treatment with D_2O). IR: ν 1646, 3242 cm^{-1}. Anal. ($C_{19}H_{19}ClFN_3O_5S_2$ (487.95)) C H N Cl F S.

5-Chloro-3-[(3,5-dimethylphenyl)sulfonyl]-*N*-(1-sulfamoylpropan-2-yl)-1*H*-indole-2-carboxamide (54). Was synthesized as **139** using **152** Yield 12%, mp 212-214 °C (from ethanol). ^{1}H NMR (DMSO-d_6): δ 1.42 (d, J = 6.6 Hz, 3H), 2.32 (s, 6H), 3.19 (dd, J = 13.9 and 8.3 Hz, 1H), 3.42 (dd, J = 13.8 and 4.4 Hz, 1H), 4.48-4.51 (m, 1H), 7.02 (broad s, 2H, disappeared on treatment with D_2O), 7.26 (s, 1H), 7.34 (dd, J = 8.6 and 1.8 Hz, 1H), 7.54 (d, J = 8.8 Hz, 1H), 7.66 (s, 2H), 7.91 (d, J = 1.8 Hz, 1H), 9.09 (broad s, 1H, disappeared with treatment with D_2O), 12.98 ppm (broad s, 1H, disappeared on treatment with D_2O). IR: ν 1643, 3255 cm^{-1}. Anal. ($C_{20}H_{22}ClN_3O_5S_2$ (483.99)) C H N Cl S.

5-Bromo-3-[(3,5-dimethylphenyl)sulfonyl]-*N*-(1-sulfamoylpropan-3-yl)-1*H*-indole-2-carboxamide (55). Was synthesized as **139** using **128** and **152**. Yield 8%, mp 155-159 °C (from ethanol). ^{1}H NMR (DMSO-d_6): δ 1.41 (d, J = 6.7 Hz, 3H), 2.32 (s, 6H), 3.17-3.23 (m, 1H), 3.38-3.43 (m, 1H), 4.46-4.53 (m, 1H), 7.03 (broad s, 2H, disappeared on treatment with D_2O), 7.27 (s, 1H), 7.46 (dd, J = 8.7 and 1.8 Hz, 1H), 7.50 (d, J = 8.7 Hz, 1H), 7.66 (s, 2H), 8.06 (d, J = 1.8 Hz,

1H), 9.11 (broad s, 1H, disappeared with treatment with D_2O), 13.00 ppm (broad s, 1H, disappeared on treatment with D_2O). IR: ν 1637, 3257 cm^{-1}. Anal. ($C_{20}H_{22}BrN_3O_5S_2$ (528.44)) C H N Br S.

3-[(3,5-Dimethylphenyl)sulfonyl]-5-nitro-*N*-(1-sulfamoylpropan-2-yl)-1*H*-indole-2-carboxamide (56). Was synthesized as **139** using **129** and **52**. Yield 21%, mp 226-229 °C (from ethanol). ^1H NMR (DMSO-d_6): δ 1.42 (d, *J* = 6.7 Hz, 3H), 2.32 (s, 6H), 3.16-3.22 (m, 1H), 3.37-3.42 (m, 1H), 4.47-4.52 (m, 1H), 7.05 (broad s, 2H, disappeared on treatment with D_2O), 7.29 (s, 1H), 7.67 (s, 2H), 7.73 (d, *J* = 9.0 Hz, 1H), 8.19 (dd, *J* = 9.0 and 2.2 Hz, 1H), 8.81 (d, *J* = 1.9 Hz, 1H), 9.15 (broad s, 1H, disappeared with treatment with D_2O), 13.44 ppm (broad s, 1H, disappeared on treatment with D_2O). IR: ν 1655, 3239 cm^{-1}. Anal. ($C_{20}H_{22}N_4O_7S_2$ (494.54) C H N S.

5-Chloro-3-[(3,5-dimethylphenyl)sulfonyl]-4-fluoro-*N*-(1-sulfamoylpropan-2-yl)-1*H*-indole-2-carboxamide (57). Was synthesized as **139** using **130** and **152**. Yield 20%, mp 193-197 °C (from ethanol). ^1H NMR (DMSO-d_6): δ 1.40 (d, *J* = 6.5 Hz, 3H), 2.31 (s, 6H), 3.13 (dd, *J* = 13.5 and 9.0 Hz, 1H), 3.45 (dd, *J* = 13.5 and 3.6 Hz, 1H), 4.43-4.50 (m, 1H), 7.01 (broad s, 2H, disappeared on treatment with D_2O), 7.25 (s, 1H), 7.31-7.41 (m, 2H), 7.65 (s, 2H), 9.16 (broad s, 1H, disappeared with treatment with D_2O), 13.19 ppm (broad s, 1H, disappeared on treatment with D_2O). IR: ν 1629, 3293 cm^{-1}. Anal. ($C_{20}H_{21}ClFN_3O_5S_2$ (501.98)) C H N Cl F S.

***N*-Benzyl-5-chloro-3-(3,5-dimethylphenylsulfonyl)-1*H*-indole-2-carboxamide (70).** Was synthesized as **139** using benzylamine. Yield: 43%. Pale yellow solid, mp 259-262 °C (from ethanol). ^1H NMR ($CDCl_3$): δ 2.26 (s, 6H), 4.80 (d, *J* = 2.9 Hz, 2H), 7.15 (s, 1H), 7.25-7.27 (m, 2H), 7.35-7.50 (m, 5H), 8.24-8.25 (m, 1H), 10.17 (broad s, 1H, disappeared on treatment with D_2O), 11.25 ppm (broad s, 1H, disappeared on treatment with D_2O). IR: ν 1638, 3209 cm^{-1}. Anal ($C_{24}H_{21}ClN_2O_3S$ (452.95)) C H Cl N S.

***N*-Benzyl-5-bromo-3-(3,5-dimethylphenylsulfonyl)-1*H*-indole-2-carboxamide (71).** Was synthesized as **139** using **128** and benzyl amine. Yield: 50%. White

solid, mp 266-269 °C (from ethanol). ^{1}H NMR (DMSO-d_6): δ 2.26 (s, 6H), 4.58 (d, *J* = 5.6 Hz, 2H), 7.24 (s, 1H), 7.27 (t, *J* = 7.7 Hz, 1H), 7.34 (t, *J* = 7.1 Hz, 2H), 7.43-7.50 (m, 4H), 7.58 (s, 2H), 8.08 (s, 1H), 9.42 (broad s, 1H, disappeared on treatment with D_2O), 13.03 ppm (broad s, 1H, disappeared on treatment with D_2O). IR: ν 1645, 3214 cm^{-1}. Anal ($C_{24}H_{21}BrN_2O_3S$ (497.40)) C H Br N S.

***N*-Benzyl-3-(3,5-dimethylphenylsulfonyl)-5-nitro-1*H*-indole-2-carboxamide (72).** Was synthesized as **139** from **129** using benzyl amine. Yield: 55%. White solid, mp 246-248 °C (from ethanol). ^{1}H NMR (DMSO-d_6): δ 2.26 (s, 6H), 4.59 (d, *J* = 5.7 Hs, 2H), 7.25 (s, 1H), 7.29 (t, *J* = 7.2 Hz, 1H), 7.37 (t, *J* = 7.5 Hz, 2H), 7.45 (d, *J* = 7.3 Hz, 2H), 7.61 (s, 2H), 7.70 (d, *J* = 9.1 Hz, 1H), 8.17 (dd, J = 9.0 and 2.3 Hz, 1H), 9.47 (broad s, 1H, disappeared on treatment with D_2O), 13.50 ppm (broad s, 1H, disappeared on treatment with D_2O). IR: ν 1637, 3190, 3281 cm^{-1}. Anal ($C_{24}H_{21}N_3O_5S$ (463.51)) C H N S.

5-Bromo-3-(3,5-dimethylphenylsulfonyl)-*N*-(2-(pyrrolidin-1-yl)ethyl)-1*H*-indole-2-carboxamide (75). Was synthesized as **139** using **128** and 2-(pyrrolidin-1-yl)ethanamine. Yield: 70%. White solid, mp 207-210 °C (from ethanol). ^{1}H NMR (DMSO-d_6): δ 1.67-1.71 (m, 4H), 2.30 (s, 6H), 2.52-2.56 (m, 4H), 2.66 (t, *J* = 6.8 Hz, 2H), 3.47 (q, *J* = 6.9 Hz, 2H), 7.25 (s, 1H), 7.38-7.48 (m, 2H), 7.61 (s, 2H), 8.1 (s, 1H), 9.00 (broad s, 1H, disappeared on treatment with D_2O), 13.05 ppm (broad s, 1H, disappeared on treatment with D_2O). IR: ν 1648, 3204 cm^{-1}. Anal ($C_{23}H_{26}BrN_3O_3S$ (504.44)) C H Br N S.

3-(3,5-Dimethylphenylsulfonyl)-5-nitro-*N*-(2-(pyrrolidin-1-yl)ethyl)-1*H*-indole-2-carboxamide (76). Was synthesized as **139** using **129** and 2-(pyrrolidin-1-yl)ethanamine. Yield: 46%. White solid, mp 216-218 °C (from ethanol). ^{1}H NMR (DMSO-d_6): δ 1.74-1.78 (m, 4H), 2.28 (s, 6H), 2.81-2.85 (m, 4H), 2.90 (t, *J* = 6.3 Hz, 2H), 3.50 (q, *J* = 6.2 Hz, 2H), 7.20 (s, 1H), 7.57-7.62 (m, 3H), 8.02 (dd, *J* = 9.0 and 2.1 Hz, 1H), 8.84-8.89 (m, 2H), 13.46 ppm (broad s,1H, disappeared on treatment with D_2O). IR: ν 1643, 3181 cm^{-1}. Anal ($C_{23}H_{26}N_4O_5S$ (470.54)) C H N S.

***N*-(2-(1*H*-pyrrol-1-yl)ethyl)-5-chloro-3-(3,5-dimethylphenylsulfonyl)-1*H*-indole-2-carboxamide (78).** Was synthesized as **139** using 2-(1*H*-pyrrol-1-yl)ethanamine. Yield: 38%. White solid, mp 200-203 °C (from ethanol). ^{1}H NMR (DMSO-d_6): δ 2.31 (s, 6H), 3.66 (q, *J* = 6.1 Hz, 2H), 4.14 (t, *J* = 6.2 Hz, 2H), 6.01 (t, *J* = 2.1 Hz, 2H), 6.87 (t, *J* = 2.1 Hz, 2H), 7.26 (s, 1H), 7.34 (dd, *J* = 8.8 and 2.0 Hz, 1H), 7.54 (d, *J* = 8.8 Hz, 1H), 7.65 (s, 2H), 7.91 (d, *J* = 1.9 Hz, 1H), 9.18 (broad s, 1H, disappeared on treatment with D_2O), 13.08 ppm (broad s, 1H, disappeared on treatment with D_2O). IR: ν 1638, 3215cm^{-1}. Anal ($C_{23}H_{22}ClN_3O_3S$ (455.96)) C H Cl N S.

***N*-(2-(1*H*-Pyrrol-1-yl)ethyl)-5-bromo-3-(3,5-dimethylphenylsulfonyl)-1*H*-indole-2-carboxamide (79).** Was synthesized as **139** using **128** and 2-(1*H*-pyrrol-1-yl)ethanamine. Yield: 29%. White solid, mp 213-216 °C (from ethanol). ^{1}H NMR (DMSO-d_6): δ 2.30 (s, 6H), 3.65 (q, *J* = 5.2 Hz, 2H), 4.12 (t, *J* = 6.4 Hz, 2H), 5.99 (s, 2H), 6.84 (s, 2H), 7.25 (s, 1H), 7.43-7.49 (m, 2H), 7.16 (s, 2H), 8.04 (s, 1H), 9.14 (broad s, 1H, disappeared on treatment with D_2O), 13.00 ppm (broad s, 1H, disappeared on treatment with D_2O). IR: ν 1655, 3195 cm^{-1}. Anal ($C_{23}H_{22}BrN_3O_3S$ (500.41)) C H Br N S.

***N*-(2-(1*H*-Pyrrol-1-yl)ethyl)-3-(3,5-dimethylphenylsulfonyl)-5-nitro-1*H*-indole-2-carboxamide (80).** Was synthesized as **139** using **129** and 2-(1*H*-pyrrol-1-yl)ethanamine. Yield: 76%. Pale yellow solid, mp 234-237 °C (from ethanol). ^{1}H NMR (DMSO-d_6): δ 2.30 (s, 6H), 3.65 (q, *J* = 5.95 Hz, 2H), 4.12 (t, *J* = 6.1 Hz, 2H), 7.27 (s, 1H), 7.65 (s, 2H), 7.69 (d, *J* = 9.1 Hz, 1H), 8.16 (dd, *J* = 9.2 and 1.7 Hz, 1H), 8.80 (d, *J* = 1.9 Hz, 1H), 9.18 (broad s,1H, disappeared on treatment with D_2O), 13.44 ppm (broad s,1H, disappeared on treatment with D_2O). IR: ν 1648, 3228 cm^{-1}. Anal ($C_{23}H_{22}N_4O_5S$ (466.51)) C H N S.

5-Chloro-3-(3,5-dimethylphenylsulfonyl)-*N*-(2-morpholinoethyl)-1*H*-indole-2-carboxamide (82). Was synthesized as **139** using 2-morpholin-4-ylethanamine. Yield: 25%. White solid, mp 208-210 °C (from ethanol). ^{1}H NMR (DMSO-d_6): δ 2.31 (s, 6H), 2.48-2.53 (m, 4H), 3.50-3.59 (m, 8H), 7.28 (s, 1H), 7.34 (d, *J* = 9.0 Hz, 1H), 7.54 (d, *J* = 8.12 Hz, 1H), 7.63 (s, 2H), 7.97 (s, 1H), 9.09 (broad s, 1H,

disappeared on treatment with D_2O), 13.04 ppm (broad s, 1H, disappeared on treatment with D_2O). IR: ν 1646, 3213 cm^{-1}. Anal ($C_{23}H_{26}ClN_3O_4S$ (475.99)) C H Cl N S.

5-Bromo-3-(3,5-dimethylphenylsulfonyl)-*N*-(2-morpholinoethyl)-1*H*-indole-2-carboxamide (83). Was synthesized as **139** using **128** and 2-morpholin-4-yl-ethanamine. Yield: 53%. White solid, mp 218-223 °C (from ethanol). ^1H NMR (DMSO-d_6): δ 2.30 (s, 6H), 2.43-2.47 (m, 4H), 2.53 (t, *J* = 6.4 Hz, 2H), 3.49 (q, *J* = 6.0 Hz, 2H), 3.56-3.59 (m, 4H), 7.26 (s, 1H), 7.43-7.49 (m, 2H), 7.60 (s, 2H), 8.10 (s, 1H), 9.06 (broad s, 1H, disappeared on treatment with D_2O), 13.01 ppm (broad s, 1H, disappeared on treatment with D_2O). IR: ν 1640, 3196 cm^{-1}. Anal ($C_{23}H_{26}BrN_3O_4S$ (520.44)) C H Br N S.

3-(3,5-Dimethylphenylsulfonyl)-*N*-(2-morpholinoethyl)-5-nitro-1*H*-indole-2-carboxamide (84). Was synthesized as **139** using **129** 2-morpholin-4-yl-ethanamine. Yield: 63%. Pale yellow solid, mp 243-246 °C (from ethanol). ^1H NMR (DMSO-d_6): δ 2.30 (s, 6H), 2.46-2.49 (m, 4H), 2.55 (t, *J* = 6.4 Hz, 2H), 3.50 (q, *J* = 6.0 Hz, 2H), 3.58-3.60 (m, 4H), 7.27 (s, 1H), 7.63 (s, 2H), 7.69 (d, *J* = 9.1 Hz, 1H), 8.17 (dd, *J* = 8.9 and 1.8 Hz, 1H), 8.86 (d, *J* = 2.1 Hz, 1H), 9.05 (broad s, 1H, disappeared on treatment with D_2O), 13.46 ppm (broad s, 1H, disappeared on treatment with D_2O). IR: ν 1648, 3163 cm^{-1}. Anal ($C_{23}H_{26}N_4O_6S$ (486.54)) C H N S.

5-Chloro-3-(3,5-dimethylphenylsulfonyl)-*N*-phenethyl-1*H*-indole-2-carboxamide (86). Was synthesized as **139** using 2-phenylethanamine. Yield: 60%. White solid, mp 227-228 °C (from ethanol). ^1H NMR (DMSO-d_6): δ 2.32 (s, 6H), 2.91 (t, *J* = 7.4 Hz, 2H), 3.58-3.63 (m, 2H), 7.23-7.37 (m, 7H), 7.47 (d, *J* = 7.1 Hz, 1H), 7.52 (s, 2H), 7.94 (d, *J* = 2.0 Hz, 1H), 9.10 (broad s, 1H, disappeared on treatment with D_2O), 13.05 ppm (broad s, 1H, disappeared on treatment with D_2O). IR: ν 1643, 3195, 3287 cm^{-1}. Anal ($C_{25}H_{23}ClN_2O_3S$ (466.98)) C H Cl N S.

5-Bromo-3-(3,5-dimethylphenylsulfonyl)-*N*-phenethyl-1*H*-indole-2-carboxamide (87). Was synthesized as **139** using **128** and 2-

phenylethanamine. Yield: 30%. White solid, mp 231-236 °C (from ethanol). ^{1}H NMR (DMSO-d_6): δ 2.29 (s, 6H), 2.90 (t, *J* = 7.4 Hz, 2H), 3.58 (q, *J* = 6.7 Hz, 2H), 7.22-7.31 (m, 6H), 7.43-7.49 (m, 2H), 7.59 (s, 2H), 8.07 (s, 1H), 9.08 (broad s, 1H, disappeared on treatment with D_2O), 13.00 ppm (broad s, 1H, disappeared on treatment with D_2O). IR: ν 1640, 3191, 3290 cm^{-1}. Anal ($C_{25}H_{23}BrN_2O_3S$ (511.43)) C H Br N S.

3-(3,5-Dimethylphenylsulfonyl)-5-nitro-*N*-phenethyl-1*H*-indole-2-carboxamide (88). Was synthesized as **139** using **129** and 2-phenylethanamine. Yield: 74%. White solid, mp 261-262 °C (from ethanol). ^{1}H NMR (DMSO-d_6): δ 2.29 (s, 6H), 2.89 (t, *J* = 7.4 Hz, 2H), 3.56 (q, *J* = 6.7 Hz, 2H), 7.20-7.24 (m, 3H), 7.28-7.31 (m, 4H), 7.63-7.67 (m, 3H), 8.11 (dd, *J* = 8.9 and 1.9 Hz, 1H), 8.85 (d, *J* = 1.9 Hz, 1H), 8.98 (broad s, 1H, disappeared on treatment with D_2O), 13.47 ppm (broad s, 1H, disappeared on treatment with D_2O). IR: ν 1641, 3176, 3284 cm^{-1}. Anal ($C_{25}H_{23}N_3O_5S$ (477.53)) C H N S.

5-Chloro-3-(3,5-dimethylphenylsulfonyl)-*N*-(2-phenoxyethyl)-1*H*-indole-2-carboxamide (90). Was synthesized as **139** using 2-phenoxyethanamine. Yield: 83%. White solid, mp 227-228 °C (from ethanol). ^{1}H NMR ($CDCl_3$): δ 2.17 (2, 6H), 3.97 (q, *J* = 6.3 Hz, 2H), 4.23 (t, *J* = 5.2 Hz, 2H), 6.95-7.00 (m, 3H), 7.09 (s, 1H), 7.26-7.34 (m, 3H), 7.39 (d, *J* = 8.8 Hz, 1H), 7.51 (s, 2H), 8.28 (d, *J* = 1.8 Hz, 1H), 10.05 (broad s, 1H, disappeared with D_2O), 10.31 ppm (broad s, 1H, disappeared with D_2O). IR: ν 1650, 3209 cm^{-1}. Anal ($C_{25}H_{23}ClN_2O_4S$ (482.98)) C H Cl N S.

5-Bromo-3-(3,5-dimethylphenylsulfonyl)-*N*-(2-phenoxyethyl)-1*H*-indole-2-carboxamide (91). Was synthesized as **139** using **128** and 2-phenoxyethanamine. Yield: 52%. White solid, mp 214-219 °C (from ethanol). ^{1}H NMR (DMSO-d_6): δ 2.18 (s, 6H), 4.62 (q, *J* = 6.2 Hz, 2H), 4.07 (t, *J* = 6.4 Hz, 2H), 6.88-6.97 (m, 3H), 7.04-7.08 (m, 2H), 7.26-7.37 (m, 3H), 7.55 (s, 2H), 8.09 (s, 1H), 8.50 (broad s, 1H, disappeared on treatment with D_2O), 13.05 ppm (broad s, 1H, disappeared on treatment with D_2O). IR: ν 1644, 3206 cm^{-1}. Anal ($C_{25}H_{23}BrN_2O_4S$ (527.43)) C H Br N S.

3-(3,5-Dimethylphenylsulfonyl)-5-nitro-*N*-(2-phenoxyethyl)-1*H*-indole-2-carboxamide (92). Was synthesized as **139** using **129** and 2-phenoxyethanamine. Yield: 93%. White solid, mp 278-280 °C (from ethanol). ^{1}H NMR (DMSO-d_6): δ 2.23 (s, 6H), 3.77 (q, *J* = 5.4 Hz, 2H), 4.18 (t, *J* = 5.2 Hz, 2H), 6.93-7.00 (m, 3H), 7.24 (s, 1H), 7.30 (t, *J* = 7.3 Hz, 2H), 7.62 (s, 2H), 7.70 (d, *J* = 9.1 Hz, 1H), 8.18 (dd, *J* = 8.8 and 1.8 Hz, 1H), 8.88 (d, *J* = 2.2 Hz, 1H), 9.33 (broad s, 1H, disappeared on treatment with D_2O), 13.48 ppm (broad s, 1H, disappeared on treatment with D_2O). IR: ν 1642, 3188, 3279 cm^{-1}. Anal ($C_{25}H_{23}N_3O_6S$ (493.53)) C H N S.

Ethyl 2-[*N*-[5-chloro-3-[(3,5-dimethylphenyl)sulfonyl]-1*H*-indole-2-carboxamido]]acetate (131). Was synthesized as **139** using ethyl glycine hydrochloride. Yield 80%, mp 209-211 °C (from ethanol). ^{1}H NMR (DMSO-d_6): δ 1.25 (t, *J* = 7.1 Hz, 3H), 2.31 (s, 6H), 4.12-4.30 (m, 4H), 7.27 (s, 1H), 7.37 (dd, *J* = 1.7 and 8.8 Hz, 1H), 7.57 (d, *J* = 8.8 Hz, 1H), 7.72 (s, 2H), 8.03 (d, *J* = 1.7 Hz, 1H), 9.49 (t, *J* = 5.6 Hz, 1H, disappeared on treatment with D_2O), 13.13 ppm (broad, 1H, disappeared on treatment with D_2O). IR (Nujol): ν 1635, 1740, 3200 cm^{-1}. Anal. ($C_{21}H_{21}ClN_2O_5S$ (448.92)), C, H, N, Cl, S.

Ethyl 2-[*N*-[5-bromo-3-[(3,5-dimethylphenyl)sulfonyl]-1*H*-indole-2-carboxamido]]acetate (132). Was synthesized as **139** using **128** and ethyl glycine hydrochloride. Yield 48%, mp 199-201 °C (from ethanol). ^{1}H NMR (DMSO-d_6): δ 1.25 (t, *J* = 7.1 Hz, 3H), 2.31 (s, 6H), 4.17-4.26 (m, 4H), 7.27 (s, 1H), 7.47-7.53 (m, 2H), 7.70 (s, 2H), 8.18 (d, *J* = 1.7 Hz, 1H), 9.48 (broad s, 1H, disappeared on treatment with D_2O), 13.13 (broad s, 1H, disappeared on treatment with D_2O). IR: ν 1639, 1732, 3213 cm^{-1}. Anal. ($C_{21}H_{21}BrN_2O_5S$ (493.37)) C H Br N S.

Ethyl 2-[3-[(3,5-dimethylphenyl)sulfonyl]-5-nitro-1*H*-indole-2-carboxamido]acetate (133). Was synthesized as **139** using **129** and ethyl glycine hydrochloride. Yield 48%, mp 224-226 °C (from ethanol). ^{1}H NMR (DMSO-d_6): δ 1.24 (t, *J* = 7.1 Hz, 3H), 2.29 (s, 6H), 4.21-4.23 (m, 4H), 7.27 (s, 1H), 7.69-7.70 (m, 3H), 8.18 (dd, *J* = 9.1 and 2.3 Hz, 1H), 8.91 (d, *J* = 2.2 Hz,

1H), 9.43 (broad s, 1H, disappeared on treatment with D_2O), 13.88 ppm (broad s, 1H, disappeared on treatment with D_2O). IR (Nujol): ν 1647, 1749, 3215 cm^{-1}. Anal. ($C_{21}H_{21}N_3O_7S$ (459.47)) C, H, N, S.

Ethyl 2-[5-chloro-3-[(3,5-dimethylphenyl)sulfonyl]-4-fluoro-1*H*-indole-2-carboxamido)acetate (134). Was synthesized as **139** using **130** and ethyl glycine hydrochloride. Yield 86%, mp 221-223 °C (from ethanol). ^1H NMR (DMSO-d_6): δ 1.23 (t, *J* = 7.1 Hz, 3H), 2.30 (m, 6H), 4.12-4.20 (m, 4H), 7.24 (s, 1H), 7.33-7.40 (m, 2H), 7.62 (s, 2H), 9.51 (broad s, 1H, disappeared on treatment with D_2O), 13.24 (broad s, 1H, disappeared on treatment with D_2O). IR: ν 1638, 1745, 3212 cm^{-1}. Anal. ($C_{21}H_{20}ClFN_2O_5S$ (466.91)) C H Cl F N S.

Ethyl 2-[*N*-[5-chloro-3-[(3,5-dimethylphenyl)sulfonyl]-1*H*-indole-2-carboxamido]]propanoate (135). Was synthesized as **139** using ethyl alanine hydrocloride. Yield 86%, mp 200-203 °C (from ethanol). ^1H NMR (DMSO-d_6): δ 1.23 (t, *J* = 7.5 Hz, 3H), 1.47 (d, *J* = 7.2 Hz, 3H), 2.30 (s, 6H), 4.18 (q, *J* = 7.5 Hz, 2H), 4.60 (m, 1H), 7.25 (s, 1H), 7.36 (dd, *J* = 1.8 and 8.8 Hz, 1H), 7.56 (d, *J* = 8.8 Hz, 1H) 7.67 (s, 2H), 8.01 (d, *J* = 1.8 Hz, 9.49 (d, *J* = 6.6 Hz, 1H, disappeared on treatment with D_2O), 13.15 ppm (broad s, 1H, disappeared on treatment with D_2O). IR (nujol): ν 1635, 1735, 3270 cm^{-1}. Anal. ($C_{22}H_{23}ClN_2O_5S$ (462.94)), C, H, N, Cl, S.

Ethyl 2-[*N*-[5-bromo-3-[(3,5-dimethylphenyl)sulfonyl]-1*H*-indole-2-carboxamido]]propanoate (136). Was synthesized as **139** using **128** and ethyl alanine hydrochloride. Yield 85%, mp 211-214 °C (from ethanol). ^1H NMR (DMSO-d_6): δ 1.47 (d, *J* = 7.2 Hz, 3H), 2.32 (s, 6H), 3.73 (s, 3H), 4.63 (q, *J* = 7.1 Hz, 1H), 7.27 (s, 1H), 7.48 (dd, *J* = 8.8 and 1.8 Hz, 1H), 7.52 (d, *J* = 8.7 Hz, 1H), 7.67 (s, 2H), 8.16 (d, *J* = 2.9 Hz, 1H), 9.49 (broad s, 1H, disappeared on treatment with D_2O), 13.11 (broad s, 1H, disappeared on treatment with D_2O). IR: ν 1644, 1752, 3216 cm^{-1}. Anal. ($C_{21}H_{21}BrN_2O_5S$ (493.37)) C H Br N S.

Ethyl 2-[3-[(3,5-dimethylphenyl)sulfonyl]-5-nitro-1*H*-indole-2-carboxamido)propanoate (137). Was synthesized as **139** using **129** and ethyl alanine hydrochloride. Yield 99%, mp 232-235 °C (from ethanol). ^1H NMR

(DMSO-d_6): δ 1.23 (t, *J* = 7.1 Hz, 3H), 1.45 (d, *J* = 7.2 Hz, 3H), 2.29 (s, 6H), 4.18 (q, *J* = 7.1 Hz, 2H), 4.56-4.60 (m, 1H), 7.27 (s, 1H), 7.66 (s, 2H), 7.70 (d, *J* = 9.1 Hz, 1H), 8.18 (dd, *J* = 9.1 and 2.3 Hz, 1H), 8.88 (s, 1H), 9.45 (broad s, 1H, disappeared on treatment with D_2O), 13.82 ppm (broad s, 1H, disappeared on treatment with D_2O). IR (Nujol): ν 1651, 1741, 3194 cm^{-1}. Anal. ($C_{22}H_{23}N_3O_7S$ (473.50)) C, H, N, S.

Ethyl 2-[5-chloro-3-[(3,5-dimethylphenyl)sulfonyl]-4-fluoro-1*H*-indole-2-carboxamido)propanoate (138). Was synthesized as **139** using **130** and ethyl alanine hydrochloride. Yield 90%, mp 198-200 °C (from ethanol). ^1H NMR (DMSO-d_6): δ 1.25 (t, *J* = 7.1 Hz, 3H), 1.45 (d, *J* = 7.2 Hz, 3H), 2.33 (m, 6H), 4.18 (q, *J* = 7.0 Hz, 2H), 4.56 (q, *J* = 7.3 Hz, 1H), 7.26 (s, 1H), 7.35-7.43 (m, 2H), 7.68 (s, 2H), 9.51 (broad s, 1H, disappeared on treatment with D_2O), 13.31 (broad s, 1H, disappeared on treatment with D_2O). IR: ν 1643, 1731, 3222 cm^{-1}. Anal. ($C_{22}H_{22}ClFN_2O_5S$ (480.94)) C H Cl F N S.

Methyl 3-[*N*-[5-bromo-3-[(3,5-dimethylphenyl)sulfonyl]-1*H*-indole-2-carboxamido]]propanoate (140). Synthesized as **139** using **128** and methyl β-alanine hydrochloride. Yield 95%, mp 208-211 °C (from ethanol). ^1H NMR (DMSO-d_6): δ 2.31 (s, 6H), 2.68 (t, *J* = 6.7 Hz, 2H), 3.58-3.63 (m, 5H), 7.25 (s, 1H), 7.44-7.50 (m, 2H), 7.62 (s, 2H), 8.08 (s, 1H), 9.12 (broad s, 1H, disappeared on treatment with D_2O), 13.03 (broad s, 1H, disappeared on treatment with D_2O). IR: ν 1644, 1736, 3291 cm^{-1}. Anal. ($C_{21}H_{21}BrN_2O_5S$ (493.37)) C H Br N S.

Methyl 3-[3-[(3,5-dimethylphenyl)sulfonyl]-5-nitro-1*H*-indole-2-carboxamido)propanoate (141). Was synthesized as **139** using **129** methyl β-alanine hydrochloride. Yield 99%, mp 224-226 °C (from ethanol). ^1H NMR (DMSO-d_6): δ 2.30 (s, 6H), 2.66 (t, *J* = 6.6 Hz, 2H), 3.56-4.62 (m, 5H), 7.26 (s, 1H), 7.62 (s, 2H), 7.68 (d, *J* = 9.0 Hz, 1H), 8.16 (dd, *J* = 9.0 and 2.12 Hz, 1H), 8.81 (d, *J* = 2.0 Hz, 1H), 9.11 (broad s, 1H, disappeared on treatment with D_2O), 14.57 ppm (broad s, 1H, disappeared on treatment with D_2O). IR: ν 1656, 1732, 3223, 3322 cm^{-1}. Anal. (($C_{21}H_{21}N_3O_7S$ (459.47)) C, H, N, S.

Methyl 3-[5-chloro-3-[(3,5-dimethylphenyl)sulfonyl]-4-fluoro-1*H*-indole-2-carboxamido)propanoate (142). Was synthesized as **139** using **130** and methyl β-alanine hydrochloride. Yield 73%, mp 205-268 °C (from ethanol). ^{1}H NMR (DMSO-d_6): δ 2.34 (s, 6H), 2.68 (d, *J* = 6.6 Hz, 2H), 3.57-3.63 (m, 5H), 7.27 (s, 1H), 7.33-7.41 (m, 2H), 7.66 (s, 2H), 9.18 (broad s, 1H, disappeared on treatment with D_2O), 13.24 (broad s, 1H, disappeared on treatment with D_2O). IR: ν 1639, 1734, 3221 cm^{-1}. Anal. ($C_{21}H_{20}ClFN_2O_5S$ (466.91)) C H Cl F N S.

Ethyl 3-[*N*-[5-chloro-3-[(3,5-dimethylphenyl)sulfonyl]-1*H*-indole-2-carboxamido]butanoate (143). Was synthesized as **139** using ethyl 3-aminobutanoate. Yield 86%, mp 179-181 °C (from ethanol). ^{1}H NMR (DMSO-d_6): δ 1.19 (t, *J* = 7.1 Hz, 3H), 1.28 (d, *J* = 6.7 Hz, 3H), 2.32 (s, 6H), 2.54 (dd, *J* = 15.7 and 7.4 Hz, 1H), 2.67 (dd, *J* = 15.6 and 6.0 Hz, 1H), 4.10 (q, *J* = 7.1 Hz, 2H) 4.36-4.42 (m, 1H), 7.27 (s, 1H), 7.35 (dd, *J* = 8.8 and 2.0 Hz, 1H), 7.54 (d, *J* = 8.7 Hz, 1H), 7.64 (s, 2H), 7.94 (d, *J* = 1.4 Hz, 1H), 9.03 (broad s, 1H, disappeared with treatment with D_2O), 13.00 ppm (broad s, 1H, disappeared on treatment with D_2O). IR: ν 1643, 1732, 3212, 3285 cm^{-1}. Anal. ($C_{23}H_{25}ClN_2O_5S$ (476.97)) C H N Cl S.

Ethyl 3-[*N*-[5-bromo-3-[(3,5-dimethylphenyl)sulfonyl]-1*H*-indole-2-carboxamido]]butanoate (144). Synthesized as **139** using **128** and ethyl 3-aminobutanoate. Yield 99%, mp 181-185 °C (from ethanol). ^{1}H NMR (DMSO-d_6): δ 1.19 (t, *J* = 7.1 Hz, 3H), 1.28 (d, *J* = 6.6 Hz, 3H), 2.30 (s, 6H), 2.49-2.53 (m, 1H), 2.69-2.74 (m, 1H), 4.01 (q, *J* = 7.1 Hz, 2H), 4.36-4.41 (m, 1H), 7.28 (s, 1H), 7.46 (dd, *J* = 8.8 and 1.8 Hz, 1H), 7.49 (d, *J* = 8.7 Hz, 1H), 7.64 (s, 2H), 8.09 (d, *J* = 1.7 Hz, 1H), 9.02 (broad s, 1H, disappeared on treatment with D_2O), 13.02 ppm (s, 1H, disappeared on treatment with D_2O). IR: ν 1643, 1730, 3193 cm^{-1}. Anal. ($C_{23}H_{25}BrN_2O_5S$ (521.42)) C H Br N S.

Ethyl 3-[3-[(3,5-dimethylphenyl)sulfonyl]-5-nitro-1*H*-indole-2-carboxamido)butanoate (145). Was synthesized as **139** using **129** and ethyl 3-aminobutanoate. Yield 82%, mp 278-279 °C (from ethanol). ^{1}H NMR (DMSO-d_6): δ 1.20 (t, *J* = 7.5 Hz, 3H), 1.29 (d, *J* = 6.6 Hz, 3H), 2.32 (s, 6H), 2.53-2.57

(m, 1H), 2.68-2.76 (m, 1H), 4.12 (q, *J* = 7.1 Hz, 2H), 4.36-4.41 (m, 1H), 7.29 (s, 1H), 7.65 (s, 2H), 7.72 (d, *J* = 9.1 Hz, 1H), 8.18 (dd, *J* = 8.3 and 2.3 Hz, 1H), 8.85 (d, *J* = 2.5 Hz, 1H), 9.05 (broad s, 1H, disappeared on treatment with D_2O), 13.46 ppm (s, 1H, disappeared on treatment with D_2O). IR: ν 1644, 1721, 3178 cm^{-1}. Anal. ($C_{23}H_{25}N_3O_7S$ (487.53)). C, H, N, S.

Ethyl 3-[5-chloro-3-[(3,5-dimethylphenyl)sulfonyl]-4-fluoro-1*H*-indole-2-carboxamido)butanoate (146). Was synthesized as **139** using **130** and ethyl 3-aminobutanoate. Yield 88%, mp 172-174 °C (from ethanol). ^1H NMR (DMSO-d_6): δ 1.19 (t, *J* = 7.1 Hz, 3H), 1.24 (d, *J* = 6.6 Hz, 3H), 2.31 (s, 6H), 2.41-2.47 (m, 1H), 2.71-2.77 (m, 1H), 4.09 (q, *J* = 7.1 Hz, 2H), 4.31-4.39 (m, 1H), 7.25 (s, 1H), 7.31-7.39 (m, 2H), 7.64 (s, 2H), 9.05 (broad s, 1H, disappeared on treatment with D_2O), 13.16 ppm (s, 1H, disappeared on treatment with D_2O). IR: ν 1643, 1731, 3218 cm^{-1}. Anal. ($C_{23}H_{24}ClFN_2O_5S$ (494.96)) C H Cl F N S.

General procedure for Preparation of Derivatives 73,74,77,81,85,89 and 93. Example: *N*-Benzyl-5-chloro-3-(3,5-dimethylphenylsulfonyl)-4-fluoro-1*H*-indole-2-carboxamide (73). A mixture of **126** (0.100 g, 0.00024 mol) and benzyl amine (0.078 g, 0.2 mL, 0.000729 mol) in ethanol (0.15 mL) was placed in microwave cavity. Microwave irradiation of 150W was used, the temperature being ramped from 25 °C to 150 °C. Once this reached, taking about 3 min, the reaction mixture was hold at this temperature for 15 min, while stirring (press max: 250 psi). After cooling the precipitate was collected and recrystallized in ethanol to give **73**. Yield: 75%. White solid, mp 229-231 °C (from ethanol). ^1H NMR (DMSO-d_6): δ 2.30 (s, 6H), 4.56 (d, *J* = 5.7 Hz, 2H), 7.25 (s, 1H), 7.28 (t, *J* = 7.2 Hz, 1H), 7.32-7.39 (m, 4H),7.48 (d, *J* = 7.1 Hz, 2H), 7.67 (s, 2H), 9.50 (broad s, 1H, disappeared on treatment with D_2O), 13.29 ppm (broad s, 1H, disappeared on treatment with D_2O). IR: ν 1638, 3220 cm^{-1}. Anal. ($C_{24}H_{20}ClFN_2O_3S$ (470.94)) C H Cl F N S.

5-Chloro-3-(3,5-dimethylphenylsulfonyl)-*N*-(2-(pyrrolidin-1-yl)ethyl)-1*H*-indole-2-carboxamide (74). Was synthesized as **73** using **123** and 2-(pyrrolidin-1-yl)ethanamine. Yield: 82%. White solid, mp 200-203 °C (from ethanol). ^1H

NMR (DMSO-d_6): δ 2.29 (s, 6H), 2.66 (t, *J* = 6.6 Hz, 2H), 3.40 (q, *J* = 6.1 Hz, 2H), 7.25 (s, 1H), 7.31 (dd, *J* = 8.8 and 1.9 Hz, 1H), 7.51 (d, *J* = 8.7 Hz,1H), 7.61 (s, 2H), 7.94 (d, *J* = 1.7 Hz, 1H), 9.00 (broad s, 1H, disappeared on treatment with D_2O), 13.02 ppm (broad s, 1H, disappeared on treatment with D_2O). IR: ν 1648, 3204 cm^{-1}. Anal ($C_{23}H_{26}ClN_3O_3S$ (459.99)) C H Cl N S.

5-Chloro-3-(3,5-dimethylphenylsulfonyl)-4-fluoro-*N*-(2-(pyrrolidin-1-yl)ethyl)-1*H*-indole-2-carboxamide (77). Was synthesized as **73** using 2-(pyrrolidin-1-yl)ethanamine. Yield: 59%. White solid, mp 194-195 °C (from ethanol).^{1}H NMR (DMSO-d_6): δ 1.69-1.71 (m, 4H), 2.32 (s, 6H), 2.55-2.58 (m, 4H), 2.68 (t, *J* = 7.0 Hz, 2H), 3.43 (q, *J* = 6.5 Hz, 2H), 7.24 (s, 1H), 7.29-7.32 (m, 2H), 7.67 (s, 2H), 8.92 (broad s, 1H, disappeared on treatment with D_2O), 13.21 ppm (broad s, 1H, disappeared on treatment with D_2O). IR: ν 1655, 3344 cm^{-1}. Anal ($C_{23}H_{25}ClFN_3O_3S$ (477.98)) C H Cl F N S.

***N*-(2-(1*H*-Pyrrol-1-yl)ethyl)-5-chloro-3-(3,5-dimethylphenylsulfonyl)-4-fluoro-1*H*-indole-2-carboxamide (81).** Was synthesized as **73** using 2-(1*H*-pyrrol-1-yl)ethanamine. Yield: 88%. White solid, mp 234-236 °C (from ethanol). ^{1}H NMR (DMSO-d_6): δ 2.31 (s, 6H), 3.59 (q, *J* = 5.9 Hz, 2H), 4.10 (t, *J* = 6.2 Hz, 2H), 5.98-5.99 (m, 2H), 6.86-6.87 (m, 2H), 7.26 (s, 1H), 7.31-7.39 (m, 2H), 7.66 (s, 2H), 9.25 (broad s, 1H, disappeared on treatment with D_2O), 13.21 ppm (broad s, 1H, disappeared on treatment with D_2O). IR: ν 1643, 3261 cm^{-1}. Anal ($C_{23}H_{21}ClFN_3O_3S$ (473.95)) C H Cl F N S.

5-Chloro-3-(3,5-dimethylphenylsulfonyl)-4-fluoro-*N*-(2-morpholinoethyl)-1*H*-indole-2-carboxamide (85). Was synthesized as **73** using 2-morpholin-4-yl-ethanamine. Yield: 93%. White solid, mp 216-217 °C (from ethanol). ^{1}H NMR ($CDCl_3$): δ 2.37 (s, 6H), 2.54-2.56 (m, 4H), 2.68 (t, *J* = 6.1 Hz, 2H), 3.69-3.71 (m, 6H), 7.20 (s, 1H), 7.22 (s, *J* = 8.8 Hz, 1H), 7.33 (dd, *J* = 8.8 and 6.4 Hz, 1H), 7.59 (s, 2H), 10.14 (broad s, 1H, disappeared on treatment with D_2O), 10.38 ppm (broad s, 1H, disappeared on treatment with D_2O). IR: ν 1646, 3181, 3266 cm^{-1}. Anal ($C_{23}H_{25}ClFN_3O_4S$ (493.98)) C H Cl F N S.

5-Chloro-3-(3,5-dimethylphenylsulfonyl)-4-fluoro-*N*-phenethyl-1*H*-indole-2-carboxamide (89). Was synthesized as **73** using **130** and 2-phenylethanamine. Yield: 88%. White solid, mp 184-185 °C (from ethanol). ^{1}H NMR (DMSO-d_6): δ 2.32 (s, 6H), 2.90 (t, *J* = 7.5 Hz, 2H), 3.54 (q, *J* = 5.5 Hz, 2H), 7.22-7.42 (m, 8H), 7.66 (s, 2H), 9.16 (broad s, 1H, disappeared on treatment with D_2O), 13.24 ppm (broad s, 1H, disappeared on treatment with D_2O). IR: ν 1649, 3197 cm^{-1}. Anal ($C_{25}H_{22}ClFN_2O_3S$ (484.97)) C H Cl F N S.

5-Chloro-3-(3,5-dimethylphenylsulfonyl)-4-fluoro-*N*-(2-phenoxyethyl)-1*H*-indole-2-carboxamide (93). Was synthesized as **73** using 2-(1*H*-pyrrol-1-yl)ethanamine. Yield: 76%. White solid, mp 198-201 °C (from ethanol). ^{1}H NMR (DMSO-d_6): δ 2.29 (s, 6H), 3.71 (q, *J* = 5.2 Hz, 2H), 5.15 (t, *J* = 5.1 Hz, 2H), 6.93-6.98 (m, 3H), 7.34-7.37 (m, 5H), 7.65 (s, 2H), 9.33 (broad s, 1H, disappeared on treatment with D_2O), 13.22 ppm (broad s, 1H, disappeared on treatment with D_2O). IR: ν 1643, 3204 cm^{-1}. Anal ($C_{25}H_{22}ClFN_2O_4S$ (500.97)) C H Cl F N S.

General Procedure for preparation of derivatives 58-69. Example (Mannich reaction in *t*-butanol): 5-Chloro-3-(3,5-dimethylphenylsulfonyl)-*N*-(pyrrolidin-1-ylmethyl)-1*H*-indole-2-carboxamide (58). A mixture of **21** (0.43 g, 0.00119 mol) in *t*-butanol (20 mL) was heated at 100 °C until dissolution and pyrrolidine (0.093 g, 1 mL, 1.31 mol) and 37% formaldehyde (39.3 mg, 0.1 mL, 1.31 mol) were added. Reaction mixture was stirred at same temperature for 4 h, and pyrrolidine (0.093 g, 1 mL, 1.31 mol) and 37% formaldehyde (39.3 mg, 0.1 mL, 1.31 mol) were added and it was stirred for additional 3 h. Reaction mixture was filtered, and *n*-hexane was added. The precipitate was collected to give **58**. Yield: 13%. White solid, 193-196 °C. ^{1}H NMR (DMSO-d_6): δ 1.66-1.69 (m, 4H), 2.30 (s, 6H), 2.63-.66 (m, 4H), 4.32 (d, *J* = 5.7 Hz, 2H), 7.25 (s, 1H), 7.32 (dd, *J* = 6.6 and 2.1 Hz, 1H), 7.52 (d, *J* = 8.7 Hz, 1H), 7.61 (d, 2H), 7.91 (d, *J* = 2.2 Hz, 1H), 9.22 (broad s, 1H, disappeared on treatment with D_2O), 13.01 ppm (very broad s, 1H, disappeared on treatment with D_2O). IR: ν 1678, 3120 cm^{-1}. Anal ($C_{22}H_{24}ClN_3O_3S$ (445.96)) C H Cl N S.

3-(3,5-Dimethylphenylsulfonyl)-5-nitro-*N*-(pyrrolidin-1-ylmethyl)-1*H*-indole-2-carboxamide (60). Was synthesized as **58** using **154**. Yield: 27%. Pale yellow solid, 256-259 °C. ^{1}H NMR (DMSO-d_6): δ 1.71-1.75 (m, 4H), 2.29 (s, 6H), 2.73-2.78 (m, 4H), 4.37 (d, *J* = 6.2 Hz, 2H), 7.24 (s, 1H), 7.62 (s, 2H), 7.67 (d, *J* = 9.0 Hz, 1H), 8.11 (dd, *J* = 9.0 and 2.2 Hz, 1H), 8.84 (d, *J* = 2.3 Hz, 1H), 9.27 (broad s, 1H, disappeared on treatment with D_2O), 13.46 ppm (broad s, 1H, disappeared on treatment with D_2O). IR: ν 1642, 3175, 3231 cm^{-1}. Anal ($C_{22}H_{24}N_4O_5S$ (456.51)) C H N S.

5-Chloro-3-(3,5-dimethylphenylsulfonyl)-*N*-(piperidin-1-ylmethyl)-1*H*-indole-2-carboxamide (62). Was synthesized as **58** using piperidine. Yield: 50%. White solid, 172-174 °C. ^{1}H NMR (DMSO-d_6): δ 1.35-1.37 (m, 2H), 1.50-1.51 (m, 4H), 2.31 (s, 6H), 2.54-2.57 (m, 4H), 4.21 (d, *J* = 5.9 Hz, 2H), 7.26 (s, 1H), 7.34 (dd, *J* = 8.8 and 1.9 Hz, 1H), 7.62 (s, 2H), 7.93 (d, *J* = 2.0 Hz, 1H), 9.19 (broad s, 1H, disappeared on treatment with D_2O), 13.47 ppm (very broad s, 1H, disappeared on treatment with D_2O). IR: ν 1634, 3189 cm^{-1}. Anal ($C_{23}H_{26}ClN_3O_3S$ (459.99)) C H Cl N S.

3-(3,5-Dimethylphenylsulfonyl)-5-nitro-*N*-(piperidin-1-ylmethyl)-1*H*-indole-2-carboxamide (64). Was synthesized as **58** using **154** and piperidine. Yield: 41%. White solid, 188-191 °C. ^{1}H NMR (DMSO-d_6): δ 1.37 (s, 2H), 1.48-151 (m, 4H), 2.30 (s, 6H), 2.56-2.60 (m, 4H), 4.22 (d, *J* = 6.0 Hz, 2H), 7.26 (s, 1H), 7.63 (s, 2H), 7.69 (d, *J* = 9.1 Hz, 1H), 8.15 (dd, *J* = 9.2 and 2.1 Hz, 1H), 8.83 (d, *J* = 2.2 Hz, 1H), 9.19 (broad s, 1H, disappeared on treatment with D_2O), 13.42 ppm (broad s, 1H, disappeared on treatment with D_2O). IR: ν 1638, 3161, 3280 cm^{-1}. Anal ($C_{23}H_{26}N_4O_5S$ (470.54)) C H N S.

5-Chloro-3-(3,5-dimethylphenylsulfonyl)-*N*-(morpholinomethyl)-1*H*-indole-2-carboxamide (66). Was synthesized as **58** using morpholine. Yield: 57%. White solid, 209-211 °C. ^{1}H NMR (DMSO-d_6): δ 2.31 (s, 6H), 2.61 (t, *J* = 4.6 Hz, 4H), 3.60 (t, *J* = 4.4 Hz, 4H), 4.22 (d, *J* = 6.1 Hz, 2H), 7.26 (s, 1H), 7.34 (dd, *J* = 8.8 and 2.0 Hz, 1H), 7.54 (d, *J* = 8.7 Hz, 1H), 7.65 (s, 2H), 7.92 (d, *J* = 2.1 Hz, 1H), 9.25 (broad s, 1H, disappeared on treatment with D_2O), 13.03 ppm (broad s,

1H, disappeared on treatment with D_2O). IR: ν 1650, 3201 cm^{-1}. Anal ($C_{22}H_{24}ClN_3O_4S$ (461.96)) C H Cl N S.

3-(3,5-Dimethylphenylsulfonyl)-*N*-(morpholinomethyl)-5-nitro-1*H*-indole-2-carboxamide (68). Was synthesized as **58** using **154** and morpholine. Yield: 41%. Yellow solid, 183-185 °C. ^1H NMR (DMSO-d_6): δ 2.30 (s, 6H), 2.58-2.62 (m, 4H), 3.57-3.62 (m, 4H), 4.21 (d, *J* = 6.0 Hz, 2H), 7.27 (s, 1H), 7.65 (s, 2H), 7.70 (d, *J* = 9.0 Hz, 1H), 8.17 (dd, *J* = 9.1 and 2.3 Hz, 1H), 8.82 (d, *J* = 2.7 Hz, 1H), 9.26 (broad s, 1H, disappeared on treatment with D_2O), 13.48 ppm (broad s, 1H, disappeared on treatment with D_2O). IR: ν 1642, 3180, 3213 cm^{-1}. Anal ($C_{22}H_{24}N_4O_6S$ (472.51)) C H N S.

Example (Mannich reaction in benzene): 5-Bromo-3-(3,5-dimethylphenylsulfonyl)-*N*-(pyrrolidin-1-ylmethyl)-1*H*-indole-2-carboxamide (59). A mixture of **153** (0.1 g, 0.00024 mol), paraformaldehyde (0.072 g, 0.00024 mol) and pyrrolidine (0.017 g, 0.02 mL, 0.00024 mol) in benzene (15 mL) was refluxed using Dean-Stark apparatus for 3h.. After cooling the precipitate was collected and washed with benzene to give **59**. Yield: 60%. White solid, mp 183-186 °C. ^1H NMR (DMSO-d_6): δ 1.66-1.70 (m, 4H), 2.29 (s, 6H), 2.63-2.67 (m, 4H), 4.32 (d, *J* = 4.2 Hz, 2H), 7.26 (s, 1H), 7.41-7.49 (m, 2H), 7.71 (s, 2H), 8.07 (d, *J* = 1.1 Hz, 1H), 9.21 (broad s, 1H, disappeared on treatment with D_2O), 13.01 ppm (broad s, 1H, disappeared on treatment with D_2O). IR: ν 1646, 3217 cm^{-1}. Anal ($C_{22}H_{24}BrN_3O_3S$ (490.41)) C H Br N S.

5-Chloro-3-(3,5-dimethylphenylsulfonyl)-4-fluoro-*N*-(pyrrolidin-1-ylmethyl)-1*H*-indole-2-carboxamide (61). Was synthesized as **59** using **32**. Yield: 58%. White solid, mp 119-124 °C ^1H NMR (DMSO-d_6): δ 1.57-1.61 (m, 4H), 2.31 (s, 6H), 2.64-2.68 (m, 4H), 4.29 (d, *J* = 5.2 Hz, 2H), 7.24 (s, 1H), 7.27-7.40 (m, 2H), 7.64 (s, 2H), 9.23 (broad s, 1H, disappeared on treatment with D_2O), 13.01 ppm (broad s, 1H, disappeared on treatment with D_2O). IR: ν 1671, 3319 cm^{-1}. Anal ($C_{22}H_{23}ClFN_3O_3S$ (463.95)) C H Cl F N S.

5-Bromo-3-(3,5-dimethylphenylsulfonyl)-*N*-(piperidin-1-ylmethyl)-1*H*-indole-2-carboxamide (63). Was synthesized as **59** using piperidine. Yield: 46%. White

solid, mp 177-180 °C. ^{1}H NMR (DMSO-d_6): δ 1.34-1.37 (m, 2H), 1.48-1.52 (m, 4H), 2.31 (s, 6H), 2.54-2.58 (m, 4H), 4.20 (d, *J* = 5.9 Hz, 2H), 7.27 (s, 1H), 7.43-7.50 (m, 2H), 7.61 (s, 2H), 8.06 (s, 1H), 9.18 (broad s, 1H, disappeared on treatment with D_2O), 12.95 ppm (broad s, 1H, disappeared on treatment with D_2O). IR: ν 1649, 3194, 3274 cm^{-1}. Anal ($C_{23}H_{26}BrN_3O_3S$ (504.44)) C H Br N S.

5-Chloro-3-(3,5-dimethylphenylsulfonyl)-4-fluoro-*N*-(piperidin-1-ylmethyl)-1*H*-indole-2-carboxamide (65). Was synthesized as **59** using **32** and piperidine. Yield: 69%. White solid, mp 175-177 °C. ^{1}H NMR (DMSO-d_6): δ 1.35-1.38 (m, 2H), 1.46-1.51 (m, 4H), 2.32 (s, 6H), 2.63-2.66 (m, 4H), 4.15 (d, *J* = 5.9 Hz, 2H), 7.26 (s, 1H), 7.36-7.43 (m, 2H), 7.63 (s, 2H), 9.24 (broad s, 1H, disappeared on treatment with D_2O), 13.01 ppm (broad s, 1H, disappeared on treatment with D_2O). IR: ν 1682, 3353 cm^{-1}. Anal ($C_{23}H_{25}ClFN_3O_3S$ (477.98)) C H Cl F N S.

5-Bromo-3-(3,5-dimethylphenylsulfonyl)-*N*-(morpholinomethyl)-1*H*-indole-2-carboxamide (67). Was synthesized as **59** using morpholine. Yield: 24%. White solid, mp 267-271 °C. ^{1}H NMR (DMSO-d_6): δ 2.30 (s, 6H), 2.56-2.58 (m, 4H), 3.57-3.61 (m, 4H), 4.21 (d, *J* = 5.8 Hz, 2H), 7.25 (s, 1H), 7.43-7.49 (m, 2H), 7.63 (s, 2H), 8.05 (s, 1H), 9.24 (broad s, 1H, disappeared on treatment with D_2O), 13.02 ppm (broad s, 1H, disappeared on treatment with D_2O). IR: ν 1654, 3210 cm^{-1}. Anal ($C_{22}H_{24}BrN_3O_4S$ (506.41)) C H Br N S.

5-Chloro-3-(3,5-dimethylphenylsulfonyl)-4-fluoro-*N*-(morpholinomethyl)-1*H*-indole-2-carboxamide (69). Was synthesized as **59** using **32** and morpholine. Yield: 69%. White solid, mp 197-199 °C. ^{1}H NMR (DMSO-d_6): δ 2.32 (s, 6H), 2.62-2.64 (m, 4H), 3.58-3.61 (m, 4H), 4.17 (d, *J* = 6.0 Hz, 2H), 7.26 (s, 1H), 7.32-7.38 (m, 2H), 7.66 (s, 2H), 9.31 (broad s, 1H, disappeared on treatment with D_2O), 13.18 ppm (broad s, 1H, disappeared on treatment with D_2O). IR: ν 1649, 3238 cm^{-1}. Anal ($C_{22}H_{23}ClFN_3O_4S$ (479.95)) C H Cl F N S.

Ethyl 3-[(3,5-dimethylphenyl)thio]-5-nitro-1*H*-indole-2-carboxylate (121). Boron trifluoride diethyletherate (0.14 g, 0.12 mL, 0.001 mol) was added to a mixture of ethyl 5-nitro-1*H*-indole-2-carboxylate (0.72 g, 0.0031 mol) and 1-(3,5-dimethylphenylthio)pyrrolidine-2,5-dione (**116**) (0.77 g, 0.0033 mol) in

anhydrous dichloromethane (20 mL) while cooling over an ice-bath. After 2 h at room temperature, boron trifluoride diethyletherate (0.28 g, 0.24 mL, 0.002 mol) was added and reaction was refluxed for 2 h. After cooling, dichloromethane was added and the organic layer was washed with brine, dried, and evaporated. The residue was purified by silica gel column chromatography (dichloromethane-petroleum ether 1:1 as eluent) to give **121**, yield 53%, mp 212-213 °C (from ethanol). ^{1}H NMR (DMSO-d_6): δ 1.29 (t, *J* = 7.1 Hz, 3H), 2.16 (s, 6H), 4.36 (q, *J* = 7.1 Hz, 2H), 6.82 (s, 3H), 7.69 (d, *J* = 9.0 Hz, 1H), 8.17 (dd, *J* = 9.0 and 2.1 Hz, 1H), 8.25 (d, *J* = 2.1 Hz, 1H), 12.99 ppm (broad s, 1H, disappeared on treatment with D_2O). IR (Nujol): ν 1660, 3270 cm^{-1}. Anal. ($C_{19}H_{18}N_2O_4S$ (370.42)) C, H, N, S.

Methyl 5-chloro-3-[(3,5-dimethylphenyl)thio]-1*H*-indole-2-carboxylate (119). Was synthesized as **121** using methyl 5-chloro-1*H*-indole-2-carboxylate. Yield 77%, mp 174-175 °C (from cyclohexane). ^{1}H NMR ($CDCl_3$): δ 2.19 (s, 6H), 3.95 (s, 3H), 6.73-6.82 (m, 3H), 7.28-7.41 (m, 2H), 7.58 (m, 1H), 9.30 ppm (broad s, 1H, disappeared on treatment with D_2O). IR (Nujol): ν 1675, 3280 cm^{-1}. Anal. ($C_{18}H_{16}ClNO_2S$ (345.84)) C, H, N, S, Cl.

Ethyl 5-bromo-3-[(3,5-dimethylphenyl)thio]-1*H*-indole-2-carboxylate (120). Was synthesized as **121** using ethyl 5-bromo-1*H*-indole-2-carboxylate. Yield 93%, mp 162-165 °C (from ethanol). ^{1}H NMR (DMSO-d_6): δ 1.25 (t, *J* = 7.1 Hz, 3H), 2.14 (s, 6H), 4.29 (q, *J* = 7.1 Hz, 2H), 6.72 (m, 2H), 6.76 (m, 1H), 7.43 (dd, *J* = 1.8 and 8.8 Hz, 1H), 7.51 and 7.53 (two d, *J* = 1.8 and 8.8 Hz, overlapped signals, 2H), 12.65 ppm (broad s, 1H, disappeared on treatment with D_2O). IR (Nujol): δ 1670, 3270 cm-1. Anal. ($C_{19}H_{18}BrNO_2S$ (404.32)) C, H, N, S, Br.

Ethyl 5-chloro-3-[(3,5-dimethylphenyl)thio]-4-fluoro-1*H*-indole-2-carboxylate (122). Was prepared as **121** using **105**. Yield 51%, mp 149-151 °C (from ethanol). ^{1}H NMR (DMSO-d_6): δ 1.19 (t, *J* = 7.1 Hz, 3H), 2.07 (s, 6H), 4.26 (q, *J* = 7.1 Hz, 2H), 6.40-7.35 ppm (m, 5H), 13.45 (broad s, 1H, disappeared on treatment with D_2O). IR (nujol): ν 1700, 3400 cm^{-1}. Anal. ($C_{19}H_{17}ClFNO_2S$ (377.86)) C H Cl FN S.

Ethyl 3-[(3,5-dimethylphenyl)sulfonyl]-5-nitro-1*H*-indole-2-carboxylate (125). 3-Chloroperoxybenzoic acid (0.69 g, 0.004 mol) was added to an ice-cooled solution of **121** (0.50 g, 0.00135 mol) in chloroform (22 mL). Reaction mixture was stirred at room temperature for 2 h. Water was added and the mixture was extracted with ethyl acetate. The organic layer was washed with brine, dried, evaporated. The residue was purified by alumina chromatography (ethyl acetate as eluent) to give **125**, yield 53%, mp 255-256 °C (from ethanol). ^{1}H NMR (DMSO-d_6): δ 1.34 (t, J = 7.1 Hz, 3H), 2.37 (s, 6H), 4.43 (q, J = 7.1 Hz, 2H), 7.34 (s, 1H), 7.72 (s, 2H), 7.83 (d, J = 9.2 Hz, 1H), 8.29 (dd, J = 9.2 and 1.9 Hz, 1H), 9.21 (d, J = 1.9 Hz, 1H), 13.72 ppm (broad s, 1H, disappeared on treatment with D_2O, 1H). IR (Nujol): ν 1680, 3375 cm^{-1}. Anal. ($C_{19}H_{18}N_2O_6S$ (402.42)) C, H, N, S.

Ethyl 5-chloro-3-[(3,5-dimethylphenyl)sulfonyl]-1*H*-indole-2-carboxylate (123). Was synthesized as **125** using **119**. Yield 74%, mp 234-236 °C (from toluene/cyclohexane). ^{1}H NMR (DMSO-d_6): δ 2.33 (s, 6H), 3.88 (s, 3H), 7.28 (m, 1H), 7.43 (dd, J = 2.0 and 8.6 Hz, 1H), 7.55-7.67 (m, 3H), 8.24 (d, J = 2.0 Hz, 1H), 13.33 ppm (broad s, 1H, disappeared on treatment with D_2O). IR (nujol): ν 1740, 3200 cm^{-1}. Anal. ($C_{18}H_{16}ClNO_4S$ (377.84)) C, H, N, S, Cl.

Ethyl 5-bromo-3-[(3,5-dimethylphenyl)sulfonyl]-1*H*-indole-2-carboxylate (124). Was synthesized as **125** using **120**. Yield 77%, mp >300 °C (from aqueous ethanol). ^{1}H NMR (DMSO-d_6): δ 1.28 (t, J = 7.1 Hz, 3H), 2.32 (s, 6H), 4.35 (q, J = 7.1 Hz, 2H), 7.28 (m, 1H), 7.55 (d, J = 1.2 Hz, 2H), 7.60 (m, 2H), 8.38 ppm (t, J = 1.2 Hz, 1H). IR (Nujol): ν 1690, 3260 cm^{-1}. Anal. ($C_{19}H_{18}BrNO_4S$ (436.32)) C, H, N, S, Br.

Ethyl 5-chloro-3-[(3,5-dimethylphenyl)sulfonyl]-4-fluoro-1*H*-indole-2-carboxylate (126). Was prepared as **125** using **122**. Yield 59%, mp 224-226 °C (from ethanol). ^{1}H NMR (DMSO-d_6): δ 1.34 (t, J = 7.1 Hz, 3H), 2.28 (s, 6H), 4.40 (q, J = 7.1 Hz, 2H), 7.24 (s, 1H), 7.32 (d, J = 8.8 Hz, 1H), 7.37 (dd, J = 6.0 and 8.8 Hz, 1H), 7.62 ppm (s, 2H), 13.66 (broad s, 1H, disappeared on treatment

with D_2O). IR (nujol): ν 1700, 3400 cm^{-1}. Anal. ($C_{19}H_{17}ClFNO_4S$ (409.86)) C H Cl F N S.

5-Chloro-3-[(3,5-dimethylphenyl)sulfonyl]-1*H*-indole-2-carboxylic acid (127). Was prepared as previously reported.[74]

5-Bromo-3-[(3,5-dimethylphenyl)sulfonyl]-1*H*-indole-2-carboxylic acid (128). Lithium hydroxide monohydrate (1.79 g, 0.0428 mol) was added to a mixture of **124**[59] (6.07 g, 0.0139 mol) in tetrahydrofuran (16 mL) and water (16 mL). After stirring at room temperature for 5 h, lithium hydroxide monohydrate (1.79 g, 0.0428 mol) was added and the reaction was maintained at room temperature for 3 days. Water and 1N HCl were added (pH ~ 2) and the mixture was extracted with ethyl acetate. The organic layer was washed with brine, dried, filtered and evaporated. The crude product was crystallized from ethanol to give **128**, yield 96%, mp 280-284 °C (from ethanol). ^{1}H NMR (DMSO-d_6): δ 2.30 (s, 6H), 7.21 (s, 1H), 7.46-7.53 (m, 2H), 7.70 (s, 2H), 8.37 (s, 1H), 13.06 (broad s, 1H, disappeared on treatment with D_2O), 14.02 (broad s, 1H, disappeared on treatment with D_2O). IR: ν 1708, 3169, 3386 cm^{-1}. Anal. ($C_{17}H_{14}BrNO_4S$ (408.27)) C H Br N S.

3-[(3,5-Dimethylphenyl)sulfonyl]-5-nitro-1*H*-indole-2-carboxylic acid (129). Was synthesized as **128** using **125**. Yield 83%, mp 266-275 °C (from ethanol). ^{1}H NMR (DMSO-d_6): δ 2.27 (s, 6H), 7.22 (s, 1H), 7.64 (s, 2H), 7.69 (d, J = 9.0 Hz, 1H), 8.18 (dd, J = 9.0 and 2.2 Hz, 1H), 9.11 (d, J = 2.17 Hz, 1H), 13.9 (broad s, 1H, disappeared on treatment with D_2O), 14.15 ppm (broad s, 1H, disappeared on treatment with D_2O). IR (Nujol): δ 1608, 1730, 3191 cm^{-1}. Anal. ($C_{17}H_{14}N_2O_6S$ (402.43)) C, H, N, S.

5-Chloro-3-[(3,5-dimethylphenyl)sulfonyl]-4-fluoro-1*H*-indole-2-carboxylic acid (130). Was synthesized as **128** starting from **126**. Yield 99%, mp 255-257 °C (from ethanol). ^{1}H NMR (DMSO-d_6): δ 2.35 (s, 6H), 7.30 (s, 1H), 7.37-7.46 (m, 2H), 7.72 (s, 2H), 13.41 (broad s, 1H, disappeared on treatment with D_2O), 13.90 ppm (broad s, 1H, disappeared on treatment with D_2O). IR (Nujol): δ 1668, 3236 cm^{-1}. Anal. ($C_{17}H_{13}ClFNO_4S$ (381.81)) C, H, N, S.

Ethyl 2-(2-(4-bromophenyl)hydrazono)propanoate (95). A mixture of 4-bromophenylhydrazine hydrochloride (**94**) (5.7 g, 0.0255 mol), ethyl pyruvate (2 g, 1.91 mL, 0.017 mol) and sodium acetate (2.79 g, 0.034 mol) in 96° ethanol (40 mL) was placed into the microwave cavity (open vessel mode). Microwave irradiation of 250W was used, the temperature being ramped from 25 °C to 100 °C. Once this reached, taking about 2 min, the reaction mixture was hold at this temperature for 5 min, while stirring and cooling. The reaction mixture was cooled at 0 °C and filtered to give 57, yield 90%, mp 142-144 °C (from ethanol). ^{1}H NMR ($CDCl_3$): δ 1.39 (t, *J* = 7.2 Hz, 3H), 2.12 (s, 3H), 4.33 (q, *J* = 7.1 Hz, 2H), 7.10 (d, *J* = 6.7 Hz, 2H), 7.40 (d, *J* = 6.9 Hz, 2H), 7.64 ppm (broad s, disappeared on treatment with D_2O, 1H). IR: ν 1576, 1675, 3290 cm^{-1}. Anal. ($C_{11}H_{13}BrN_2O_2$ (285.14)) C H Br N.

Ethyl 5-bromo-1H-indole-2-carboxylate (96). 95 (35.15 g, 0.123 mol) was added by portions to preheated at 110 °C polyphosphoric acid (350 g). The mixture was stirred at the same temperature for 30 min and then quenched on ice-water. The solid was filtered, washed with water, dried and recrystallized from ethanol to give 58 as brown solid (32.95 g, 60%), mp 160-161 °C. ^{1}H NMR ($CDCl_3$): δ 1.43 (t, *J* = 7.1 Hz, 3H), 4.43 (q, *J* = 7.1 Hz, 2H), 7.15-7.16 (m, 1H), 7.31 (d, *J* = 8.1 Hz, 1H), 7.41 (dd, *J* = 7.0 Hz, 1H), 7.84 (m, 1H), 9.98 ppm (broad s, disappeared on treatment with D_2O, 1H). IR: ν 1690, 3311 cm^{-1}. Anal. ($C_{11}H_{10}BrNO_2$ (268.11)) C H Br N.

***N*-(3-Fluoro-2-methylphenyl)pivalamide (110).**- Pivaloyl chloride (1.59 g, 1.62 mL, 0.0132 mol) was added dropwise at 0 ºC to a solution of 3-fluoro-2-methylaniline (**103**) (1.50 g, 0.012 mol), triethylamine (1.33 g, 1.84 mL, 0.0132 mol) in anhydrous tetrahydrofuran (20 mL). The reaction mixture was stirred at room temperature for 1 h. The solvent was evaporated at reduced pressure to give a residue which was treated with water (30 mL) and extracted with ethyl acetate. The organic layer was washed with brine, dried, filtered and evaporated to dryness. The crude solid residue was crystallized from cyclohexane to give **110** as a white solid (1.93 g, 77%), mp 99-101 ºC (from

cyclohexane). ^{1}H NMR ($CDCl_3$): δ 1.35 (s, 9H), 2.16 (d, *J* = 1.8 Hz, 3H), 6.86 (t, *J* = 8.8 Hz, 1H), 7.16 (q, *J* = 7.6 Hz, 1H), 7.26 (broad s, 1H, disappeared on treatment with D_2O), 7.64 ppm (d, *J* = 8.2 Hz, 1H). IR: ν 1648, 3294 cm^{-1}. Anal. ($C_{12}H_{16}FNO$ (209.26)) C H F N.

***N*-(4-Chloro-3-fluoro-2-methylphenyl)pivalamide (112)**. A solution of **110** (1.77 g, 0.0084 mol) in anhydrous DMF (10 mL) was added dropwise and under an argon stream to a solution of *N*-chlorosuccinimide (NCS) (1.12 g, 0.0084 mol) in the same solvent (10 mL). The reaction mixture was heated at 80 ºC in the argon atmosphere for 30 min. After cooling, water was added and the mixture was extracted with ethyl acetate. The organic layer was washed with brine, dried, filtered and evaporated at reduced pressure. The crude solid residue was crystallized from cyclohexane to give **112** as a white solid (1.83 g, 89%), mp 114-116 ºC (from cyclohexane). ^{1}H NMR ($CDCl_3$): δ 1.34 (s, 9H), 2.18 (d, *J* = 2.1 Hz, 3H), 7.19-7.24 (m, 2H, t, *J* = 8.5 Hz, 1H after treatment with D_2O), 7.59 ppm (dd, *J* = 8.8 and 1,6 Hz, 1H). IR: ν 1649, 3319 cm^{-1}. Anal. ($C_{12}H_{15}ClFNO$ (243.71)) C H Cl F N.

4-Chloro-3-fluoro-2-methylaniline (113).- A solution of **112** (1.37 g, 0.0056 mol) in dioxane (20 mL) and 6N HCl (10 mL) was heated at 100 ºC overnight. After cooling, a saturated aqueous solution of potassium carbonate was added to reach pH ~ 9 (CO_2 evolution!) and the mixture was extracted with ethyl acetate. The organic layer was washed with brine, dried, filtered and evaporate at reduced pressure. The crude residue was purified by silica gel column chromatography (dichloromethane as eluent) to give **113** as a yellow oil (0.88 g, 99%), ^{1}H NMR ($CDCl_3$): δ 2.10 (d, *J* = 2.0 Hz, 3H), 3.70 (broad s, 2H, disappeared on treatment with D_2O), 6.41 (dd, *J* = 8.6 and 1.5 Hz, 1H), 7.01 ppm (t, *J* = 8.3 Hz, 1H). IR: ν 3394, 3476 cm^{-1}. Anal. (C_7H_7ClFN (159.59)) C H Cl F N.

1-Chloro-2-fluoro-3-methyl-4-nitrobenzene (114). A mixture of **113** (0.61 g, 0.0038 mol), 3-chloroperoxybenzoic acid (70% wt, 4.68 g, 0.019 mol) in toluene (15 mL) was refluxed for 3 h. After cooling, dichloromethane was

added; the mixture was filtered and the solid was washed with the same solvent. The organic layer was washed with a saturated solution of sodium hydrogen carbonate, with brine and dried. After concentration to a small volume under reduced pressure, the crude oily residue was purified by silica gel column chromatography (dichloromethane as eluent) to give **114** as a colorless oil (0.60 g, 83%). ^{1}H NMR ($CDCl_3$): δ 2.54 (d, *J* = 2.5 Hz, 3H), 7.40 (t, *J* = 8.0 Hz, 1H), 7.75 ppm (dd, *J* = 8.9 and 1.5 Hz, 1H). Anal. ($C_7H_5ClFNO_2$ (189.57)) C H Cl F N.

Ethyl 3-(3-Chloro-2-fluoro-6-nitrophenyl)-2-oxopropanoate (115). A solution of **114** (3.43 g, 0.018 mol) in anhydrous ethanol (5 mL) was added to a solution of sodium ethoxide (obtained for the dissolution of sodium (0.62 g, 0.027 ga) in the same solvent (35 mL). Diethyl oxalate (20 mL) was added, and the reaction mixture was stirred at room temperature overnight. The excess of diethyl oxalate was distilled off. A saturated solution of ammonium chloride was added and the mixture was extracted with ethyl acetate (20 mL). The organic layer was washed with brine, dried, filtered and evaporated at reduced pressure. The residue was purified by silica gel column chromatography (ethyl acetate:*n*-hexane 3:7 as eluent) to give **115** as an yellow oil (3.47 g, 67%). ^{1}H NMR ($CDCl_3$): δ 1.43 (t, *J* = 7.2 Hz, 3H), 4.43 (q, *J* = 7.1 Hz, 2H), 4.64 (d, *J* = 1.4 Hz, 2H), 7.57 (dd, *J* = 8.1 and 7.3 Hz, 1H), 7.98 ppm (dd, *J* = 9.0 and 1.7 Hz, 1H). IR: ν 1730 cm^{-1}. Anal. ($C_{11}H_9ClFNO_5$ (289.64)) C H Cl F N.

Ethyl 5-Chloro-4-fluoro-1*H*-indole-2-carboxylate (105). Iron powder (0.41 g, 0.0074 ga) was added to a solution of **115** (0.40 g, 0.0014 mol) in acetic acid (8 mL) at 60 °C, and the reaction mixture was heated at same temperature overnight. After cooling, the solvent was evaporated to dryness at reduced pressure. Water was added and the mixture was extracted with ethyl acetate. The organic layer was washed with a saturated solution of sodium hydrogen carbonate and with brine, dried, filtered and evaporated at reduced pressure. The crude solid residue was purified by silica gel column chromatography (ethyl acetate:*n*-hexane 3:7 as eluent) to give **105** as a white solid (0.33 g, 100%), mp

191-193 °C (from ethanol). Lit.[75] 186-190 ºC. ^{1}H NMR and IR spectra were identical to those of the sample we previously described.[74]

Cbz-Ala-ψ-[CH_2SAc] (148). Potassium thioacetate (3.03 g, 26.5 mmol) was added in one portion to a solution of mesylate **147**[76] (1.51 g, 5.26 mmol) in DMF (26 mL) and stirring was maintained at room temperature overnight. The mixture was diluted with water (50 mL) and extracted with ethyl acetate. The pooled organic phases were washed with water, 5% sodium hydrogen sulphate and brine. After removal of the solvent, the crude product was triturated with *n*-hexane to give 69 as a pale yellow solid (yield 60%). ^{1}H NMR: δ 1.20 (d, *J* = 6.6 Hz, 3H), 2.40 (s, 3H), 3.02 (d, *J* = 6.2 Hz, 2H), 3.99-4.05 (m, 1H), 5.05 (s, 2H), 6.99 ppm (broad s, 1H, disappeared on treatment with D_2O), 7.39-7.41 (m, 5H). IR: ν 1715, 3435 cm^{-1}. Anal ($C_{13}H_{17}NO_3S$ (267.34)) C H N S.

Cbz-Ala-ψ-[CH_2SO_2]-Cl (150). A solution of **148** (0.82 g, 3.06 mmol) in acetic acid (5 mL) was treated with a solution hydrogen peroxide [30% w/w in water (3 mL)] and acetic acid (7 mL). After stirring overnight at room temperature, the excess of peroxide was destroyed by addition of 10% Pd/C (0.050 g). The mixture was filtered on celite, concentrated and coevaporated with toluene. To the crude sulfonic acid **149** was suspended in anhydrous dichloromethane (20 mL), and a solution of phosgene in toluene (20% m/m, 2.5 mL) and dry DMF (0.4 ml) was added under nitrogen atmosphere. After 1 h was added an additional 1 mL of phosgene solution and the mixture was stirred for 2 h under the same conditions. After removal of the solvent, the crude product was purified by silica gel flash chromatography (chloroform-methanol 97:3) to give **150** as a white solid (yield 70%). ^{1}H NMR: δ 1.50 (d, *J* = 6.7 Hz, 3H), 3.86-3.89 (m, 1H), 4.15-4.18 (m, 1H), 4.33-4.37 (m, 1H), 5.12 (s, 2H), 7.01 (broad s, 1H, disappeared on treatment with D_2O), 7.34-7.37 ppm (m, 5H). IR: ν 1719, 3439 cm^{-1}. Anal ($C_{11}H_{14}ClNO_4S$ (291.75)) C H Cl N S.

Cbz-Ala-ψ-[CH_2SO_2]-NH_2 (151). Gaseous ammonia was bubbled for 30 min through an ice-cooled solution of **150** (0.52 g, 1.8 mmol) in benzene (15 mL). The mixture was heated at 60 °C for 2 h. After cooling, the precipitate was

collected, washed with benzene and dried to afford **152** as a white solid (yield 73%). ^{1}H NMR: δ 1.24 (d, *J* = 6.6 Hz, 3H), 3.13-3.18 (m, 2H), 4.04-4.09 (m, 1H), 5.08 (s, 2H), 6.95 (broad s, 2H, disappeared on treatment with D_2O), 7.34-7.39 ppm (m, 5H). IR: ν 1728, 3452 cm^{-1}. Anal ($C_{11}H_{16}N_2O_4S$ (272.32)) C H N S.

HCl-Ala-ψ-[CH_2SO_2]-NH_2 (152). The sulfonilamide hydrochloride **152** was obtained by treating **151** with hydrogen in methanol/water/37% HCl (10:10:1, 20 mL) in the presence of 10% Pd/C for 3 h at room temperature. The solution was filtered on celite and the solvent removed under reduced pressure. The crude salt was triturated with diethyl ether and used without further purification in the next coupling step. Anal. ($C_3H_{11}ClN_2O_2S$ (174.65)) C H Cl N S.

Molecular Modeling. All molecular modelling studies were performed on a MacPro dual 2.66 GHz Xeon running Ubuntu 8. The RTS structures were downloaded from the PDB data bank (http://www.rcsb.org/). Hydrogen atoms were added to the protein, using Molecular Operating Environment (MOE) 2007.09,[67] and minimized keeping all the heavy atoms fixed until a RMSD gradient of 0.05 kcal mol^{-1} Å^{-1} was reached. Ligand structures were built with MOE and minimized using the MMFF94x forcefield until a RMSD gradient of 0.05 kcal mol^{-1} Å^{-1} was reached. The docking simulations were performed using FlexX[77] with the MOE interface using default settings and getting 20 poses for compound, with SurfleX[78] with the Sybyl8.0[79] interface also in this case using default settings and getting 10 poses for compound and PLANTS[80] with the Zodiac[81] interface. In the Zodiac GUI for PLANTS we setted the binding lattice as a sphere of 12Å binding site radius from the centre of 2zd1[53] co-crystallized inhibitor. Also in this case we used all default settings. The Y181I mutation was obtained by mutating the specific residue in the 1jkh[67] crystal using the rotamer explorer tool in MOE and using the lowest energy conformation obtained. The calculation of the RMSDs values between the co-crystallized and docked conformation were calculated by MOE SVL script.[82] The images in the manuscript were created with Zodiac[79] and PyMOL.[83]

Cell Based Antiviral Assay Procedures

Antiviral activity assays. The compounds were evaluated against the following viruses: human immunodeficiency virus type 1 strain IIIB and human immunodeficiency virus type 2 strain ROD. Viral cytopathicity was recorded as soon as it reached completion in the control virus-infected cell cultures that were not treated with the test compounds. Antiviral activity was expressed as the EC_{50} or concentration required to reduce virus-induced cytopathogenicity by 50%.

Inhibition of HIV-induced cytopathicity in CEM cells. The methodology for the anti-HIV assays had been described previously.[84] Briefly, human CEM cell cultures (~3 x 10^5 cells/ml^{-1}) were infected with ~ 100 $CCID_{50}$ HIV-1(IIIB) or HIV-2 (ROD) per ml and seeded in 200 µl-well microtiter plates, containing appropriate dilutions of the test compounds. After 4 days of incubation at 37°C, syncytia cell formation was examined microscopically in the CEM cell cultures.

Cytotoxicity assays. The cytostatic concentration was calculated as the CC_{50}, or the compound concentration required to reduce cell proliferation by 50% relative to the number of cells in the untreated controls. CC_{50} values were estimated from graphic plots of the number of cells (percentage of control) as a function of the concentration of the test compounds. Alternatively, cytotoxicity of the test compounds was expressed as the minimum cytotoxic concentration (MCC) or the compound concentration that caused a microscopically detectable alteration of cell morphology.

Enzymatic Assay Procedures

Chemicals. [^{3}H]dTTP (40 Ci/mmol) was from Amersham and unlabelled dNTP's from Boehringer. Whatman was the supplier of the GF/C filters. All other reagents were of analytical grade and purchased from Merck or Fluka.

Nucleic acid substrates. The homopolymer poly(rA) (Pharmacia) was mixed at weight ratios in nucleotides of 10:1, to the oligomer $oligo(dT)_{12\text{-}18}$ (Pharmacia) in 20 mM Tris-HCl (pH 8.0), containing 20 mM KCl and 1 mM EDTA, heated at 65 °C for 5 min and then slowly cooled at room temperature.

Expression and purification of recombinant HIV-1 RT forms. The coexpression vectors pUC12N/p66(His)/p51with the wild-type or the mutant forms of HIV-1 RT p66 were kindly provided by Dr. S. H. Hughes (NCI-Frederick Cancer Research and Development Center). Proteins were expressed in E.coli and purified as described.[85]

HIV-1 RT RNA-dependent DNA polymerase activity assay. RNA-dependent DNA polymerase activity was assayed as follows: a final volume of 25 µl contained reaction buffer (50 mM Tris-HCl pH 7.5, 1 mM DTT, 0.2 mg/ml BSA, 4% glycerol), 10 mM $MgCl_2$, 0.5 µg of poly(rA)/oligo(dT)$_{10:1}$ (0.3 µM 3'-OH ends), 10 µM [^{3}H]-dTTP (1Ci/mmol) and 2-4 nM RT. Reactions were incubated at 37°C for the indicated time. 20 µl-Aliquots were then spotted on glass fiber filters GF/C which were immediately immersed in 5% ice-cold TCA. Filters were washed twice in 5% ice-cold TCA and once in ethanol for 5 min, dried and acid-precipitable radioactivity was quantitated by scintillation counting.

Inhibition assays. Reactions were performed under the conditions described for the HIV-1 RT RNA-dependent DNA polymerase activity assay. Incorporation of radioactive dTTP into poly(rA)/oligo(dT) at different substrate (nucleic acid or dTTP) concentrations was monitored in the presence of increasing fixed amounts of inhibitor. Data were then plotted according to Lineweaver-Burke and Dixon. For K_i determination, an interval of inhibitor concentrations between 0.2 K_i and 5 K_i was used.

Kinetic Procedures.

Chemicals. All the reagents were of analytical grade and purchased from Sigma–Aldrich (St. Louis, MO), Merck Sharp & Dohme (Readington, NJ), ICN (Research Products Division, Costa Mesa, CA), or AppliChem GmbH (Darmstadt, Germany). Radioactive 2'-deoxythymidine 5'-triphosphate [^{3}H]dTTP (40 Ci/mmol) was purchased from Amersham Bio-Sciences (GE Healthcare, Buckinghamshire, GB), while unlabeled dNTPs were from Boehringer Ingelheim

GmbH (Ingelheim, Germany). GF/C filters were provided byWhatman Int. Ltd. (Maidstone, England).

Template/primer. The homopolymer poly(rA) and the oligomer oligo(dT)12–18 (Pharmacia & Upjohn Inc. Pfizer, Peapack, NJ) were mixed atweight ratios in nucleotides of 10:1 with 25mMTris–HCl (pH 8.0) containing 22 mM KCl, heated at 70 °C for 5min and then slowly cooled at room temperature.

Steady-state kinetic assays. Steady state kinetic assays were also performed to evaluate the activity of HIV-1 RT in the presence of fixed concentrations (ID_{50}), of selected inhibitors and variable concentrations of either poly(rA)/oligo(dT) or [^{3}H]TTP, while the other was maintained at saturating doses. [^{3}H]TTP concentrations varied between 0.2 and 20 μM, while poly(rA)/oligo(dT) doses ranged from 10 to 200 nM. These experiments led to the determination of V_{max}, K_m and k_{cat} parameters from Michaelis Menten curves, as mentioned in the "calculation of kinetic parameters" section. The true inhibitor dissociation constant (Ki) values were derived as described.

Kinetics of inhibitor binding. Kinetics of inhibitor binding experimentswere as described previously. Briefly, HIV-1 RT (20–40 nM) was incubated for 2 min at 37 ◦C in a final volume of 4 μl in the presence of TDB buffer, with 10 mM $MgCl_2$ alone or with 100 nM 3'-OH ends (for the formation of the RT/TP complex), or in the same mixture complemented with 10 μM unlabeled dTTP (for the formation of the RT/TP/dNTP complex). The inhibitor to be tested was then added to a final volume of 5 μl at a concentration at which $[EI]/[E_0] = [1-1/(1 + [I]/K_i)] > 0.9$. Then, 145 μl of a mix containing TDB buffer, 10mM $MgCl_2$, and 10 μM [^{3}H]dTTP (5 Ci/mmol) was added at different time points. After an additional 10 min of incubation at 37 ◦C, 50-μl aliquots were spotted on GF/C filters, and acid-precipitable radioactivity was measured as described for the HIV-1 RT RNA-dependent DNA polymerase activity assay. The v_t/v_0 ratio, representing the normalized difference between the amount of dTTP incorporated at the zero time point and at different time points, was then

plotted against time. The k_{app} values, the association rate (k_{on}) and the dissociation rate (k_{off}) values were calculated as described in the kinetic parameter calculation section.

Data analysis and statistics. Data obtained were analyzed by non-linear regression analysis using GraphPad Software (San Diego, CA, USA).

Kinetic parameter calculation. All valueswere calculated by non-least-squarescomputer fitting of the experimental data to the appropriate rate equations. Steady-state inhibitor binding was analysed according to the equation for mixed type inhibition:

$$v = \left\{ \frac{\left[V_{\max} / \left(1 + I / K_i''\right)\right]}{\left[1 + \left(K_m / S\right)\right]} \frac{\left(1 + I / K_i'\right)}{\left(1 + I / K_i''\right)} \right\} \quad (1)$$

According to Figure26B, when TP was saturating, left part, $K_i' = K_i^{free}$, whereas at saturating dNTP (right part), $K_i' = K_i^{bin}$. In all cases, $K_i'' = K_i^{ter}$. According to the mixed-type mechanism of Equation (1) it follows that, if $K_i' = K_i''$, then both K_m and V_{max} values will decrease at increasing inhibitor concentrations. When $K_i' = K_i''$, then Equation (1) can be simplified to the one describing a fully non-competitive mechanism. The equilibrium dissociation constants (K_i' and K_i'') were calculated under the conditions shown in Figure 26B, right panel, from the variations of the K_m and V_{max} values as a function of the inhibitor concentrations according to the equations:

$$K_i' = \frac{I}{\left\{\left[K_p\left(1 + I / K_i'\right) / K_m\right] - 1\right\}} \quad (2)$$

$$K_i'' = \frac{I}{\left[\left(V_{\max} / V_p\right) - 1\right]} \quad (3)$$

where K_p and V_p are the apparent K_m and V_{max} values, respectively, at each given inhibitor concentration.

The true inhibition constant K_i (which according to the kinetic model was assumed as $K_i^{bin} = K_i^{ter}$) was calculated under the conditions shown in Figure 26B, left panel.

The apparent catalytic rates were calculated from the relationship: $v_0 = k_{cat}[E]_0$

The apparent binding rate (k_{app}) values were determined by fitting the experimental data to the single-exponential equation:

$$\frac{v_t}{v_0} = e^{-K}app^t \qquad (4)$$

where t is time. If $[E]_0$ is the input enzyme concentration, $[E]_t$ is the enzyme available for the reaction at time *t*, and $[E:I]_t$ is the enzyme bound to the inhibitor at time *t*, it follows that

$$[E]_t = [E]_0 - [E:I]_t$$

Since $v_0 = k_{cat}[E]_0$ and $v_t = k_{cat}[E]_t$, then $v_t/v_0 = 1 - [E:I]_t/[E]_0$. Thus, the v_t/v_0 value is proportional to the fraction of enzyme bound to the inhibitor.

The true association (k_{on}) and dissociation (k_{off}) rates were calculated from the equations:

$$k_{app} = k_{on}([I] + K_i) \qquad (5)$$

$$k_{off} = k_{on}K_i \qquad (6)$$

Table 19. Elemental Analyses of Derivatives **34-93**.

Compd	Calculated	Found
34	**C, 54.35; H, 4.32; Cl, 8.44; N, 10.01; O, 15.24; S, 7.64**	**C, 54.16; H, 4.28; Cl, 8.40; N, 9.95; O, 15.16; S, 7.60**
35	C, 49.15; H, 3.91; Br, 17.21; N, 9.05; S, 6.91	C, 48.97; H, 3.90; Br, 17.18; N, 8.99; S, 6.86
36	C, 53.02; H, 4.22; N, 13.02; S, 7.45	C, 52.87; H, 4.20; N, 12.97; S, 7.41
37	C, 52.12; H, 3.91; Cl, 8.10; F, 4.34; N, 9.60; S, 7.32	C, 51.98; H, 3.89; Cl, 8.08; F, 4.31; N, 9.57; S, 7.29
38	**C, 55.36; H, 4.65; Cl, 8.17; N, 9.68; O, 14.75; S 7.39**	**C, 55.27; H, 4.63; Cl, 8.13; N, 9.64; O, 14.68; S, 7.34**
39	C, 50.22; H, 4.21; Br, 16.70; N, 8.78; S, 6.70	C, 50.03; H, 4.19; Br, 16.66; N, 8.75; S, 6.67
40	C, 54.05; H, 4.54; N, 12.61; S, 7.21	C, 53.79; H, 4.53; N, 12.57; S, 7.17
41	C, 53.16; H, 4.24; Cl, 7.85; F, 4.20; N, 9.30; S, 7.10	C, 52.89; H, 4.23; Cl, 7.81; F, 4.18; N, 9.27; S, 7.05
42	C, 55.36; H, 4.65; Cl, 8.17; N, 9.68; S, 7.39	C, 55.11; H, 4.63; Cl, 8.15; N, 9.63; S, 7.32
43	C, 50.22; H, 4.21; Br, 16.70; N, 8.78; S, 6.70	C, 50.01; H, 4.19; Br, 16.61; N, 8.71; S, 6.66
44	C, 54.05; H, 4.54; N, 12.61; S, 7.21	C, 53.77; H, 4.52; N, 12.57; S, 7.18
45	C, 53.16; H, 4.24; Cl, 7.85; F, 4.20; N, 9.30; S, 7.10	C, 52.88; H, 4.22; Cl, 7.81; F, 4.18; N, 9.27; S, 7.09
46	C, 56.31; H, 4.95; Cl, 7.91; N, 9.38; S, 7.16	C, 56.02; H, 4.94; Cl, 7.89; N, 9.31; S, 7.14
47	C, 51.22; H, 4.50; Br, 16.23; N, 8.53; S, 6.51	C, 50.98; H, 4.48; Br, 16.17; N, 8.51; S, 6.49
48	C, 55.01; H, 4.84; N, 12.22; S, 6.99	C, 54.78; H, 4.82; N, 12.20; S, 6.97
49	C, 54.13; H, 4.54; Cl, 7.61; F, 4.08; N, 9.02; S, 6.88	C, 52.89; H, 4.53; Cl, 7.58; F, 4.05; N, 8.99; S, 6.85
50	C, 48.56; H, 4.29; Cl, 7.54; N, 8.94; S, 13.65	C, 48.29; H, 4.27; Cl, 7.51; N, 8.89; S, 13.58
51	C, 44.36; H, 3.92; Br, 15.53; N, 8.17; S, 12.47	C, 44.12; H, 3.91; Br, 15.42; N, 8.09; S, 12.39
52	C, 47.49; H, 4.20; N, 11.66; S, 13.35	C, 47.32; H, 4.18; N, 11.61; S, 13.29
53	C, 46.77; H, 3.92; Cl, 7.27; F, 3.89; N, 8.61; S, 13.14	C, 46.56; H, 3.90; Cl, 7.23; F, 3.85; N, 8.58; S, 13.10
54	C, 49.63; H, 4.58; Cl, 7.33; N, 8.68; S, 13.25	C, 49.45; H, 4.55; Cl, 7.27; N, 8.62; S, 13.19
55	C, 45.46; H, 4.20; Br, 15.12; N, 7.95; S, 12.14	C, 45.24; H, 4.19; Br, 15.07; N, 7.91; S, 12.1
56	C, 48.57; H, 4.48; N, 11.33; S, 12.97	C, 48.29; H, 4.45; N, 11.28; S, 12.85
57	C, 47.85; H, 4.22; Cl, 7.06; F, 3.78; N, 8.37; S, 12.78	C, 47.62; H, 4.19; Cl, 7.01; F, 3.74; N, 8.31; S, 12.71

Table 19. Elemental Analyses of Derivatives **34-93**. (*Continued...*)

Compd	Calculated	Found
58	**C, 59.25; H, 5.42; Cl, 7.95; N, 9.42; O, 10.76; S, 7.19**	**C, 59.27; H, 5.38; Cl, 7.90; N, 9.35; O, 10.69; S, 7.12**
59	**C, 53.88; H, 4.93; Br, 16.29; N, 8.57; O, 9.79; S, 6.54**	C, 53.66; H, 4.90; Br, 16.21; N, 8.50; O, 9.72; S, 6.52
60	**C, 57.88; H, 5.30; N, 12.27; O, 17.52; S, 7.02**	**C, 57.59; H, 5.27; N, 12.19; O, 17.43; S, 6.99**
61	**C, 56.95; H, 5.00; Cl, 7.64; F, 4.09; N, 9.06; O, 10.35; S, 6.91**	**C, 56.76; H, 4.97; Cl, 7.59; F, 4.03; N, 9.00; O, 10.29; S, 6.86**
62	**C, 60.05; H, 5.70; Cl, 7.71; N, 9.14; O, 10.43; S, 6.97**	C, 59.88; H, 5.67; Cl, 7.67; N, 9.11; O, 10.38; S, 6.94
63	**C, 54.76; H, 5.20; Br, 15.84; N, 8.33; O, 9.52; S, 6.36**	C, 54.59; H, 5.18; Br, 15.79; N, 8.29; O, 9.44; S, 6.31
64	**C, 58.71; H, 5.57; N, 11.91; O, 17.00; S, 6.81**	**C, 58.44; H, 5.53; N, 11.84; O, 16.91; S, 6.84**
65	C, 57.79; H, 5.27; Cl, 7.42; F, 3.97; N, 8.79; O, 10.04; S, 6.71	C, 57.66; H, 5.22; Cl, 7.37; F, 3.94; N, 8.72; O, 9.99; S, 6.68
66	**C, 57.20; H, 5.24; Cl, 7.67; N, 9.10; O, 13.85; S, 6.94**	**C, 56.97; H, 5.22; Cl, 7.62; N, 9.04; O, 13.78; S, 6.88**
67	C, 52.18; H, 4.78; Br, 15.78; N, 8.30; O, 12.64; S, 6.33	C, 51.89; H, 4.75; Br, 15.69; N, 8.24; O, 12.57; S, 6.29
68	C, 63.64; H, 4.67; Cl, 7.83; N, 6.18; O, 10.60; S, 7.08	C, 63.48; H, 4.63; Cl, 7.78; N, 6.13; O, 10.55; S, 7.02
69	C, 57.95; H, 4.26; Br, 16.06; N, 5.63; O, 9.65; S, 6.45	C, 57.78; H, 4.23; Br, 16.02; N, 5.60; O, 9.61; S, 6.40
70	C, 62.19; H, 4.57; N, 9.07; O, 17.26; S, 6.92	C, 61.89; H, 4.54; N, 9.03; O, 17.19; S, 6.89
71	C, 61.21; H, 4.28; Cl, 7.53; F, 4.03; N, 5.95; O, 10.19; S, 6.81	C, 69.98; H, 4.26; Cl, 7.49; F, 4.01; N, 5.91; O, 10.11; S, 6.78
72	C, 55.92; H, 5.12; N, 11.86; O, 20.32; S, 6.79	C, 55.66; H, 5.07; N, 11.77; O, 20.21; S, 6.69
73	C, 55.05; H, 4.83; Cl, 7.39; F, 3.96; N, 8.76; O, 13.33; S, 6.68	C, 54.76; H, 4.80; Cl, 7.36; F, 3.94; N, 8.72; O, 13.27; S, 6.63
74	C, 60.05; H, 5.70; Cl, 7.71; N, 9.14; O, 10.43; S, 6.97	C, 59.68; H, 5.68; Cl, 7.67; N, 9.12; O, 10.35; S, 6.92
75	C, 54.76; H, 5.20; Br, 15.84; N, 8.33; O, 9.52; S, 6.36	C, 54.58; H, 5.18; Br, 15.80; N, 8.29; O, 9.48; S, 6.31

Table 19. Elemental Analyses of Derivatives **34-93**. (*Continued...*)

Compd	Calculated	Found
76	C, 58.71; H, 5.57; N, 11.91; O, 17.00; S, 6.81	C, 58.67; H, 5.54; N, 11.84; O, 17.05; S, 6.77
77	C, 57.79; H, 5.27; Cl, 7.42; F, 3.97; N, 8.79; O, 10.04; S, 6.71	C, 57.59; H, 5.24; Cl, 7.38; F, 3.94; N, 8.72; O, 9.98; S, 6.66
78	C, 60.59; H, 4.86; Cl, 7.78; N, 9.22; O, 10.53; S, 7.03	C, 60.36; H, 4.81; Cl, 7.72; N, 9.15; O, 10.47; S, 7.00
79	C, 55.20; H, 4.43; Br, 15.97; N, 8.40; O, 9.59; S, 6.41	C, 55.01; H, 4.42; Br, 15.92; N, 8.33; O, 9.50; S, 6.37
80	**C, 59.22; H, 4.75; N, 12.01; O, 17.15; S, 6.87**	**C, 58.98; H, 4.73; N, 11.96; O, 17.08; S, 6.84**
81	**C, 58.29; H, 4.47; Cl, 7.48; F, 4.01; N, 8.87; O, 10.13; S, 6.77**	C, 58.02; H, 4.44; Cl, 7.42; F, 3.99; N, 8.83; O, 10.07; S, 6.73
82	**C, 58.04; H, 5.51; Cl, 7.45; N, 8.83; O, 13.45; S, 6.74**	**C, 57.89; H, 5.48; Cl, 7.42; N, 8.78; O, 13.38; S, 6.69**
83	C, 53.08; H, 5.04; Br, 15.35; N, 8.07; O, 12.30; S, 6.16	C, 52.97; H, 5.02; Br, 15.27; N, 8.02; O, 12.25; S, 6.14
84	**C, 56.78; H, 5.39; N, 11.52; O, 19.73; S, 6.59**	**C, 56.59; H, 5.35; N, 11.47; O, 19.60; S, 6.51**
85	C, 55.92; H, 5.10; Cl, 7.18; F, 3.85; N, 8.51; O, 12.96; S, 6.49	C, 55.77; H, 5.08; Cl, 7.15; F, 3.84; N, 8.48; O, 12.88; S, 6.46
86	C, 64.30; H, 4.96; Cl, 7.59; N, 6.00; O, 10.28; S, 6.87	C, 64.18; H, 4.94; Cl, 7.53; N, 5.89; O, 10.20; S, 6.83
87	C, 58.71; H, 4.53; Br, 15.62; N, 5.48; O, 9.39; S, 6.27	C, 58.58; H, 4.51; Br, 15.57; N, 5.45; O, 9.33; S, 6.24
88	C, 62.88; H, 4.85; N, 8.80; O, 16.75; S, 6.71	C, 62.65; H, 4.83; N, 8.75; O, 16.68; S, 6.69
89	C, 61.91; H, 4.57; Cl, 7.31; F, 3.92; N, 5.78; O, 9.90; S, 6.61	C, 61.91; H, 4.57; Cl, 7.31; F, 3.92; N, 5.78; O, 9.90; S, 6.59
90	C, 62.17; H, 4.80; Cl, 7.34; N, 5.80; O, 13.25; S, 6.64	C, 61.88; H, 4.78; Cl, 7.31; N, 5.77; O, 13.19; S, 6.62
91	C, 56.93; H, 4.40; Br, 15.15; N, 5.31; O, 12.13; S, 6.08	C, 56.72; H, 4.42; Br, 15.11; N, 5.28; O, 12.05; S, 6.05
92	C, 60.84; H, 4.70; N, 8.51; O, 19.45; S, 6.50	C, 60.57; H, 4.68; N, 8.47; O, 19.39; S, 6.48
93	C, 59.94; H, 4.43; Cl, 7.08; F, 3.79; N, 5.59; O, 12.77; S, 6.40	C, 59.65; H, 4.42; Cl, 7.02; F, 3.78; N, 5.55; O, 12.69; S, 6.37

Acknowledgments:

Prof. Romano Silvestri, Dip. Chimica e Tecnologie del Farmaco, Sapienza Università di Roma.

Dr Giuseppe La Regina, Dip. Chimica e Tecnologie del Farmaco, Sapienza Università di Roma.

Dr Antonio Coluccia and Dr Valerio Gatti, Istituto Pasteur - Fondazione Cenci Bolognetti, Sapienza Università di Roma.

Dr Cesare Giordano, Dip. di Chimica e Tecnologie del Farmaco, Sapienza Università di Roma.

Dr Andrea Brancale, Welsh School of Pharmacy, Cardiff University.

Prof. Jean Balzarini, Rega Institute for Medical Research.

Dr Giovanni Maga, Istituto di Genetica Molecolare, Consiglio Nazionale delle Ricerche, Pavia.

I would like to thank my co-workers Valentina Gentili, Giuliana Robortaccio, Alessandra Di Pasquale, Maria De Rosa, Carmela Mazzoccoli, Cinzia D'Amico, Emanuala Aversa, Lea Cresca, Elisa D'Ascenzi, Raffaella Campagna, Lara Minelli, Lorenza Cianci, Grazia Di Fraia, Barbara Montuori, Monica Armenti, Maria Antonietta Brando, Emanuela Iacobelli, Martina Perciballi, Beatrice Di Pierro, Antonia Contento, Federica Belmaggio, Gabriele Bagaglini, Valentina Gattinara and my friends Valentina Pepe, Alberto Iacovo, Maria Giovanna Siniscalco, Benedetto Milelli, Luca Carola, Fabrizio Barberi, Paolo Mugione, Alessio Basili, Rossella Palumbo, Simone Bianchini and Paola Listo.

A special thank to Domenica Torino, Anna Sansone and Pasqualina Punzi.

References:

1. http://data.unaids.org/pub/GlobalReport/2008/jc1510_2008_global_report_pp211_234_en.pdf.
2. Wang, L. X. New approaches to HIV-1 inhibitor and vaccine design. *Curr. Pharm. Des.* **2007**, *13*, 127-128.
3. http://www.fda.gov/oashi/aids/status.html.
4. Orkin, C.; Stebbing, J.; Nelson, M.; Bower, M.; Johnson, M.; Mandalia, S.; Jones, R.; Moyle, G.; Fisher, M.; Gazzard, B. A randomized study comparing a three- and four-drug HAART regimen in first-line therapy. *J. Antimicrob. Chemoth.* **2005**, *55*, 246-251.
5. Li, X.; Margolick, J. B.; Conover, C. S.; Badri, S.; Riddler, S. A.; Witt, M. D.; Jacobson, L. P. Interruption and discontinuation of highly active antiretroviral therapy in the multicenter AIDS cohort study. *J. Acquired Immune Defic. Syndr.* **2005**, *38*, 320-328.
6. Vandamme, A.-M.; Van Vaerenbergh, K.; De Clercq, E. Anti-human immunodeficiency virus drug combination strategies. *AntiViral Chem. Chemother.* **1998**, *9*, 187-203.
7. Luciw, P. A. Human immunodeficiency virus and its replication. In: Fields BM, editor. Fields virology. 3rd ed. Philadelphia: Lippincott-Raven Publishers, 1996.
8. Ferguson, M. R.; Rojo, D. R.; von Lindern, J. J.; O' Brien, W. A. HIV-1 replication cycle. *Clin. Lab. Med.* **2002**, *22*, 611-635.
9. (a). Dalgleish, A. G.; Beverleym, P. C.; Clapham, P. R.; Crawford, D. H.; Greaves, M. F.; and Weiss, R. A. The CD4 (T4) antigen is an essential component of the receptor for the AIDS retrovirus. *Nature (London)* **1984**, *312*, 763-767. (b) Klatzmann, D.; Champagne, E.; Chamaret, S.; Gruest, J.; Guetard, D.; Hercend, T; Gluckman, J. D.; and Montagnier, L. T-lymphocyte T4 molecule behaves as the receptor for human retroviral LAy. *Nature (London)* **1984**, 312, 767-768. (c) McDougal, J. S.; Mawle, A.; Cort, S. F.; Nicholson, K. A.; Cross, D. G.; Scheppler-Campbell, J. A.; Hicks, D.; and Sligh, J. Cellular tropism of the human retrovirus HTLV III/LAy. I. role of T cell activation and expression of the T4 antigen. *Immunology* **1985**, *135*, 3151-3162
10. (a) McDougal, J. S.; Klatzmann, D. R.; Maddon, P. J. CD4-gp120 interactions. *Curr. Opin. Immunol.* **1991**, *3*, 552-558. (b) Rosenberg, Z. F. and Fauci, A. S. Immunopathogenesis of HIV infection. *FASEB J.* **1991**, *5*, 2382-2390.
11. (a) Stein, B. S.; Gowda, S. D.; Lifson, J. D.; Penhallow, R. C.; Bensch, K.G. and Engleman, E.G. pH-independent HIV entry into $CD4^+$ cells via virus envelope fusion to the plasma membrane. *Cell* **1987**, *49*, 659–668. (b) McClure, M. O.; Marsh, M. and Weiss, R. A. HIV infection of CD4-bearing cells occurs by a pH-independent mechanism. *EMBO* **1988**, *7*, 513-518.

12. (a) Famet, C.M. and Haseltine, W. A. Determination of viral proteins present in HIV-1 preintegration complex. *J. Virol.* **1991**, *65*, 1910-1915. (b) Lewis, P.; Gensel, M. and Emerman, M. HIV infection of cells arrested in the cell cycle. *EMBO* **1992**, *11*, 3053–3058. (c) Stevenson, M.; Bukrinsky, M. and Haggerty S: HIV-1 replication and potential targets for intervention. *AIDS Res Hum Retroviruses* **1992**, *8*; 107-117. (d) Bkrinsky, M.I.; Sharova, N.; McDonald, T. L.; Pushkarskaya, T.; Tarpley, W. G. and Stevenson M. Association of IN, MA and RT antigens of HIV-1 with viral nucleic acids following acute infection. *Proc. Natl. Acad. Sci. USA.* **1993**, *90*, 6125-6129.
13. Fujiwara, T. and Mizuuchi, K. Retroviral DNA integration: structure of an integration intermediate. *Cell* **1988**, *54*, 497-504.
14. (a) Kulkosky, J. and Skalka, A. M. HIV DNA integration: observations and inferences. *J. AIDS* **1990**, *3*, 839-851. (b) Bushman, F. D. and Craigie, R. Activities of HIV integration protein *in vitro:* specific cleavage and integration of HIV DNA. *Proc. Natl. Acad. Sci. USA.* **1991**, *88*, 1339-1343. (c) Engelman, A.; Mizuuchi, K. and Craigie, R. HIV-1 DNA integration: mechanism of viral DNA cleavage and DNA strand transfer. *Cell* **1991**, *67*, 1211-1221.
15. Chen, B. K.; Saksela, K.; Andino, R. and Baltimore, D. Distinct modes of HIV-1 proviral latency revealed by superinfection of non-productive infected cell lines with recombinant luciferase-encoding viruses. *J. Virol.* **1994**, *68*, 654-660.
16. Newman, M.; Harrison, J.; Saltavelli, M.; Hedjiyannis, E.; Erfle, V.; Felber, B. K. and Pavlakis, G. Splicing variability in HIV-1 revealed by quantitative RNA polymerase chain reaction. *AIDS ResHuman Retroviruses* **1994**, *10*, 1531-1542.
17. Truus, E. M. and Abbink, B. B. HIV-1 reverse transcription initiation: A potential target for novel antivirals? *Virus Research* **2008**, *134*, 4–18.
18. (a) Lever, A.; Gottinger, H.; Haseltine, W. A. and Sodroski, J. G. Identification of a sequence required for efficient packaging of HIV-1 RNA into virions. *J. Virol.* **1989**, *63*, 4085-4087. (b) Aldovini, A. and Young, R. A. Mutations of RNA and protein sequences involved in HIV-1 packaging result in production of non-infectious virus. *J. Virol.* **1990**, *64*, 1920-1926. (c) Hayashi, T.; Shioda, T.; Iwakura, Y. and Shibuta, H. RNA Ψ signal of HIV-1. *Virology* **1992**, *188*, 590-599. (d) Hayashi, T.; Ueno, Y. and Okamoto, T. Elucidation of a conserved RNA stem-loop structure in the Ψ signal of HIV-1. *FEBS Lett.* **1993**, *327*, 213-218. (e) Luban, J. and Goff, S. Mutational analysis of *cis-acting* signals Ψ in HIV-1. *J. Virol.* **1994**, *68*, 3784-4793. (f) Clever, J.; Sassetti, C. and Parslow, T. G. RNA secondary structure and binding sites for *gag* gene products in the 5' Ψ signal of HIV-1. *J. Virol.* **1995**, *69*, 2101-2109.

19. Richardson, J. H. and Child, L. A. Lever AM Packaging of HIV-1 RNA requires *cis*acting sequences outside the 5' leader region. *J. Virol.* **1993**, *67*, 3997-4005.
20. (a) Darlix, J. L.; Gabus, C.; Nugeyre, M. T.; Clavel, F. and Barre-Sinoussi, F.: *Cis* elements and *trans-acting* factors involved in the RNA dimerization of the HIV-1. *J. Mol. Biol.* **1990**, *216*, 689-699. (b) Awang, G. and Sen, D. Mode of dimerization of HIV-1 genomic RNA. *Biochemistry* **1993**, *32*, 11453-11457. (c) Sundquist, W. I. and Heaphy, S. Evidence for interstrand quadruplex formation in the dimerization of HIV-1 genomic RNA. *Proc. Natl. Acad. Sci. USA* **1993**, *90*, 3393-3397.
21. Dannull, J.; Surovoy, A.; Jung, G. and Moelling, K. Specific binding of HIV-1 nucleocapsid protein to PSI RNA *in vitro* requires N-terminal zinc finger and flanking basic amino acid residues. *EMBO* **1994**, *13*, 1525-1533.
22. Nguyen, D. H. and Hildreth, J. E. Evidence for budding of human immunodeficiency virus type 1 selectively from glycolipid-enriched membrane lipid rafts. *J. Virol.* **2000**, *74*, 3264–3272.
23. Gould, S. J.; Booth, A. M. and Hildreth, J. E. The Trojan exosome hypothesis. *Proc. Natl. Acad. Sci. USA* **2000**, *100*, 10592–10597.
24. Raiborg, C.; Rusten, T. E. and Stenmark, H. Protein sorting into multivesicular endosomes. *Curr. Opin. Cell. Biol.* **2003**, *15*, 446–455.
25. McDonald, D.; Wu, L.; Bohks, S. M.; Kewa, V. N.; Ramani, I.; Unutmaz, D. and Hope, T. J. Recruitment of HIV and its receptors to dendritic cell – T cell junctions. *Science* **2003**, *300*, 1295–1297.
26. Jolly, C.; Kashefi, K.; Hollinshead, M. and Sattentau, Q. J. HIV-1 cell to cell transfer across an Env-induced, actin-dependent synapse. *J. Exp. Med.* **2004**, *199*, 283–293.
27. Pearce-Pratt, R.; Malamud, D. and Phillips, D. M. Role of the cytoskeleton in cell-to-cell transmission of human immunodeficiency virus. *J. Virol.* **2004**, *68*; 2898–2905.
28. Perotti, M. E.; Tan, X. and Phillips, D. M. Directional budding of human immunodeficiency virus from monocytes. *J. Virol.* **1996**, *70*, 5916–5921.
29. Brik, A. B. and Wong, C. H. HIV-1 protease: mechanism and drug discovery. *Org. Biomol. Chem.* **2003**, *1*, 5-14.
30. McDonald, S. K. and Kuritzkes, D. R. Human immunodeficiency virus type 1 protease inhibitors. *Arch. Intern. Med.* **1997**, *157*, 951-959.
31. Lalezari, J. P.; Henry, K. and O' Hearn, M. Enfuvirtide, an HIV-1 fusion inhibitor, for drug resistant HIV infection in North and South America. *N. Engl. J. Med.* **2003**, *348*, 2175-2185.

32. (a) Cooper, D. *et al*. Results of BENCHMRK-1, a Phase III study evaluating the efficacy and safety of MK-0518, a novel HIV-1 integrase inhibitor, in patients with triple class resistant virus. Abstract 105aLB. *14th Conference on Retroviruses and Opportunistic Infections web site* [online], <http://www.retroconference.org/2007/Abstracts/30687.htm> (2007). (b) Stiegbigel, R. *et al*. Results of BENCHMRK-2, a Phase III study evaluating the efficacy and safety of MK-0518, a novel HIV-1 integrase inhibitor, in patients with triple class resistant virus. Abstract 105bLB. *14th Conference on Retroviruses and Opportunistic Infections web site* [online], <http://www.retroconference.org/2007/Abstracts/30688.htm> (2007).
33. Jones, G. *et al*. Resistance profile of HIV-1 mutants *in vitro* selected by the HIV-1 integrase inhibitor, GS-9137 (JTK-303). Abstract 627.*14th Conference on Retroviruses and Opportunistic Infections web site* [online], <http://www.retroconference.org/2007/Abstracts/29251.htm> (2007).
34. (a) Nelson, M. *et al*. Efficacy and safety of maraviroc plus optimized background therapy in viremic, ARTexperienced patients infected with CCR5-tropic HIV-1 in Europe, Auastralia, and North America: 24-week results. Abstract 104aLB.*14th Conference on Retroviruses and Opportunistic Infections web site* [online], <http://www.retroconference.org/2007/Abstracts/30636.htm> (2007). (b) Lalezari, J. *et al*. Efficacy and safety of maraviroc plus optimized background therapy in viremic, ARTexperienced patients infected with CCR5-tropic HIV-1, 24-week results of a Phase 2b/3 study in the U. S. & Canada. Abstract 104bLB. *14th Conference on Retroviruses and Opportunistic Infections* [online], <http://www.retroconference.org/2007/Abstracts/30635.htm> (2007).
35. De Clercq, E. From adefovir to AtriplaTM via tenofovir, VireadTM and TruvadaTM. *Future Virol.* **2006**, *1*, 709–715.
36. Kohlstaedt, L. A.; Wang, J.; Friedman, J. M.; Rice, P. A. and Steitz, T. A. Crystal structure at 3.5 Å resolution of HIV-1 reverse transcriptase complexed with an inhibitor. *Science* **1992**, *256*, 1783–1790.
37. (a) Jacobo-Molina, A.; Ding, J.; Nanni, R. G.; Clarck; A. D.; Lu, X.; Antillo, C.; Williams, R. l.; Kame, G.; Ferris, A. L.; Clarck, P.; Hitzi, A.; Hughes, S. H. and Arnold, E. Crystal structure of human immunodeficiency virus type 1 reverse transcriptase complexed with double-stranded DNA at 3.0 A resolution shows bent DNA *Proc. Natl. Acad. Sci. USA* **1993**, *90*, 6320-6324. (b) Huang, H.; Chopra, R.; Verdine, G. L. and Harrison, S. C. Structure of a Covalently Trapped Catalityc Complex of HIV-1 Reverse Transcriptase: Implications for Drug Resistence *Science* **1998**, *282*, 1669-1675.

38. Esnouf, R.; Ren, J.; Ross, C.; Jones, Y.; Stammers, D.; Stuart, D. Mechanism of inhibition of HIV-1 reverse transcriptase by non-nucleoside inhibitors *Nat. Struct. Biol*., **1995**, *2*, 303.
39. Spence, R. A.; Kati, W. A.; Anderson, K. S. and Johnson, K.A. Mechanism of inhibition of HIV-1 reverse transcriptase by nonnucleoside inhibitors *Science*, **1995**, *267*, 988.
40. Ren, J.; Bird, L. E.; Chamberlain, P. P.; Stewart-Jones, G. B. and Stammers, D. Structure of HIV-2 reverse transcriptase at 2.35-Å resolution and the mechanism of resistance to non-nucleoside inhibitors *Proc. Natl. Acad. Sci. USA,* **2002**, *99*, 14410.
41. Temiz, N. and Bahar, I. A unifold, mesofold, and superfold model of protein fold use ***Proteins*** **2002**, *49*, 61.
42. (a) Tachedjian, G.; Orlova, M.; Sarafianos, S.; Arnold, E. and Goff, S. Molecular matchmaking: NNRTIs can enhance the dimerization of HIV type 1 reverse transcriptase *Proc. Natl. Acad. Sci. USA,* **2001**, *98,* 7188. (b) Sluis-Cremer, N.; Arion, D. and Parniak, M. A. Destabilization of the HIV-1 Reverse Transcriptase Dimer upon Interaction with *N*-Acyl Hydrazone Inhibitors *Mol. Pharmacol*. **2002**, *62,* 398-405.
43. (a) Merluzzi, V.; Hargrave, M.; Labadia, K.; Grozinger, M.; Skoog, J.; Wu, C.K.; Shih, K.; Eckner, S.; Hattox, J.; Adams, A. S.; Rosendahl, R.; Faanes, R.; Eckner, R.; Koup, R. and Sullivan, J. Inhibition of HIV-1 replication by a nonnucleoside reverse transcriptase inhibitor *Science,* **1990**, *250,* 1411-1413. (b) Hargrave, K.; Schmidt, G.; Engel, W.; Trummlitz, G. and Eberlein, W. 5,11-Dihydro-6*H*-dipyrido(3,2-b:2',3'-e) (1,4) diazepines and their use in the prevention or treatment of HIV infection, **1991**, EP 00429987.
44. Richman, D.; Rosenthahl, A.; Skoog, M.; Eckner, R.; Chou, T.; Sabo, J. and Merluzzi, V. BI-RG-587 is active against zidovudine-resistant human immunodeficiency virus type 1 and synergistic with zidovudine. *Antimicrob. Agents Chemother*., **1991**, *35*, 305.
45. Havlir, D.; McLaughlin, M. M. and Richman, D.D. [titolo] *J. Infect. Dis*. **1995**, *172*, 1379.
46. Johnson, J. A.; Li, J. F.; Morris, L.; Martinson, N.; Gray, G.; McIntyre, J. and Heneine, W. Emergence of Drug-Resistant HIV-1 after Intrapartum Administration of Single-Dose Nevirapine Is Substantially Underestimated *J. Infect. Dis.,* **2005**, *192*, 16.
47. Romero, D.; Mitchell, M.; Thomas, R.; Palmer, J.; Tarpley, W.; Aristoff, P. and Smith, H. Diaromatic substituted anti-AIDS compounds, **1989**, WO09109849.
48. (a) Dueweke, T.; Kezdy, F.; Waszak, G.; Deibel, M.; Tarpley, W. The binding of a novel bisheteroarylpiperazine mediates inhibition of human immunodeficiency virus type 1 reverse transcriptase *J. Biol. Chem*. **1992**, *267*, 27. (b) Romero, D.; Morge, R.; Genin, M.; Bile, C.; Busso, M.; Resnick, L.; Althaus, I.; Reusser, F.; Thomas, R. and Tarpley, W. Bis(heteroaryl)piperazine (BHAP) reverse transcriptase inhibitors: structure-activity

relationships of novel substituted indole analogs and the identification of 1-[(5-methanesulfonamido-1H-indol-2-yl)carbonyl]-4-[3-[(1-methylethyl)amino]pyridinyl]piperazinemonomethanesulfonate (U-90152S), a second-generation clinical candidate *J. Med. Chem*., **1993**, *36*, 1505. (c) Dueweke, T.; Poppe, S.; Romero, D.; Swaney, S.; So, A.; Downey, K.; Althaus, I.; Reusser, F.; Buso, M.; Resnick, L.; Mayer, D.; Lane, J.; Aristoff, P.; Thomas, R. and Tarpley, W. U-90152, a potent inhibitor of human immunodeficiency virus type 1 replication *Antimicrob. Agents Chemother*. **1993**, *37*, 1127. (d) Romero, D.; Morge, R.; Biles, C.; Pena, N.; May, P.; Palmer, J.; Johnson, P.; Smith, P.; Busso, M.; Tan, C.; Voorman, R.; Reusser, F.; Althaus, I.; Downey, K.; So, A.; Resnick, L.; Tarpley, W. and Aristof, P. Discovery, Synthesis, and Bioactivity of Bis(heteroaryl)piperazines. 1. A Novel Class of Non-Nucleoside HIV-1 Reverse Transcriptase Inhibitors *J. Med. Chem*. **1994**, *37*, 999. (e) Genin, M.; Poel, T.; Yagi, Y.; Biles, C.; Althaus, I.; Keiser, B.; Kopta, L.; Friis, J.; Reusser, F.; Adams, W.; Olmsted, R.; Voorman, R.; Thomas, R.; Romero, D. Synthesis and Bioactivity of Novel Bis(heteroaryl)piperazine (BHAP) Reverse Transcriptase Inhibitors: Structure−Activity Relationships and Increased Metabolic Stability of Novel Substituted Pyridine Analogs *J. Med. Chem*. **1996**, *39*, 5267. (f) Romero, D.; Olmsted, R.; Poel, T.; Morge, R.; Biles, C.; Keiser, B.; Kopta, L.; Friis, J.; Hosley, J.; Stefanski, K.; Wishhka, D.; Evans, D.; Moris, J.; Stehle, R.; Sharma, S.; Yagi, Y.; Voorman, R.; Adams, W.; Tarpley, W. and Thomas, R. Targeting Delavirdine/Atevirdine Resistant HIV-1: Identification of (Alkylamino)piperidine-Containing Bis(heteroaryl)piperazines as Broad Spectrum HIV-1 Reverse Transcriptase Inhibitors *J. Med. Chem*. **1996**, *39*, 3769-3789

49. Esnouf, R.; Ren, J.; Hopkins, A.; Ross, C.; Jones, Y.; Stammers, D. and Stuart, D. Unique features in the structure of the complex between HIV-1 reverse transcriptase and the bis(heteroaryl)piperazine (BHAP) U-90152 explain resistance mutations for this nonnucleoside inhibitor *Proc. Natl. Acad. Sci. USA,* **1997** , *94*, 3984-3989.
50. Young, S. D.; Britcher, S. F.; Payne, L. S.; tran, L. O. and Lumma, W. C. Jr. Benzoxazinones as inhibitors of HIV reverse transcriptase, **1994**, WO 09403440.
51. Ren, J.; Milton, J.; Weaver, K. L.; Short, S. A.; Stuart, D. I. and Stammers, D. K. Structural basis for the resilience of efavirenz (DMP-266) to drug resistance mutations in HIV-1 reverse transcriptase. *Struct. Fold. Des.* **2000**, *8*, 1089-1094.
52. Corbett, J. W.; Ko, S. S.; Rodgers, J. D.; Jeffrey, S.; Bacheler, L. T.; Klabe, R. M.; Diamond, S.; Lai, C. M.; Rabel, S. R.; Saye, J. A.; Adams, S. P.; Trainor, G. L.; Anderson, P. S. and Erickson-Viitanen, S. K. Expanded-Spectrum Nonnucleoside Reverse Transcriptase Inhibitors Inhibit Clinically Relevant Mutant Variants of Human

Immunodeficiency Virus Type 1 *Antimicrob. Agents Chemother.*, **1999**, *43*, 2893-2897.

53. Heather, A. K.; Jacqueline, L. O. and Bryan, L. L. Etravirine a non-nucleoside reverse transcriptase inhibitor for the treatment or resistent HIV-1 infection. *Formulary* **2008**; *43*, 105-11.
54. Janssen, P. A. J.; Lewi, P. J.; Arnold, E.; Daeyaert, F.; de Jonge, M.; Heeres, J.; Koymans, L.; Vinkers, M.; Guillemont, J.; Pasquier, E.; Kukla, M.; Ludovici, D.; Andries, K.; de Béthune, M. P.; Pauwels, R.; Das, K.; Clark, A. D. Jr.; Frenkel, Y. V.; Hughes, S. H.; Medaer, B.; De Knaep, F.; Bohets, H.; De Clerck, F.; Lampo, A.; Williams, P. and Stoffels, P. In Search of a Novel Anti-HIV Drug: Multidisciplinary Coordination in the Discovery of 4-[[4-[[4-[(1*E*)-2-Cyanoethenyl]-2,6-dimethylphenyl]amino]-2-pyrimidinyl]amino]benzonitrile (R278474, Rilpivirine). *J. Med. Chem.* **2005**, *48*, 1901-1909.
55. (a) Williams, T. M.; Ciccarone, M.; MacTough, S. C.; Rooney, C. S.; Balani, S. K.; Condra, J. H.; Emini, E. A.; Goldman, M. E.; Greenlee, W. J. 5-Chloro-3-(phenylsulfonyl)indole-2-carboxyamide: a novel non-nucleoside inhibitor of the HIV-1 reverse transcriptase. *J. Med. Chem.* **1993**, *36*, 1291-1294. (b) Williams, T. A., Ciccarone, T. M.; Saari, W. S.; Wai, J. S.; Greenlee, W. J.; Balani, S. K.; Indoles as inhibitors of HIV reverse transcriptase. **1992**; EP 0530907 A1. (c) Williams, T. A.; Ciccarone, T.M.; Greenlee, W. J.; Balani, S. K.; Goldman, M. E.; Hoffman J. M. Jr, **1994**, WO 94/19321.
56. (a) Artico, M.; Silvestri, R.; Stefancich, G.; Massa, S.; Pagnozzi, E.; Musu, D.; Scintu, F.; Pinna, E.; Tinti, E. and La Colla, P. Synthesis of pyrryl aryl sulfones targeted at the HIV-1 reverse transcriptase. *Arch. Pharm.* (Weinheim) **1995**, *328*, 223-29. (b) Artico, M.; Silvestri, R.; Massa, S.; Loi, A. G.; Corrias, S.; Piras, G. and La Colla, P. 2-Sulfonyl-4-chloroanilino moiety: a potent pharmacophore for the anti-human immunodeficiency virus type 1 activity of pyrrolyl aryl sulfones. *J. Med. Chem.* **1996**, *39*, 522-30. (c) Artico, M.; Silvestri, R.; Pagnozzi, E.; Bruno, B.; Novellino, E.; Greco, G.; Massa, S.; Ettore, A.; Loi, A. G.; Scintu, F. and La Colla, P. Structure-based design, synthesis and biological evaluation of novel pyrrolyl aryl sulfones (PASs), HIV-1 non-nucleoside reverse transcriptase inhibitors active at nanomolar concentrations. *J. Med. Chem.* **2000**, *43*, 1886-1891. (d) Artico, M.; Silvestri, R.; Massa, S.; Loi, A. G. and La Colla, P. Pirril-(indolil-)aril-solfoni e relativo processo di produzione ed impiego nella terapia delle infezioni da virus. **1995**, MI95A000812.
57. (a) Artico, M.; Silvestri, R.; Pagnozzi, E.; Stefancich, G.; Massa, S.; Loi, A. G.; Putzolu, M.; Corrias, S.; Spiga, M. G. and La Colla, P. 5*H*-Pyrrolo[1, 2-*b*][1, 2, 5]benzothiadiazepines

(PBTDs): a novel class of HIV-1-specific non-nucleoside reverse transcriptase inhibitors. *Bioorg. Med. Chem.* **1996**, *4*, 837-50. (b) Silvestri, R,; Artico, M.; Pagnozzi, E.; Stefancich, G.; Massa, S.; La Colla, M.; Loddo, R. and La Colla, P. Synthesis and anti-HIV activity of 10, 11-dihydropyrrolo[1, 2-*b*][1, 2, 5]benzothiadiazepine-11-acetic acid 5, 5-dioxide derivatives and related compounds. *Farmaco* **1996**, *51*, 425-30. (c) Artico, M.; Massa, S.; Silvestri, R.; Loi, A. G.; De Montis, A. and La Colla, P. 1*H*-Pyrrol-1-yl and 1H-indol-1-yl sulphones, processes for their preparation and use for therapy of HIV-1 infections. **1996**, WO 96/33171.

58. Silvestri, R.; De Martino, G.; La Regina, G.; Artico, M.; Massa, S.; Vargiu, L.; Mura, M.; Loi, A. G.; Marceddu, T. and La Colla, P. Novel indolyl aryl sulfones active against HIV-1 carrying NNRTI resistance mutations: Synthesis and SAR studies. *J. Med. Chem.* **2003**, *46*, 2482-93..
59. Behforouz, M.; Kerwood, J. E. Alkyl and aryl sulfenimides. *J. Org. Chem.* **1969**, *34*, 51-55.
60. Hara, T.; Durell, S. R.; Myers, M. C. and Appella, D. H. Probing the structural requirements of peptoids that inhibit HDM2-p53 interactions. *J. Am. Chem. Soc.* **2006**, *128*, 1995-2004.
61. Hsiao, Y. and Hegedus, L. S. Synthesis of optically active imidazolines, azapenams, dioxocyclams, and bis-dioxocyclams. *J. Org. Chem.* **1997**, *62*, 3586-3591.
62. Zhao, Z.; Wolkenberg, S. E.; Lu, M.; Munshi, V.; Moyer, G.; Feng, M.; Carella, A. V.; Ecto, L. T.; Gabryelski, L. J.; Lai, M.-T.; Prasad, S. G.; Yan, Y.; McGaughey, G. B.; Miller, M. D.; Lindsley, C. W.; Hartman, G. D.; Vacca, J. P. and Williams, T. M. Novel indole-3-sulfonamides as potent HIV non-nucleoside reverse transcriptase inhibitors (NNRTIs). *Bioorg. & Med. Chem. Lett.* **2008**, *18*, 554-559.
63. (a) Ragno, R.; Artico, M.; De Martino, G.; La Regina, G.; Coluccia, A.; Di Pasquali, A. and Silvestri, R. Docking and 3-D QSAR studies on indolyl aryl sulfones (IASs). binding mode exploration at the HIV-1 reverse transcriptase non-nucleoside binding site and design of highly active *N*-(2-hydroxyethyl)carboxyamide and *N*-(2-hydroxyethyl)carboxyhydrazide derivatives. *J. Med. Chem.* **2005**, *48,* 213-223; (b) Ragno, R.; Coluccia, A.; La Regina, G.; De Martino, G.; Piscitelli, F.; Lavecchia, A.; Novellino, E.; Bergamini, A.; Ciaprini, C.; Sinistro, A.; Maga, G.; Crespan, E.; Artico, M. and Silvestri, R. Design, molecular modeling, synthesis and anti-HIV-1 activity of new indolyl aryl sulfones. Novel derivatives of the indole-2-carboxamide. *J. Med. Chem.* **2006**, *49,* 3172-3184.
64. Goodsell, D. S.; Morris, G. M. and Olson, A. J. Automated docking of flexible ligands:

Applications of AutoDock. *J. Mol. Recog.* **1996**, *9*, 1−5.
65. Biosolveit FlexX 2.2; BioSolveIT GmbH An der Ziegelei 75, 53757 Sankt Augustin, Germany; http://www.biosolveit.de/flexx.
66. Molecular Operating Environment (MOE). Chemical Computing Group, Inc. Montreal, Quebec, Canada; www.chemcomp.com.
67. Das, K.; Bauman, J. D.; Clark Jr., A.D.; Frenkel, Y. V.; Lewi, P. J.; Shatkin, A. J.; Hughes, S. H. and Arnold, E. High-resolution structures of HIV-1 reverse transcriptase/TMC278 complexes: Strategic flexibility explains potency against resistance mutations. *Proc. Nat. Acad. Sci. Usa* **2008,** *105,*1466-1471.
68. Ren, J.; Nichols, C. E.; Chamberlain, P. P.; Weaver, K. L.; Short, S. A. and Stammers, D. K. Crystal structures of HIV-1 reverse transcriptases mutated at codons 100, 106 and 108 and mechanisms of resistance to non-nucleoside inhibitors. *J. Mol. Biol.* **2004**, *336,* 569-578.
69. Ren, J.; Nichols, C. E.; Chamberlain, P. P.; Weaver, K. L.; Short, S. A.; Chan, J. H.: Kleim, J. P. and Stammers, D. K. Relationship of potency and resilience to drug resistant mutations for GW420867X revealed by crystal structures of inhibitor complexes for wild-type, Leu100Ile, Lys101Glu, and Tyr188Cys mutant HIV-1 reverse transcriptases. *J. Med. Chem.* **2007**, *50,* 2301-2309.
70. Ren, J.; Nichols, C.; Bird, L.; Chamberlain, P.; Weaver, K.; Short, S.; Stuart, D. I. and Stammers, D. K. Structural mechanisms of drug resistance for mutations at codons 181 and 188 in HIV-1 reverse transcriptase and the improved resilience of second generation non-nucleoside inhibitors. *J. Mol. Biol.* **2001**, *312*, 795-805.
71. La Regina, G.; Coluccia, A.; Piscitelli, F.; Bergamini, A.; Sinistro, A.; Cavazza, A.; Maga, G.; Samuele, A.; Zanoli, S.; Novellino, E.; Artico, M. and Silvestri, R. Indolyl aryl sulfones as HIV-1 non-nucleoside reverse transcriptase inhibitors: role of two halogen atoms at the indole ring in developing new analogues with improved antiviral activity. *J. Med. Chem.* **2007**, *50*, 5034-5038.
72. (a) Patel, P. H.; Jacobo-Molina, A.; Ding, J.; Tantillo, C.; Clark Jr., A. D.; Raag, R.; Nanni, R. G.; Hughes, S. H. and Arnold, E. Insights into DNA polymerization mechanisms from structure and function analysis of HIV-1 reverse transcriptase. *Biochemistry* **1995**, *34*, 5351–5363. (b) Patel, P. H. and Preston, B. D. Marked infidelity of human immunodeficiency virus type 1 reverse transcriptase at RNA and DNA template ends. *Proc. Natl. Acad. Sci. USA* **1994**, *91*, 549–553.
73. Crespan, E.; Locatelli, G. A.; Cancio, R.; Hubscher, U.; Spadari, S. and Maga, G. Drug resistance mutations in the nucleotide binding pocket of human immunodeficiency

virus type 1 reverse transcriptase differentially affect the phosphorolysis-dependent primer unblocking activity in the presence of stavudine and zidovudine and its inhibition by efavirenz. *Antimicrob. Agents Chemother.* **2005**, *49*, 342–349.

74. Silvestri, R.; Artico, M.; De Martino, G.; La Regina, G.; Loddo, R.; La Colla, M. and La Colla, P. Simple, Short Peptide Derivatives of a Sulfonylindolecarboxamide (L-737,126) Active *in vitro* against HIV-1 Wild Type and Variants Carrying Non-Nucleoside Reverse Transcriptase Inhibitor Resistance Mutations *J. Med. Chem.* **2004**, *47*, 3892-3896.
75. R. Silvestri, G. De Martino and G. Sbardella. A Simplified Synthesis of Ethyl 5-Chloro-4-fluoro-1*H*-indole-2-carboxylate and of Ethyl 5-Chloro-6-fluoro-1*H*-indole-2-carboxylate *Org. Prep. Proced. Int.* **2002**, *34*, 517-523.
76. Hsiao, Y.; Hegedus, L. S. Synthesis of optically active imidazolines, azapenams, dioxocyclams, and bis-dioxocyclams. *J. Org. Chem.* **1997**, *62*, 3586-3591.
77. Biosolveit FlexX 2.2; BioSolveIT GmbH An der Ziegelei 75, 53757 Sankt Augustin, Germany; http://www.biosolveit.de/flexx.
78. Surflex, version 2.1 ed.; Tripos, Inc.: St. Louis, MO 63144.
79. Tripos SYBYL 8.0; Tripos Inc., 1699 South Hanley Rd, St. Louis, MO 63144, USA. http://www.tripos.com.
80. Korb, O.; Stützle, T.; Exner, T. E. PLANTS: Application of ant colony optimization to structure-based drug design. In M. Dorigo, L. M. Gambardella, M. Birattari, A. Martinoli, R. Poli, and T. Stützle (Eds.) *Ant. Col. Opt. Swarm Int., 5th Int.l Workshop, ANTS 2006*, LNCS 4150, pp. 247-258; http://dx.doi.org/10.1007/11839088_22.
81. Zodiac: www.zeden.org.
82. Code "scoring.svl" obtained from SLV exchange website http://svl.chemcomp.com, Chemical Computing Group, Inc., Montreal, Canada.
83. PyMOL: DeLano Scientific LLC, San Carlos, California, USA. www.pymol.org.
84. Van Nhien, A. N.; Tomassi, C.; Len, C.; Marco-Contelles, J. L.; Balzarini, J.; Pannecouque, C.; De Clercq, E.; Postel, D. First synthesis and evaluation of the inhibitory effects of aza analogues of TSAO on HIV-1 replication. *J. Med. Chem.* **2005**, *48,* 4276-4284.
85. Maga, G.; Amacker, M.; Ruel, N.; Hubsher, U.; Spadari, S. Resistance to nevirapine of HIV-1 reverse transcriptase mutants: loss of stabilizing interactions and thermodynamic or steric barriers are induced by different single amino acid substitutions. *J. Mol. Biol.* **1997**, *274*, 738-747.